The TLS Proto-Oncoprotein Modulates NF-κB-Directed Gene Expression

By

Warren John Law

A thesis submitted to the Faculty of Graduate Studies of The University of Manitoba in partial fulfillment of the requirement of the degree of

Master of Science

Department of Biochemistry and Medical Genetics
Faculty of Medicine
University of Manitoba
2005

THE UNIVERSITY OF MANITOBA

FACULTY OF GRADUATE STUDIES

*****

COPYRIGHT PERMISSION

"The TLS Proto-Oncoprotein Modulates Nf-κB-Directed Gene Expression"

BY

Warren John Law

A Thesis/Practicum submitted to the Faculty of Graduate Studies of The University of Manitoba in partial fulfillment of the requirement of the degree

Of

MASTER OF SCIENCE

TABLE OF CONTENTS

Acknowledgements

I will keep this short and sweet. I would like to thank my supervisor Dr. Geoff Hicks for allowing me to join his team and for his guidance and support over the years. I would also like to thank all of my fellow lab mates that I have had the pleasure of working alongside during this same period of time. I would especially like to thank Kendra Cann and Dr. Ludger Klewes for all of their help and for their friendship.

I would like to thank my graduate committee members Dr. Jim Davie, Dr. R. Daniel Gietz and Dr. Michael Czubryt for their input and support. I would like to thank the Montreal Genome Centre technical staff for their help on our microarray experiments. I would also like to thank the Manitoba Health Research Council, University of Manitoba, CancerCare Manitoba and the Canadian Institute of Health Research Strategic Training Program for all of their financial support.

I would like to thank my family: Dad (Gil), Mom (Tina), Wes (Rach and Evan) and Ryan for their love and support. I would also like to thank a few members of the animal kingdom: Pepper, Sugar (RIP) and Max (RIP). Finally, I would like to thank my wonderful and beautiful girlfriend Jaimie for so many things (I could write another thesis-sized book on this topic), but I unfortunately promised to keep this short and sweet. End communication.

List of Figures

List of Tables

Abstract

The *TLS* gene is translocated in several human cancers, including myxoid liposarcoma[1,2] and acute myeloid leukemia[3]. The molecular and cellular mechanisms by which the resultant oncogenic fusion proteins initiate these cancers are unknown. Our lab has determined that a logical approach to deduce TLS' role in the development of cancer is to first characterize the normal cellular function of the wild type TLS protein. We have previously shown that TLS knockout mice possess defects in B cell maturation and in the maintenance of genome stability[4]. Recently we identified an impaired ionizing radiation (IR)-induced apoptotic response in TLS -/- pre-B cells. TLS has been described as an *in vitro* transcriptional coactivator to the well-characterized IR-responsive NF-κB transcription factor[5,6]. Our hypothesis is that TLS loads onto the promoters of specific IR-induced NF-κB target genes and modulates their gene expression. In this study, we have established that modulation of endogenous NF-κB-directed gene expression is TLS-dependent *in vivo*. Utilizing microarray technology we have also identified IR-induced NF-κB target genes that were differentially expressed between wild type and TLS deficient mouse pre-B cells. Here we report the identification of *TNFaip2*, *TNFrsf5*, and *Ier3* as putative TLS-dependent target genes. Interestingly, these candidate genes are known to be involved in several of the cellular processes that were determined to be defective in our TLS -/- mice and cells. The identification of these candidate genes will allow us to molecularly characterize the role of TLS in the modulation of NF-κB-directed gene expression. In addition, the discovery of these novel TLS-dependent target genes may serve as new therapeutic targets in the treatment of patients with TLS-associated cancers such as myxoid liposarcoma and acute myeloid leukemia.

Chapter 1: Introduction

1.1 TLS - Translocated in Liposarcoma

1.1.1 Background

Translocated in ***L***ipo***S***arcoma (**TLS,** also known as FUS or hnRNP-P2) is a nuclear protein of 526 amino acids in length and is widely expressed in mammalian tissues[7]. Based on its primary sequence, the TLS protein was originally classified as an RNA binding protein[3]. Since then, *in vitro* studies have demonstrated functional roles for TLS at several levels of gene expression, such as: transcription[8], splicing[9] and mRNA transport[10]. Additionally, TLS is capable of binding several types of polynucleotides including RNA[11], single-[12] and double-stranded DNA[13,14] and has been shown to engage in nucleo-cytoplasmic shuttling[15]. Despite these reports, the molecular and cellular functions of TLS *in vivo* remain largely unknown.

TLS shares a high sequence similarity to the EWS (55.6% identity)[3] and TAF15 (74% identity)[16] proteins. Collectively known as the **TET** family (***T***LS, ***E***WS, and ***T***AF15), these genes are commonly found to be translocated in several cancers (section 1.1.2). Functional inferences can be drawn from one TET family member to another because of the high sequence identity and conservation of unique structural motifs that are shared by these proteins (see below). For this reason, several references to studies of the EWS and TAF15 proteins will be discussed throughout the thesis.

The TLS protein consists of several distinct motifs (Figure 1). The amino terminus consists of a high frequency of serine, tyrosine and glutamine repeats, and is

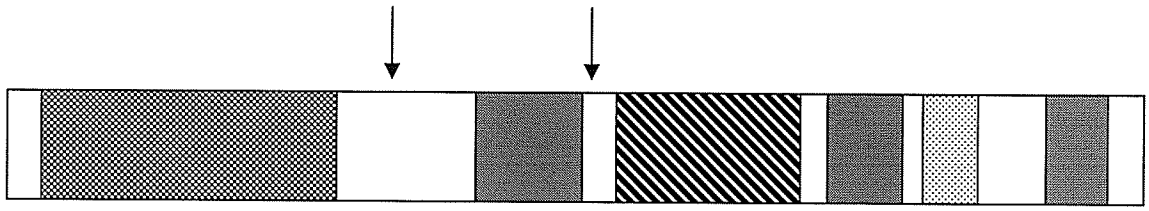

ser-tyr-gln (SYQ)-rich (12-149)
arg-gly-gly (RGG)-repeat (213-261, 377-409 and 473-505)
RNA recognition motif (RRM) (278-364)
Zinc finger motif (415-446)

Figure 1. Schematic representation of the functional motif organization of the TLS protein. Amino acid numbers are indicated below the diagram and in legend (within brackets). Arrows indicate the common translocation breakpoints in myxoid liposarcoma and acute myeloid leukemia.

unique to the TET family. The charged amino acid residues within this motif are most likely responsible for the transactivational properties that are attributed to TLS by way of *in vitro* luciferase reporter assays[8]. The EWS protein is the only other reported protein that possesses this unique motif [17]. TLS and EWS oncogenic fusion proteins retain their unique amino termini and lose their carboxy-termini (see section 1.1.2 for more on the TLS and EWS fusion proteins). The TAF15 protein (formerly TAF68) has been described as a transcription factor in its own right[16]. The amino portion of the TAF15 peptide is phosphorylated by the v-Src tyrosine kinase[18], however it has not been determined if this modification affects the transcriptional function of TAF15.

The carboxy-terminal domain of the TLS protein consists of several functional motifs, such as an RNA recognition motif (RRM), a series of arginine-glycine-glycine (RGG) repeats and a single Ran-GDP-like zinc finger motif. As the name suggests, the RRM motif is important for both recognition and interaction with RNA[19]. The RGG

motifs stabilize polynucleotide binding and have been identified as sites of post-translational modification by asymmetric dimethylation[20]. Cytoplasmic relocalization of the EWS protein has been observed upon methylation of its RGG motifs and may indicate an important point of regulation[21]. Further experimentation will be required to determine whether TLS can also translocate to the cytoplasm upon methylation of its RGG motifs. Finally, the TLS zinc finger motif has recently been shown to be important in the determination of RNA-binding specificity[22]. While unique to the hnRNP protein superfamily, several other proteins that have multiple roles in the regulation of gene expression, like TLS, have been shown to contain zinc finger motifs[23].

Taken together, the various functional motifs of TLS appear to contribute to its role in a broad range of cellular processes. The multifunctional nature of TLS and the TET family of proteins will be further discussed in section 1.1.3.

1.1.2 TLS and Cancer

Myxoid liposarcoma, a cancer of the adipose tissue that occurs primarily in the extremities of adults, is the most predominant form of liposarcoma[24,25]. It has been reported that over 90% of all cases of myxoid liposarcoma have a characteristic balanced translocation between chromosomes 12 and 16 t(12;16)(q13;p11)[26]. Examination of the translocation breakpoint region led to the discovery of the *TLS* gene and the resultant expression of an aberrant TLS-CHOP fusion protein[3,27]. The CHOP protein, also referred to as growth arrest and DNA damage-inducible 153 (GADD153), is involved in adipocyte differentiation[28] and the regulation of cell cycle growth arrest[29]. The latter function has been shown to be disrupted upon fusion with the TLS protein[29].

Additionally, it has been shown that TLS-CHOP is involved in the aberrant regulation of expression levels of specific target genes[30]. More recent discoveries using transgenic mice have directly linked TLS-CHOP with the development of a liposarcoma phenotype[31,32]. Therefore, the progression of myxoid liposarcoma is likely attributed, in part, to both the disruption of normal TLS- and CHOP-regulated cellular mechanisms and the gain of function properties attributed with the fusion protein.

In addition to the TLS-fusions reported in myxoid liposarcoma, subsequent discoveries of translocation events involving human chromosome 16 and the *TLS* locus were identified in other cancers. For example, fusion of TLS to the *ets* transcription factor ERG t(16;21)(p11;q22) has been identified in acute myeloid leukemia[1]. Retroviral induction of TLS-ERG into early hematopoietic cells has been shown to result in the progression of a leukemogenic-like pathogenesis, thereby demonstrating a direct correlation between the expression of the TLS-ERG fusion protein and the development of a leukemia-like cancer[33]. It is important to note that many examples of similar translocations involving TLS, EWS and TAF15 have been described to date (Table 1). In each case the carboxy-RNP domain of the TET protein is replaced with the DNA-binding domain of an *ets*-like transcription factor and the resultant fusion proteins are oncogenic. Taken together, it is clear that chromosomal translocations involving TET proteins are important initiating events in a broad spectrum of human cancers.

Table 1. TLS, EWS and TAF15 translocations in cancer.

Effector	DNA-Binding Domain	Human Tumor	Reference
TLS	ERG1	acute myeloid leukemia	1,2,34,35
TLS	CHOP	myxoid liposarcoma	3,27,36,37
TLS	ATF-1	angiomatoid fibrous hystiocytoma	38
TLS	BBF2H7	low-grade fibromyxoid sarcoma	39
EWS	FLI-1	Ewing sarcoma (peripheral) neuroectodermal tumor	40,41
EWS	ERG	Ewing sarcoma (PNET)	42,43
EWS	E1A-F	Ewing sarcoma (PNET)	44
EWS	WT-1	desmoplastic small round cell tumor	45-48
EWS	CHOP	myxoid sarcoma	49,50
EWS	CHN/TEC	skeletal myxoid chondrosarcoma	51,52
EWS	ATF-1	soft tissue clear cell sarcoma (PNET); malignant melanoma	53-55
EWS	ETV1	Ewing sarcoma (PNET)	56
EWS	CIZ/NMP4	myeloid leukemia	57
TAF15	CIZ/NMP4	myeloid leukemia	57
TAF15	CHN/TEC	myxoid chondrosarcoma	58-60

1.1.3 TLS and Gene Expression

Gene expression consists of several processes including transcription, splicing, mRNA stabilization and transport. Transcription and splicing are known to occur concomitantly with one another[61]. Interestingly, TLS has been characterized as a

potential bridging factor between these two processes[62]. This section will focus on TLS' roles in the regulation of gene expression and will further examine the multifunctional nature of the TET proteins.

Transcriptional Initiation and Spliceosomal Assembly

The TET proteins have been shown to associate with integral components of the transcriptional pre-initiation complex, which is essential for the induction of transcription. The human TLS protein and its *drosophila* homologue both interact with the RNA polymerase II enzyme[62,63]. RNA polymerase II is an essential component of the general transcriptional machinery that regulates the transcription of eukaryotic protein-coding genes (see reviews[61,64,65]). TLS also associates with the $TF_{II}D$ complex, a DNA-binding component of the general transcriptional machinery, and thus has been implicated in early transcriptional initiation and elongation[16]. The TFIID complex consists of the TATA-binding protein (TBP) and several TBP-associated factors (TAF) proteins[66]. EWS and TAF15 have also been shown to interact with both the RNA polymerase II enzyme and $TF_{II}D$ complex[16,67].

The RNA polymerase II enzyme has also been shown to be involved in spliceosome assembly[68,69]. Interestingly, TLS interacts with components of the nuclear matrix and has also been implicated in spliceosome assembly[70]. Y-box-binding-1 (YB-1), a multifunctional protein involved in both transcription and splicing (see review[71]), has been identified as an interaction partner of TLS, EWS, and the RNA polymerase II enzyme[72]. TLS fusion proteins have been shown to disrupt YB-1-mediated splicing by failing to recruit the YB-1 protein to RNA polymerase II[72,73]. The EWS-Fli1 fusion

proteins have also been shown to interrupt both YB-1- and serine-arginine protein-mediated splicing in a similar mechanism[72,74]. These findings suggest that TLS may act as a functional link bringing together the processes of transcription and spliceosome assembly through interactions with multifunctional proteins like RNA polymerase II and YB-1.

TLS can also associate with several gene-specific transcription factors, which suggests a more specialized, gene-specific regulatory role for TLS in the regulation of gene expression. TLS is an interaction partner to several nuclear hormone receptors, including the glucocorticoid, estrogen and thyroid hormone receptors, as well as, the retinoid X receptor-α[75]. When associated with the TLS protein, the thyroid hormone receptor is still able to retain its ability to bind its target DNA sequences[75]. This indicates that in addition to TLS' ability to bind DNA directly (see above), it is also capable of being loaded onto gene promoter sequences through interactions with gene-specific transcription factors.

The Spi-1 (PU.1) and NF-κB proteins are major transcription factors that regulate signal transduction pathways often disrupted in cancer. The PU.1 oncogene is an important transcription factor in the differentiation of white blood cells[76-78], while NF-κB is a key regulator of apoptosis (see recent reviews[79,80]). TLS has been shown to interact with PU.1 *in vivo*[81] resulting in functional consequences for both transcription and splicing. PU.1, itself, has been recently described as having splicing activity[82]. While this is surprising intrinsic activity for a *bona fide ets*-like transcription factor, it does support the hypothesis that transcription and RNA processing events are integrally linked and that it is increasingly more common to find such interaction partners that have gene-

specific multifunctional activities. TLS' role in gene splicing will be discussed in the next subsection. TLS has also been identified as an interaction partner to the p65 subunit of NF-κB. When overexpressed together, TLS and NF-κB were able to co-activate *in vitro* expression from the intercellular adhesion molecule-1 (*ICAM-1*) gene promoter[6]. NF-κB will be introduced and discussed in greater detail in section 1.3.3.

The EWS protein has also been implicated in the process of transcriptional initiation. EWS interacts with the POU homeodomain transcription factor Brn-3a[83,84], an important factor in neuronal differentiation. Interestingly, EWS activates *in vitro* transcription of a specific isoform of Brn-3a [85]. Additionally, EWS and the histone acetyl-transferase proteins CREB-binding (CBP) and p300 transcriptional activator proteins have been shown to interact and co-transactivate several *in vitro* promoters in a cell-type specific manner[86]. Finally, the ZFM1 protein, a known transcriptional repressor, was identified as an interaction partner of all three TET proteins in a yeast two-hybrid screen[87]. Taken together, the literature indicates that TLS, EWS and TAF15 may play an important role in the recruitment of both general and more specialized factors for the initiation of transcription.

Splicing, mRNA Stabilization and Transport

In addition to its role in transcriptional initiation, TLS has also been described as a splicing factor that contributes to alternative splice site selection. TLS has been shown to interact with the well-established splicing protein SC35 and another serine-arginine factor, which has been named TLS-associated serine-arginine (TASR) splicing protein, through the RGG motifs of its carboxy-terminus[9]. In a separate study, the RGG and

RRM motifs of TLS were determined to be important in the determination of alternate splice site selection *in vitro*[11]. Finally, TLS can interact with the 3' splice site early in the splicing process[88] and promote the use of distal alternate splice sites *in vitro*[81]. These findings suggest that TLS' role in splicing is likely a regulated and gene targeted activity. Alternative splicing and transcriptional elongation have been shown to affect each others rate of progress[61]. It can be speculated that TLS may be initially loaded onto the promoter during transcriptional initiation, remain associated with the elongation complex, and affect alternative splice site selection from the transcription complex.

In addition to its role in alternative splicing, TLS has been shown to associate with RNP complexes and mature transcripts [8], suggesting a possible role for TLS in mRNA transport, stabilization or subcellular targeting. Moreover, TLS may stabilize and/or transport specific mRNA transcripts, as opposed to being a more generalized RNA-binding factor. TLS' RNA-binding specificity was demonstrated by the *in vitro* identification of a GGUG consensus binding sequence[11], and structural analysis showing the TLS zinc-finger domain is responsible for sequence-specific interaction [22]. Finally, we have recently demonstrated that TLS directs the transport of specific mRNA to post-synaptic sites for local protein synthesis in the dendritic spikes of hippocampal neurons[10]. As a result, mice deficient for TLS failed to develop normal interneuronal connections. These data establish that TLS is important in the delivery of specific RNA cargo molecules to localized areas in neurons. Additional experimentation will be required to determine if this function of TLS exists in different cell types.

1.1.4 In vivo analysis of TLS function

In order to determine the *in vivo* function of the TLS protein, our lab has developed TLS knockout mice that were generated by retroviral gene-trap insertion[4]. Mice homologous for the TLS mutation were demonstrated to be deficient for TLS expression. These mice did not survive longer than 16 h after birth and had undersized thymus glands, but otherwise appeared histologically normal.

TLS deficient (TLS -/-) cells were derived from the knockout embryos to further study defects at the cellular level. A high degree of genomic instability was observed in E14.5 TLS -/- mouse embryonic fibroblast cells (MEF), which implies a role for TLS in the maintenance of genomic stability. In addition, a defect in pre-B to B-cell maturation, as determined by the reduced number of IgM+ B-cells in comparison to unchanged levels of precursor cells, was observed in hematopoietic tissues of TLS -/- mice at various stages of development. In order to test B-cell function, mature TLS -/- B-cells were derived by adoptive transfer of fetal liver hematopoietic stem cells into irradiated congenic mice and determined to be defective in response to B cell receptor (BCR) activation by α-IgM and α-CD40. In contrast, a normal BCR activation response to lipopolysaccharide was observed[4]. These findings suggest that TLS is essential for specific antigen-dependent BCR activation. It can be speculated that TLS may regulate the gene expression of essential components of the BCR signaling pathway, for example, specific BCR cell surface proteins. In the absence of functional TLS, these proteins may be differentially or incorrectly expressed thereby affecting B cell receptor activation.

Our lab has also identified that the genomic instability phenotype is linked to defects in the biological response to DNA damage, and more specifically, double-strand

DNA repair. TLS -/- pre-B cells, for example, have a defective apoptotic response to a low-level of ionizing radiation (IR) at 2.5 Gy in comparison to wild type cells (Figure 2 – unpublished data). The impairment of normal IR-induced apoptosis in the TLS -/- cells may be attributed to either a defect in the gene expression or activation of known apoptotic factors. One of the aims of this thesis project is to identify TLS-dependent target genes that are implicated in IR-induced apoptosis. Additionally, genes involved in the maintenance of genomic stability and BCR activation are of particular interest to our lab, given the defects in these processes that we have reported.

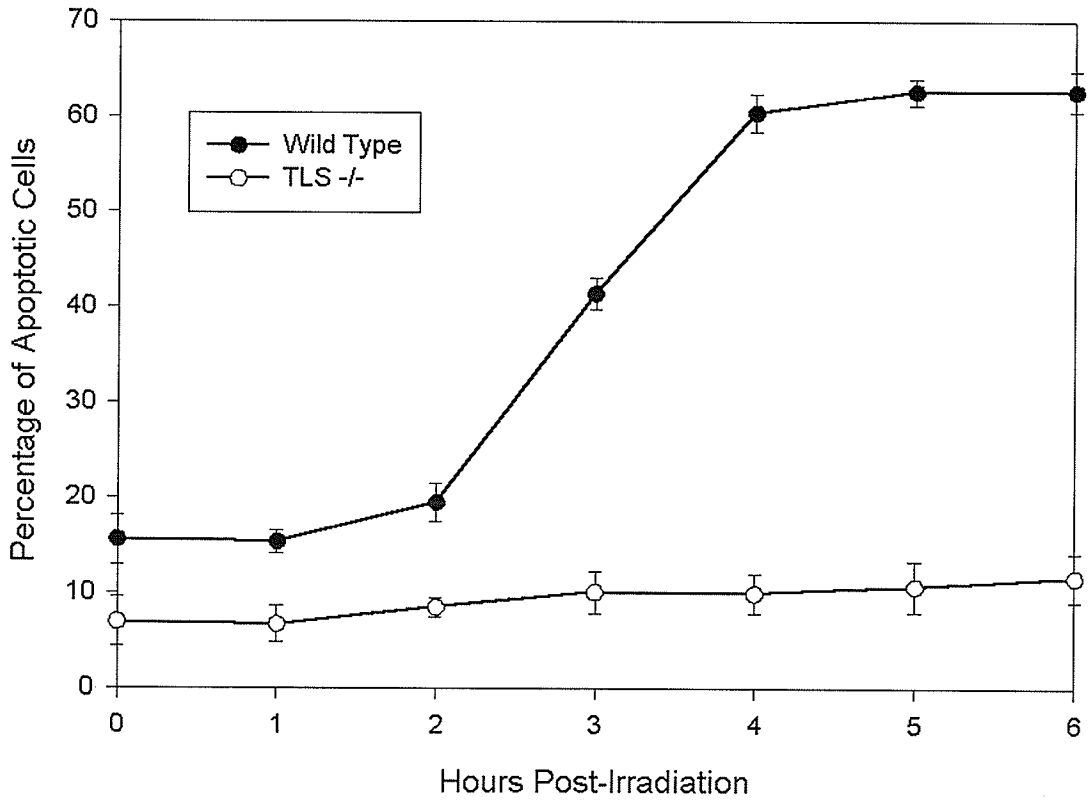

Figure 2. Reduced apoptotic response to ionizing radiation in TLS deficient pre-B cells. Pre-B cells were irradiated (2.5Gy) prior to harvest (0, 1, 2, 3, 4, 5 and 6 h). Cells were sorted by fluorescence activated cell sorting (FACS) to determine the percentage of apoptotic cells (AnnexinV positive). FACS analysis performed by Dr. L. Klewes.

1.2 Nuclear Factor Kappa B

1.2.1 Background

A major goal of my thesis research is to identify TLS-dependent genes that are implicated in the defective cellular processes that we have observed in TLS -/- mice and cells. Based on the existing literature, it is clear that TLS is a multifunctional protein that may be involved in the regulation of gene expression at several levels from gene promoter activation through to site-specific protein translation (section 1.1.3). Prior to the thesis work presented here, I previously identified the Y-box-binding-1 (YB-1) protein as an interaction partner of TLS in a yeast two-hybrid screen (performed in collaboration with Dr. R. Daniel Gietz of the University of Manitoba) and confirmed that the two proteins interact *in vivo*. This finding was also independently reported[72]. YB-1 is a multifunctional protein characterized as both a DNA-binding transcription factor[89-91] and a splicing protein[72]. To examine whether TLS could modulate YB-1 transcriptional activity, I chose to investigate the effects of TLS overexpression on YB-1-directed gene expression from the matrix metalloproteinase-1 (MMP-1) reporter promoter. My results indicated an approximate two-fold TLS-dependent increase in YB-1-directed luciferase reporter gene levels. Although, these results were consistent with other *in vitro* reporter gene assays involving the modulation of YB-1[90,92], we decided that YB-1 was not the best transcription factor model to study TLS' role in gene expression. NF-κB, on the other hand, is an extensively characterized transcription factor with well-defined molecular mechanisms, signaling pathways and target genes. We rationalized that using NF-κB as model transcription factor system would allow us to evaluate the functional role of TLS in a more comprehensive and direct manner.

Nuclear factor-kappa β (NF-κB) is a key transcription factor that is important in the regulation of gene expression in response to many intrinsic and extrinsic stresses, including: cytokines, viral and bacterial infections, DNA-damaging agents and therapeutic drugs[79,93-95]. NF-κB coordinates both adaptive and innate immune responses and is also a key regulator of apoptosis, cellular proliferation and differentiation (see reviews[96,97]).

NF-κB was originally discovered as an essential transcription factor in the expression of the kappa (κ) light chain gene[98,99] which is important in the differentiation of B lymphocytes[100]. The family of NF-κB factors consists of five mammalian members: RelA (p65), NF-κB1 (p50), NF-κB2 (p52), Rel (c-Rel) and RelB, which form homo- and heterodimers (see review[101]). These subunits share a common 300 amino acid Rel homology domain in their amino termini that is responsible for DNA-binding and dimerization[93,102]. Subsequent reference to NF-κB will specify the predominant p65/p50 form[101], unless otherwise noted.

NF-κB is normally located in the cytoplasm in an inactive state. Activation of NF-κB leads to its translocation from the cytoplasm into the nucleus. Once in the nucleus, NF-κB interacts directly with the promoter regions of its target genes. NF-κB binds to 10 base pair consensus binding sequences, called κB sites through interactions with the Rel homology domain. Most NF-κB dimers function as transcriptional activators, however, homodimers of the p50 subunit have been shown to act as repressors[103]. The next section will feature an in-depth introduction to the signaling pathways of the NF-κB protein.

1.2.2 NF-κB Signaling Pathway

The NF-κB signaling pathway has been extensively studied and is well characterized (see review[104]). For the purposes of our research project, we have focused on the classical activation pathway of NF-κB, which is described below. A non-classical activation pathway involving the p52 subunit has also been described (for review of the two NF-κB signaling pathways, see[105]). NF-κB is normally found within the cytoplasm bound to inhibitory protein molecules, called inhibitors of kappa B (IκB) (Figure 3). In the classical activation pathway the upstream IκB kinase (IKK) complex, which consists of three different subunit types (α, β and γ), is phosphorylated in response to induction stimuli. This results in the subsequent phosphorylation of the IκB molecule, which permits the release and translocation of the NF-κB dimer from the cytoplasm to the nucleus. The phosphorylated IκB molecule is targeted for degradation by the 26S proteosomal complex. Once in the nucleus, NF-κB is able to regulate its target genes, including the transcription of the IκB gene, which ultimately extinguishes the activation signal via a negative feedback mechanism[80]. Post-translational modifications of the NF-κB molecule itself has been shown to affect its nuclear function and ability to regulate transcription of its target genes[103,106-108].

The manner in which NF-κB regulates expression of each of its individual target genes is largely undefined. The diverse range of stimuli that activate NF-κB and the large number of target genes that it regulates[97] suggest that novel mechanisms exist to control gene-specific expression in a cell-specific manner. Modulatory factors may serve to integrate multiple signaling pathways by potentiating or coordinating individual target

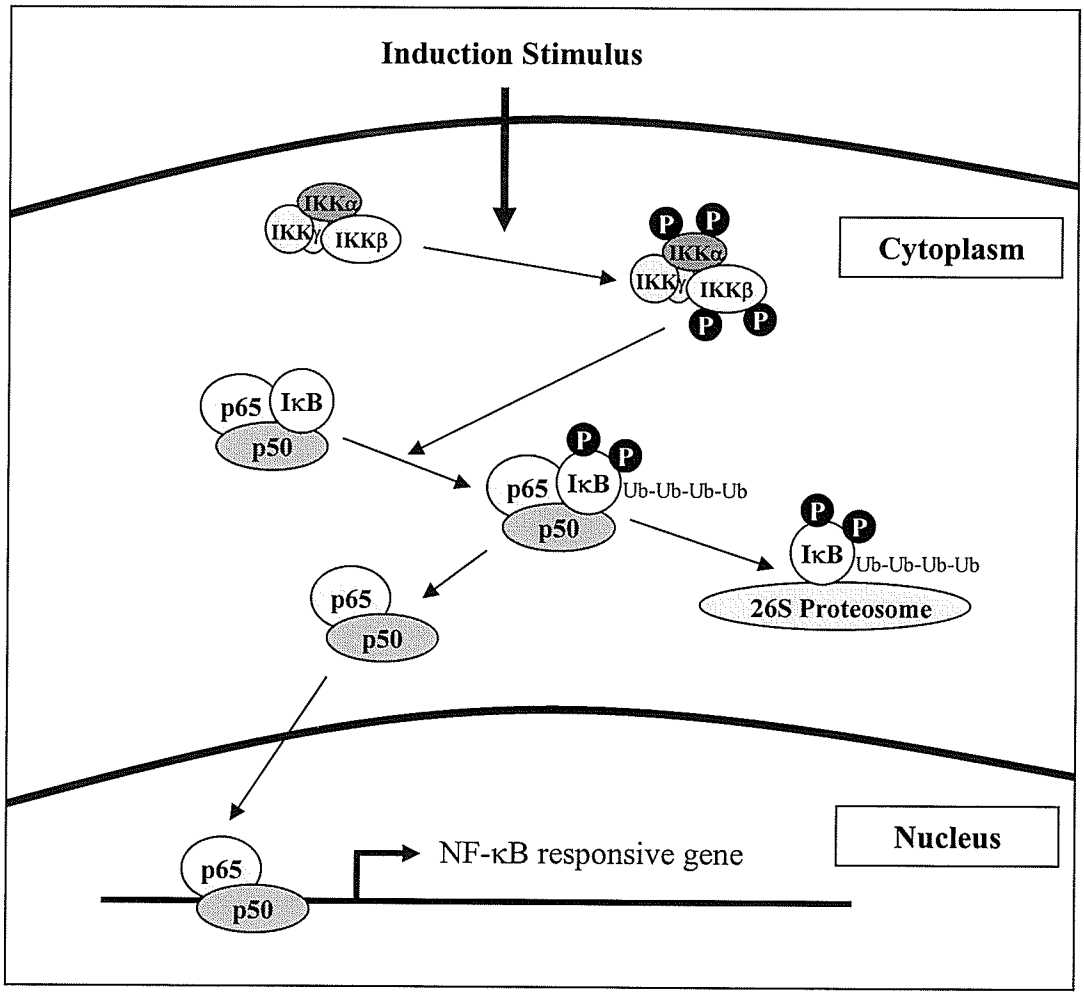

Figure 3. Schematic representation of the NF-κB activation pathway. NF-κB is normally sequestered in the cytoplasm in an inactive form. Upon activation of NF-κB (shown in figure as p65-p50 heterodimer) the IκB protein is degraded resulting in the translocation of NF-κB into the nucleus. Once in the nucleus, NF-κB activates gene transcription on its target promoters. Black circles marked with the letter P represent phosphate groups.

gene promoter regions. The next section of the thesis introduces several known transcription factors that interact with NF-κB and modulate expression levels of its target genes.

1.2.3 NF-κB-Directed Gene Expression

NF-κB has been shown to interact with several proteins that are involved in transcriptional regulation. The CREB-binding protein (CBP) and p300 are coactivators of NF-κB-directed gene expression that possess histone acetyl-transferase (HAT) activity[109,110]. Histone acetylation is important in making DNA more accessible to transcriptional machinery[111,112]. $TAF_{II}105$, a component of the $TF_{II}D$ complex, is also a co-activator of the p65 subunit[113]. TLS has also been shown to interact with components of the $TF_{II}D$ complex (section 1.1.3). The YB-1 protein can interact directly with the p65 subunit of NF-κB and modulate its transcriptional functions in both a DNA-binding-dependent[114] and non-DNA-binding-dependent manner[115]. This is important because TLS has also been described as an interaction partner to YB-1[72]. The PU.1 transcription factor, an important factor in hematopoiesis[116] and interaction partner of TLS[81,82], was shown to interact with NF-κB to upregulate expression levels from a reporter gene construct *in vitro*[117]. Based on these studies, and those discussed in section 1.1.3, it is clear that the NF-κB and TLS proteins share several transcriptional interaction partners and likely form functional complexes *in vivo*.

As discussed previously, the TLS protein was identified as a transcriptional co-activator to p65-mediated gene expression *in vitro*[6]. In this study, a yeast two-hybrid screen using a human placenta cDNA library was used to identify the TLS protein as an

interaction partner. Glutathione S-transferase pull-down and co-immunoprecipitation experiments, using exogenously expressed TLS- and p65-tagged fusion proteins, were able to further establish that the amino acids 477-521 of p65 were responsible for the interaction. Finally, reporter gene assays revealed that exogenously expressed TLS could further enhance TNF-α-induced transcription from the *ICAM-1* gene promoter in a p65-dependent manner[6]. These findings were of particular interest to our lab and thus were influential in the design of our initial experiments.

Taken together, these *in vitro* data support my hypothesis that TLS is involved in the modulation of NF-κB-directed gene expression in some capacity. There is, however, no *in vivo* evidence to validate these *in vitro* experiments. There has also been no attempt to identify *in vivo* NF-κB candidate genes or to characterize the exact mechanism(s) involved in TLS' modulation of NF-κB-directed gene expression. The work presented in this thesis has been performed to address these issues.

1.3 Microarray Analysis

We have employed microarray technology to directly test the modulatory effects of TLS on NF-κB-directed gene expression. Microarray technology permits the simultaneous measurement of gene expression changes for thousands of genes. Due to the large number of NF-κB target genes that have been characterized to date[97], we chose to utilize this technology to identify *in vivo* TLS-dependent NF-κB candidate genes. The identification of a *bona fide* TLS target gene would allow us the opportunity to determine the *in vivo* mechanism(s) involved in TLS' modulation of gene expression.

Since its inception more than 10 years ago, DNA chip technology has revolutionized the way that biological samples are analyzed for large-scale changes in gene expression[118,119]. The technology is designed to compare the relative abundance of mRNA between two biological samples to identify differentially expressed genes. Microarrays capitalize on a well-established molecular biology principle known as nucleic acid hybridization, which allows labeled messenger RNA molecules to bind specifically to the DNA template from which it was transcribed.

Several technologies for microarraying DNA probes exist. The two most common techniques utilize either full-length cDNA or *in situ* synthesized oligonucleotide probes. For our experimental purposes, we chose to use the latter in Affymetrix GeneChip® Expression Arrays and thus will focus on this technology. Affymetrix GeneChips consist of a 5"x 5" quartz wafer with millions of 25 base pair oligonucleotide probes photolithographically attached to the chip surface. Oligonucleotide probes that are adhered to the GeneChips are designed and tested by Affymetrix from raw sequences available from public domain databases. The Affymetrix website provides more in-depth information on the synthesis and quality testing of their GeneChip products (http://www.affymetrix.com).

The experimental process begins with the isolation of mRNA from cells or tissue. The mRNA is first reverse transcribed into cDNA (Figure 4). *In vitro* transcription is performed to yield cRNA which is then labeled with biotin. The biotinylated cRNA is fragmented and hybridized to the GeneChips. The hybridized microarray chips are stained with streptavidin phycoerythrin and are scanned using a GeneArray Scanner at an excitation wavelength of 488nm (http://www.affymetrix.com). The amount of labeled

target that is bound to a given oligonucleotide spot on the microarray chip is determined by measuring fluorescence or phospho-imaging[120]. Fluorescent light emissions are recorded at a wavelength of 570nm. The resultant expression profile is determined through analysis and comparison of experimental chip data by software algorithms and statistical analysis.

We chose the Affymetrix GeneChip technology over the less costly cDNA microarray technology for several reasons. Affymetrix microarray technology allows for more extensive coverage of the mouse genome. The U74Av2 and 430A 2.0 murine GeneChips that were used for our experiments provided the most updated coverage of the mouse genome in the form of approximately 12,000 and 39,000 oligonucleotide probe sets, respectively. The chips are extensively tested and quality control and reproducibility are made easier. Affymetrix-derived microarray data is compatible with other experimental data and can be entered into public databases for the purpose of sharing ones findings with the scientific community. Finally, we were able to access the services and bioinformatic expertise of the Montreal Genome Centre, an Affymetrix core facility, to ensure quality results and proper interpretation of the data.

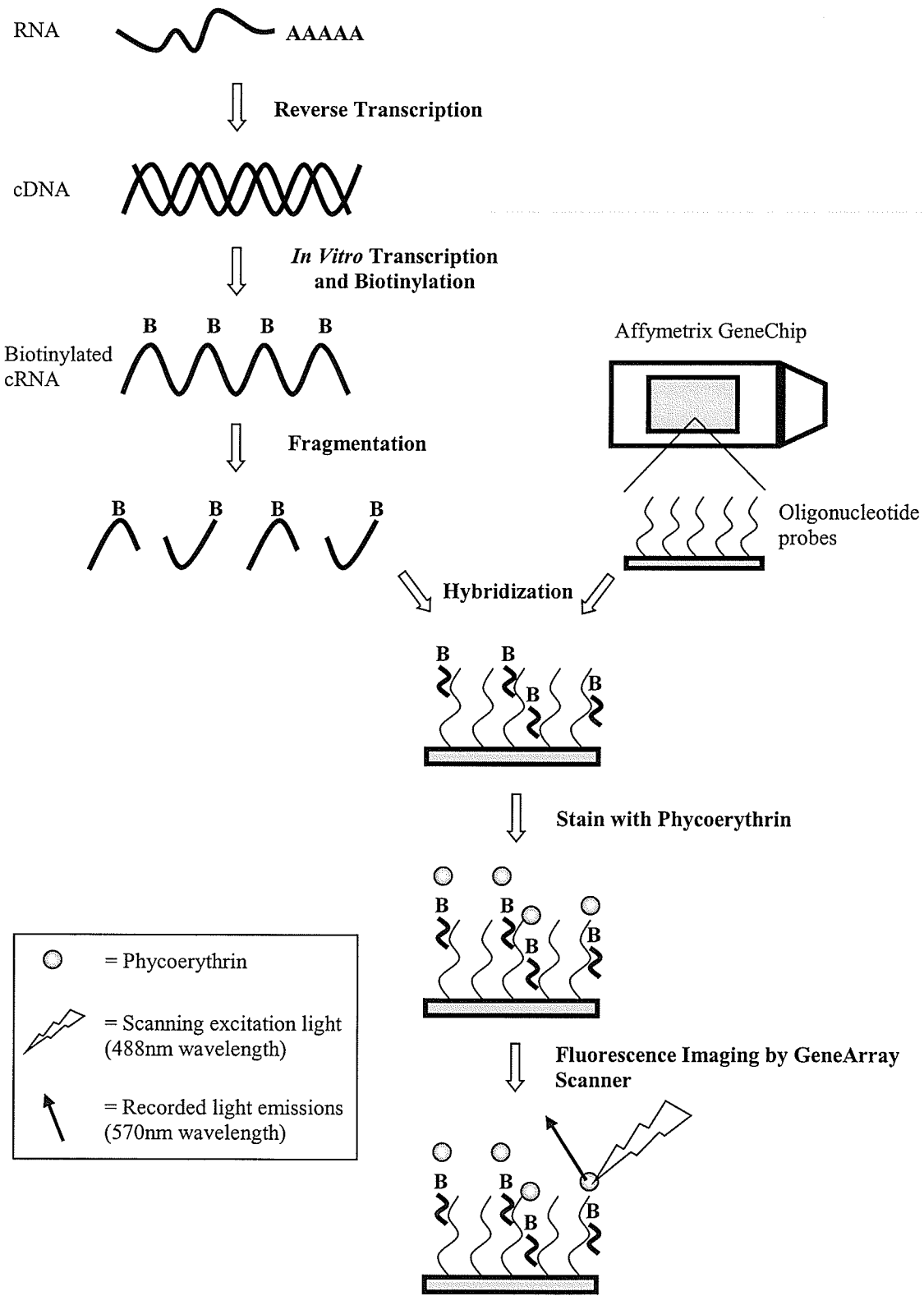

Figure 4 - Microarray analysis flow diagram.

1.4 Rationale and Hypotheses

The *TLS* gene is translocated in several human cancers, including myxoid liposarcoma and acute myeloid leukemia; however, the exact cellular mechanisms involved in the initiation and progression of these cancers are unknown. Our lab has rationalized that the best approach to determine the role of TLS in the development of cancer is to first characterize its normal cellular function. While its multiple functional motifs, nuclear cellular localization and ability to bind various nucleic acids undoubtedly support a role in the regulation of gene expression, the normal cellular functions of the TLS protein are largely undefined.

Our hypothesis is that TLS specifically modulates NF-κB-directed gene expression in response to DNA damage. In our model, TLS is loaded directly onto the promoters of specific NF-κB target genes, either through direct DNA-binding or by interacting with the NF-κB protein itself. Once loaded onto the promoter, TLS can modulate NF-κB-directed gene expression. We also hypothesize that improper expression of these candidate target genes will contribute to the phenotypes observed in both our TLS deficient mice and cells if they are indeed dependent on TLS for proper gene expression. To test our hypotheses directly, we first required the identification of bona fide TLS-dependent target genes. Here we have demonstrated that NF-κB-directed gene expression of reporter genes is TLS-dependent *in vivo*, and secondly, have performed microarray analysis experiments to identify endogenous TLS-dependent NF-κB candidate genes. The identification of these candidate genes will allow us to determine the molecular mechanisms involved in TLS' role in the regulation of gene expression.

Chapter 2: Materials and Experimental Methods

2.1 Cell Culture

2.1.1 General Maintenance of Mammalian Cells

Mammalian cells were cultured on treated, non-pyrogenic polystyrene tissue culture plates (Corning Incorporated) and maintained at 37°C in 6.0% CO_2 in a humidified incubator. Mouse embryonic fibroblasts (MEF) and 293T cells were cultured in Dulbecco's Modified Eagle Medium (DMEM) and supplemented with 1% Sodium Pyruvate, 1% Gluta MAX-1, and 1% Penicillin-Streptomycin (GIBCO (Grand Island Biological Co.) – Invitrogen Incorporated 100X stock solutions) and 10% Bovine Growth Serum (BGS) (Hyclone). MEF cells were derived from day E14.5 mouse embryos, as described[4]. Mouse pre-B cells were cultured in suspension in Roswell Park Memorial Institute (RPMI)-1640 media with L-glutamine (GIBCO; cat. #12-702F) and supplemented with 10% BGS, 50 μM 2-Mercaptoethanol, 1% Sodium Pyruvate, 1% Gluta MAX-1, and 1% Penicillin-Streptomycin.

Cultured cells were monitored daily and passaged when >70% confluence was reached. Typically, cells were washed with PBS buffer (135 mM NaCl, 8 mM $Na_2HPO_4 \cdot H_2O$, 3 mM KCl, 2 mM KH_2PO_4, pH 7.4) prior to splitting 1/10 into fresh media. Cells were detached from the culture plates by treatment with 0.05% Trypsin-EDTA (GIBCO) for 2 min at 37°C followed by addition of 2 ml fresh media to inhibit the enzyme. A record of passage history was maintained.

2.1.2 Cryopreservation

Aliquots of low passage cells were cryopreserved in culture media containing 12% DMSO, 50% BGS in DMEM for MEFs (RPMI for pre-B cells). Typically, 10^6 cells were suspended in 1 ml of cryopreservation media, aliquoted into CryoTube vials (NUNC) and cooled at a controlled rate of 1°C/min. Cells were stored for short term at -80°C and in liquid nitrogen for long term storage. To reanimate cryopreserved cells, vials were quickly brought to 37°C and added to increasing volumes of prewarmed cell culture media to avoid hypotonic shock.

2.2 DNA Molecular Cloning

2.2.1 Preparation and Transformation of E. coli cells

Bacterial DH5α (*E. coli*) cells were routinely maintained on Luria-Bertani (LB)-agar plates (10 g Tryptone, 5 g yeast extract, 5 g NaCl, and 1 ml of NaOH in 1 litre of H_2O plus 15 g agar) or grown in suspension in LB broth (same as plates minus the agar). Transformed colonies were selected by culture on plates containing antibiotics (50-100 μg/ml of ampicillin or kanamycin).

To prepare competent DH5α cells, cloned colonies from LB plates were picked with sterile toothpicks, inoculated into 2 ml of LB broth and incubated overnight at 37°C with shaking. Typically, a subculture was inoculated and cultured to an OD_{590} of 0.400 and was then placed on ice. Cells were aliquoted into microfuge tubes and centrifuged at 4°C for 5 min at 3000 rpm in a desktop microfuge. Pellets were resuspended in cold 30 mM $CaCl_2$ and centrifuged again (as above). Cell pellets were resuspended in fresh 30 mM $CaCl_2$, aliquoted and quickly frozen at -80°C.

Frozen competent DH5α cells were quickly thawed and aliquoted into 50 µl transformation reactions. Typically, 10 ng of plasmid DNA was added directly to the cells, snap mixed and left on ice for 30 min. Samples were heat shocked at 42°C for 2 min followed by the addition of 1 ml of LB broth for recovery at 37°C for 60 min. A 200 µl aliquot was transferred onto LB agar plates (with antibiotic resistance) and incubated overnight at 37°C to achieve growth of well isolated colonies. Single colonies were picked and expanded in 2 ml of fresh media for plasmid DNA preparations.

2.2.2 Isolation, Quantification and Verification of Plasmid DNA

Individual colonies of transformed cells, as selected for by antibiotic resistance, were picked using sterile toothpicks, inoculated in 4 ml of LB-antibiotic broth and incubated for 8 h at 37°C. The starter culture was then diluted 1:100 in fresh media and incubated at 37°C for 16 h. Isolation of plasmid DNA was performed using Plasmid Maxi-Kits from QIAGEN as per the manufacturer's instructions.

DNA preparations were diluted in sterile H_2O and concentrations were determined by taking the absorbances (A) at 260 nm using an UltroSpec 2000 UV/visible spectrophotometer (Amersham Pharmacia Biotech). Concentrations were calculated in µg/µl using the following equation:

$$\frac{(A_{260}\text{ value}) \times (\text{dilution factor}) \times 50\ (\text{absorbance of } 1 = 50\ \mu g/ml\ \text{of dsDNA})}{1000}$$

Restriction endonuclease (New England BioLabs) digestions were performed to verify that the correct plasmid was amplified. Briefly, this was achieved by the selection

and use of restriction endonucleases to yield unique and predictable DNA digestion fragments. DNA fragments were typically separated on a 1% agarose gel in 1 × TAE buffer (50 × TAE buffer is 2 M Tris base, 5.71% v/v glacial acetic acid, 50 mM EDTA) with 0.1 μl/ml of ethidium bromide stock solution (10 mg/ml) by electrophoresis at approximately 13 V/cm for 30-60 min. DNA fragment lengths were determined by visualization on a Gene Genius Bioimaging System in comparison with a control 1 kb ladder marker standard (New England BioLabs). Imaging and analysis (when required) was performed using Gene Snap software (Syngene).

2.3 Luciferase Reporter Gene Assay

2.3.1 Transient Transfections

Transient transfections were performed in triplicate by the calcium phosphate precipitation procedure[121,122] and transfectants were analyzed at 24 h. Briefly, 10^5 cells were cultured in 6-well plates and transfected at 30-50% confluency to ensure maximal transfection efficiency. Cells were transfected with 2 μg of the pGL2B or pGL2B-3κb reporter constructs (Promega). To normalize luciferase measurements of individual samples for transfection efficiency, cells were co-transfected with 1 μg of pcDNA3.1-lacZ. A total of 2 μg of expression and control (empty vector) constructs were transfected for exogenous protein expression experiments. These expression constructs consisted of: **1**. pCMV4 and NF-κB expression vector (pCMV4-p65) were generous gifts from Dr. Dean Ballard from the Vanderbilt University Medical Center in Nashville, Tennessee. **2**. pCMV-tag1 and the TLS expression vector (pCMV-tag1-

TLS)(Stratagene). Full length TLS cDNA from a pACT2 human fetal liver library was cloned into the pCMV-tag1 vector (K. Cann of the University of Manitoba).

DNA constructs were added to sterile tubes followed by the addition of 100 µl of HEPES buffered saline (HBS; 4 g NaCl, 2.5 g HEPES, 0.179 g KCl, 0.052 g $Na_2HPO_4 \cdot H_2O$, pH 7.1). The addition of 100 µl of 2.5 M $CaCl_2$ (in 10mM HEPES) was added dropwise to the contents of the tube while gently mixing (modified from[121,122]). The contents were immediately transferred to the cell media of the appropriate well of cells and incubated for 8 h at 37°C followed by washes with PBS buffer and the addition of fresh media. After a 24 h incubation at 37°C, transiently transfected, low passage MEFs were treated with 10 ng/ml of mouse Tumor Necrosis Factor-alpha (TNF-α) (Sigma-Aldrich) for 0, 2, 4, or 6 h and assayed as described in the next section.

2.3.2 Luciferase Reporter Assay

Transiently transfected cells were analyzed for NF-κB-directed transcriptional activation using the Luciferase Assay System (Promega). Briefly, cells were washed with PBS prior to lysis with Cell Culture Lysis Reagent (Promega). Lysates were manually scraped from the culture plates and transferred to microfuge tubes. To remove cellular debris, cell lysates were vortexed, centrifuged for 20 seconds at 12000 rpm at room temperature (RT) and the supernatants were transferred to new microfuge tubes. In 96 well clear, flat bottomed culture plates (Costar - Corning Incorporated), 20 µl of supernatant was mixed with 100 µl of Luciferase Assay Reagent (Promega). Luciferase levels were promptly measured using a luminometer (Molecular Devices Lmax) and analyzed with SOFTmaxR software (version 1.1L).

Variations in transfection efficiency were normalized to β-galactosidase activity from co-transfected expression vectors. Briefly, 20 µl of lysate supernatant was added to 600 µl of Z buffer (15 mM $Na_2HPO_4 \cdot 7\ H_2O$, 10 mM $NaH_2PO_4 \cdot H_2O$, 2.5 mM KCl, 0.25 mM $MgSO_4 \cdot 7\ H_2O$, pH to 7.0), fresh dithiothreitol (DTT) (2 mM), 1 mg/ml of o-nitrophenyl β-D-galactopyranoside (ONPG) (Sigma) and incubated at 37°C until the color of the mixture turned yellow. Reactions were terminated with 300 µl of Na_2CO_3 (1 M) and absorbances were measured at 405 nm on a spectrophotometer.

2.4 Immunohistochemistry

2.4.1 Cell Treatment and Fixation

Mouse pre-B cells (10^5) in log phase were exposed to 2.5 Gy of ionizing radiation from a ^{137}Cesium source (GammaCell 1000 – University of Manitoba). Treated cells were then seeded onto standard borosilicate microscope slides by centrifugation at 400 rpm for 7 min using a Cytospin 4 centrifuge (ThermoShandon). Cells were fixed to the microscope slides with 4% paraformaldehyde in PBS for 30 min at RT. Slides were then washed three times with PBS with 0.05% Triton-X 100 for 10 min with shaking before being incubated in a blocking buffer (5% BGS, 0.2% Triton-X 100, 0.02% Na azide, 0.1% BSA in PBS) for 2 h at RT with shaking. Fixed cells were either used immediately, or stored at 4°C for up to 2 days.

2.4.2 Immunohistochemistry

Fixed cells were incubated overnight at 4°C in a humidified chamber with a 1:25 dilution of the primary α-p65 NF-κB goat affinity-purified polyclonal antibody (8 µg/ml;

C-20 sc-372 from Santa Cruz Biotechnology, Inc) in blocking buffer. Slides were then washed three times in PBS with Triton-X 100 with shaking before being incubated with a 1:750 dilution of the secondary rabbit α-goat biotin-conjugated IgG antibody (1.5 mg/ml; BA-5000 from Vector Laboratories) for 2 h at RT. This was followed with three additional washes in PBS with Triton-X 100 for 10 min each with shaking and a 2 h incubation at RT with a 1:750 dilution of the tertiary streptavidin-fluorescein conjugate (1 mg/ml; SA-5001 from Vector Laboratories). Slides were again washed three times in PBS with Triton-X 100 for 10 min with shaking followed by a final wash with PBS. Slides were mounted with Vectashield mounting media with DAPI stain from Vector Laboratories.

2.4.3 Imaging and Analysis

Microscopy was carried out using a Leica DMRXA Widefield microscope and a Leica 63 × oil immersion lens (63 × /1.32-0.6 Oil). Digital Images were captured using a Retiga EXi Cooled Mono12-bit camera (QImaging) and Open Lab software (Improvision, ver 4.0.2).

2.5 Microarray Analysis

2.5.1 RNA Sample Preparation

Total RNA from 4×10^7 mouse pre-B cells was isolated using a Midi RNeasy RNA isolation kit (QIAGEN). Briefly, cells were lysed in a denaturing guanidine isothiocyanate buffer, added to ethanol and passed through a silica-gel-based membrane to isolate total cellular RNA. RNA concentrations were determined by measuring the

absorbance at 260 nm on the UltroSpec 2000 UV/visible spectrophotometer (Amersham Pharmacia Biotech) and calculated using the same formula described in section 2.2.2 for DNA quantification with the exception that A_{260} is multiplied by 40 (absorbance of 1 corresponds approximately to 40 μg/ml of RNA) instead of 50.

RNA was precipitated by adding 1/10 volume of 3 M sodium acetate at pH 5.2 and 2.5 volumes of ethanol, mixed well and centrifuged at 10000 g for 10 min at RT. Supernatants were aspirated and RNA pellets were washed three times in 1 ml of 80% ethanol followed by 1 min centrifugations at 10000 g. Pellets were air dried for 30 min and then resuspended in sterile H_2O to bring the sample to a final concentration of at least 2 μg/μl.

To determine whether samples were high quality and pure, RNA was elecrophoresed on a 1.2% formaldehyde agarose gel as described in the RNeasy Midi kit instruction manual (QIAGEN) and visualized to inspect the integrity of the 18S and 28S ribosomal RNA bands. The purity of the RNA samples was determined by calculating the ratio of the absorbances taken at 260/280 nm. Measured RNA sample ratios were all above 2.0 and therefore were determined to be acceptable.

2.5.2 Microarray Analysis

The preliminary expression microarray experiment was performed using Affymetrix Murine Genome Array MG_U74Av2 chips (http://www.affymetrix.com). These chips provided extensive coverage of approximately 12,000 mouse genes and expressed sequence tags (ESTs); and were provided to us as a generous gift from Dr. Tom Hudson of the Montreal Genome Centre (MGC) for the purpose of running the pilot

screen. The full microarray experiment was performed using Affymetrix GeneChip® Mouse Genome 430A 2.0 arrays. These particular chips utilize newly developed technology and provide the most updated and comprehensive coverage of approximately 39,000 mouse genes and expressed sequence tags (ESTs) on a single amalgamated array chip.

RNA samples (at least 20 μg total RNA/sample) were packaged on dry ice and delivered to the Montreal Genome Centre (MGC). Upon arrival, the samples were first reverse transcribed into cDNA, converted to cRNA and labeled with biotin. Labeled cRNA was then hybridized with our Affymetrix GeneChips (see above) and stained with a streptavidin phycoerythrin fluorescent conjugate. Hybridized chips were scanned for fluorescent signal intensities with an excitation light (488 nm wavelength) and recorded light emissions (570 nm) were then measured with a GeneArray Scanner. Raw data, in the form of fluorescent signal intensities corresponding to gene expression levels, were available for download from the Montreal Genome Centre's microarray platform website.

2.5.3 Analysis and Visualization of Data

Raw microarray data for both the pilot screen and full micorarray experiment were normalized using the Affymetrix Microarray Analysis Suite 5.0 (MAS5)[123,124] and Robust Multiple-array averaging (RMA)[125] programs, respectively. Subsequent analysis of the normalized data was performed on identified genes that were differentially expressed at least 2.5-fold. In particular, known NF-κB target genes represented on Affymetrix GeneChips were identified using available resources ([97] and http://www.panomics.com/MA2010.cfm).

Microarray data of interest were visualized using several software packages including: Cluster / TreeView (http://rana.lbl.gov/EisenSoftware.htm)[126], GeneCluster 2.0 (available at http://www.broad.mit.edu/cancer/software/genecluster2/gc2.html)[127,128] and the Bioconductor/R software (available at http://www.bioconductor.org/)[129]. The Cluster/TreeView software was used both to normalize and visualize the raw micorarray data, whereas the GeneCluster 2.0 and Bioconductor/R software packages were used strictly for visualization of selected data.

2.6 Reverse Transcriptase-PCR amplification of Candidate Genes

2.6.1 Oligonucleotide Primer Design and Synthesis

For each target gene of interest (*TNFaip2*, *TNFrsf5*, *Ier3* and the control gene *ActB*) a gene specific primer was designed to anneal to the 3' untranslated region (UTR) for first strand synthesis. In addition, two primers specific to the flanking exonic regions within the coding sequence for each gene were designed for the second step cDNA amplification (Figure 5).

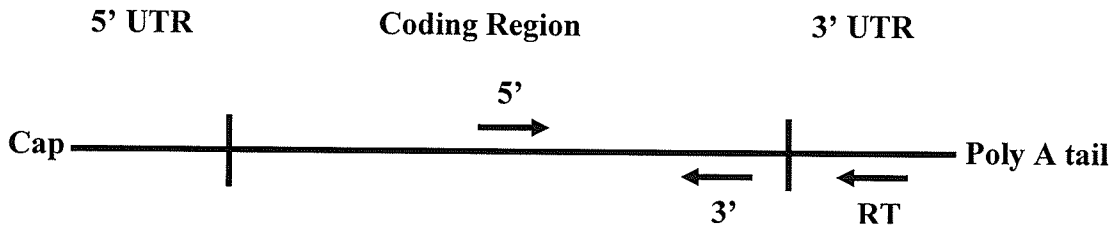

Figure 5. Strategy for oligonucleotide primer design for RT-PCR. Schematic diagram of a typical mRNA transcript. Reverse transcriptase (RT) primer, untranslated region (UTR).

For primer sequence selection, the Ensembl gene database was used to analyze the transcripts of the candidate target genes of interest to ensure that amplification primers were designed to amplify exons known not to be involved in alternate splicing. The amplification primers were designed to yield fragment sizes of roughly 300-500 base pairs in length and were 19-24 base pairs in length with approximate annealing temperatures of 53°C. Table 2 contains the sequences of the individual primers used in the RT-PCR experiments. All primers were synthesized by Invitrogen – Life Technologies.

2.6.2 Reverse Transcriptase – Polymerase Chain Reaction

First strand synthesis reactions were performed using 500 ng of starting RNA template that was isolated from mouse pre-B cells using the Mini RNeasy RNA isolation kit from QIAGEN as per the manufacturer's instructions. Briefly, reactions were performed using the Moloney Murine Leukemia Virus (M-MLV) reverse transcriptase enzyme (Invitrogen - Life Technologies). Gene specific oligonucleotide primers (2 pmoles) designed to hybridize to the 3' UTR regions of the target mRNA transcripts (section 2.6.1) were used in the reaction.

PCR reactions were performed using the DNA Engine DYAD – Peltier Thermal Cycler (MJ Research). Deoxynucleoside triphosphates (PCR grade, Boehringer Manheim) were used for both steps of RT-PCR. All other experimental conditions (i.e. temperatures, duration of incubation, etc.) used in the RT-PCR experiments were performed as recommended by the M-MLV manual that accompanied the enzyme. The Taq DNA polymerase enzyme (New England BioLabs; Cat. # M0273S) and gene-

specific amplification primers (final concentration of 10 μM) were used for cDNA amplification in the second step of the RT-PCR reaction.

The PCR amplification program used for all reactions was performed as follows: an initial denaturing step for 2 min at 94°C; followed by repeating cycles of denaturation for 20 s at 94°C, annealing for 30 s at 57°C, extension for 1 min at 72°C; followed by a final extension of 8 min at 72°C. The optimal annealing temperature was determined by performing temperature gradient experiments. The number of cycles

Table 2. Primer design and sequences.

Gene	Primer Name	Sequence (5' to 3' orientation)	Primer Location
TNFaip2	TNFaip2 RT	CAGATCTTGTTCCAGAGCCAG	3' UTR
	TNFaip2 5'	CTGAAGCCGCTGTTTAAGAAG	Exons 7-8
	TNFaip2 3'	CACTGCTTGGTAGATTGCCC	Exon 11
TNFrsf5	CD40 RT	CACTGGGCTCTGTCTTGGC	3' UTR
	CD40 5'	GAAGCCGACTGACAAGCCAC	Exon 3
	CD40 3'	CTGATTGGAGAAGAAGCCGAC	Exon 5
Ier3	Ier3 RT	CAGGTACCCATCCATGGTGC	3' UTR
	Ier3 5'	TGCCACTCGCGCAACCATCTCCAC	Exon 1
	Ier3 3'	GAAGGCCGCCGGATGTTGCTGGAG	Exon 2
ActB	ActB RT	GGTACCACCAGACAGCACTG	3' UTR
	Actb 5'	TACAATGAGCTGCGTGTGGC	Exon 3
	ActB 3'	ATAGCTCTTCTCCAGGGAGG	Exon 4

needed to ensure that PCR products remain in the linear phase of amplification was determined for each individual gene transcript. For example, the amplification of ActB cDNA was tested over a range of 17-25 cycles. Quantification of the PCR bands (section 2.6.3) revealed that 22 cycles was still in the linear phase for ActB amplification.

2.6.3 Visualization and Quantification of RT-PCR Products

RT-PCR products were resolved on 1% TAE agarose gels (section 2.2.2). Gels were visualized using the Gene Genius Bioimaging System and recorded with Gene Snap software (Syngene). The GeneTools feature of the Gene Snap package was used to quantify the band intensities of the PCR reactions. The Manual Band Quantification analysis option was selected to manually highlight each PCR band. A sample of the background was also taken and subtracted from the measured band intensities. Quantification was performed by dividing each band by its corresponding Actin B (ActB) control band for the same experimental conditions. Quantified band intensities were subsequently visualized graphically using Microsoft Excel 2003.

2.7 Candidate Promoter Sequence Analysis

The promoters for the *TNFaip2* (-1637 to +1) and *TNFrsf5* (-1621 to +1) genes were analyzed using the TFSearch transcription factor prediction software (http://www.cbrc.jp/research/db/TFSEARCH.html)[130]. Putative NF-κB binding sites were predicted based on sequence homology to the consensus NF-κB-binding sequence GGGACTTTCC[131]. Manual analysis of these same promoters yielded potential TLS-binding sites based on high sequence identity with the known TLS-binding 21bp double-

stranded DNA oligonucleotide[14]. Binding sites were deemed to be potential TLS-binding sites if the promoter sequences shared at least 80% identity to the 21bp sequence within a segment of 7-12 consecutive nucleotides (i.e. 6 of 7 base pairs match (85.7%) or 10 of 12 base pairs (83.3%)). Transcription factors are known to bind short degenerate sequences in the range of 6-20 base pairs[132]. As such, potential TLS-binding sites were required to have at least 6 matched base pairs to be deemed a putative binding site.

Chapter 3: Results

3.1 TLS is coactivator of NF-κB-mediated gene expression *in vitro*

To examine whether TLS has the potential to modulate the transcriptional activity of NF-κB, we investigated whether exogenous expression of TLS would enhance NF-κB-directed gene expression in human embryonic kidney 293T cells. Our first objective was to confirm NF-κB-mediated activation of the luciferase reporter gene from an NF-κB-responsive element called 3κB. This element is comprised of three adjacent NF-κB consensus binding sequences. Exogenous expression of the p65 protein, which has been demonstrated to activate NF-κB intracellularly[133], was used to induce an NF-κB activation response in our experiments. The 3κB reporter construct was transiently transfected into 293T cells along with increasing amounts of the pCMV4-p65 expression vector. As expected, luciferase reporter levels were upregulated between 2.5- to 6-fold upon transient transfection of the p65 construct (500 ng and 2 μg, respectively) (Figure 6).

Once we had established the conditions for our NF-κB-induced luciferase reporter system, we proceeded to investigate the effect of exogenous TLS expression on this experimental model (Figure 7). We did not observe an increase in transcription levels upon transfection of increasing amounts of the TLS expression construct alone (lanes 3-6). However, upon cotransfection of both TLS and p65 (1μg each), we observed an 8-fold induction of transcription (lane 8), nearly 2 times greater than the p65-alone -induced expression levels (lane 7). Our results support previously published reports supporting a role for TLS as a coactivator of NF-κB-mediated transcriptional regulation[6].

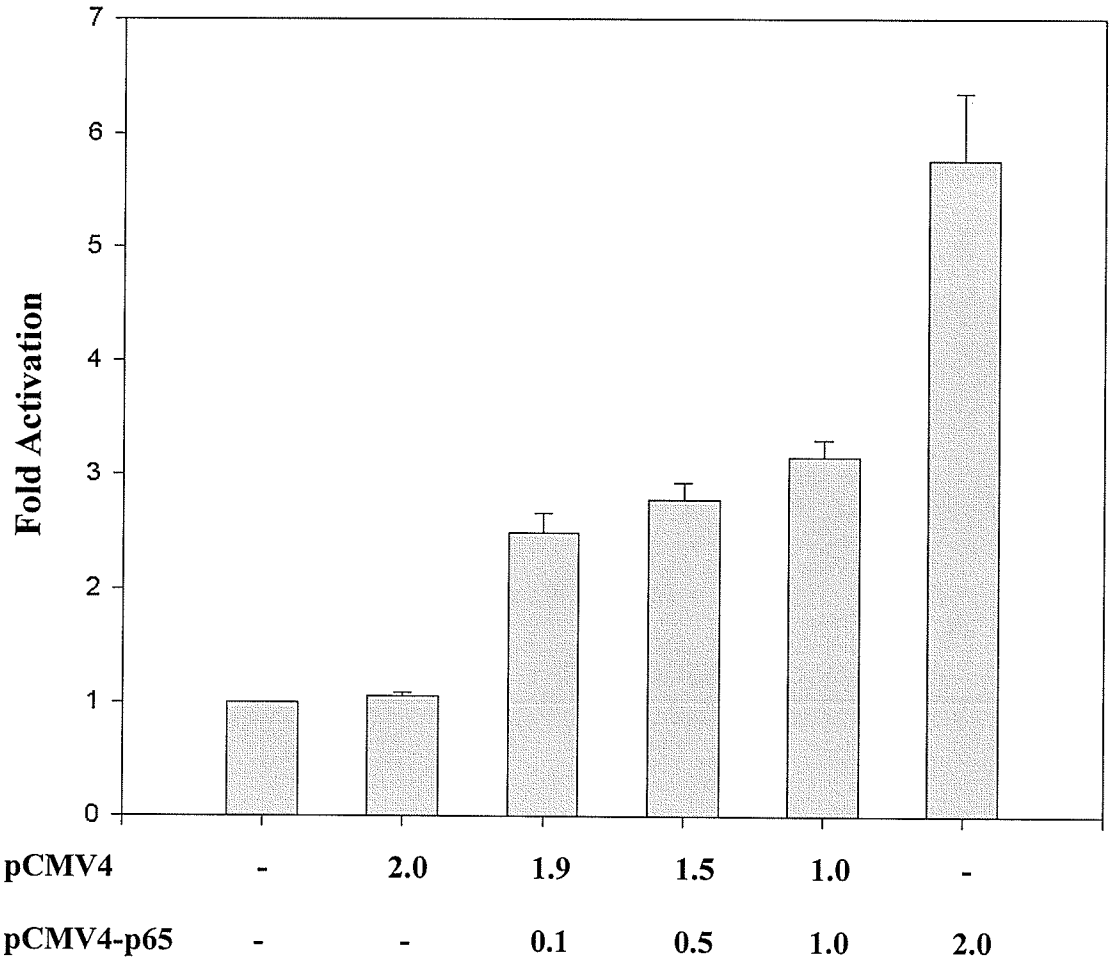

Figure 6. The p65 subunit of NF-κB upregulates *in vitro* luciferase reporter gene levels from an NF-κB-responsive element . Human embryonic kidney 293T cells were transiently transfected with the pGL2B-3κb reporter construct with increasing amounts of the pCMV4-p65 construct (μg). The pCMV4 vector was used to keep the total amount of transfected DNA constant at 2 μg as required. Fold activation values were determined from the means +/- standard error (S.E.) of three independent transfections each performed in triplicate.

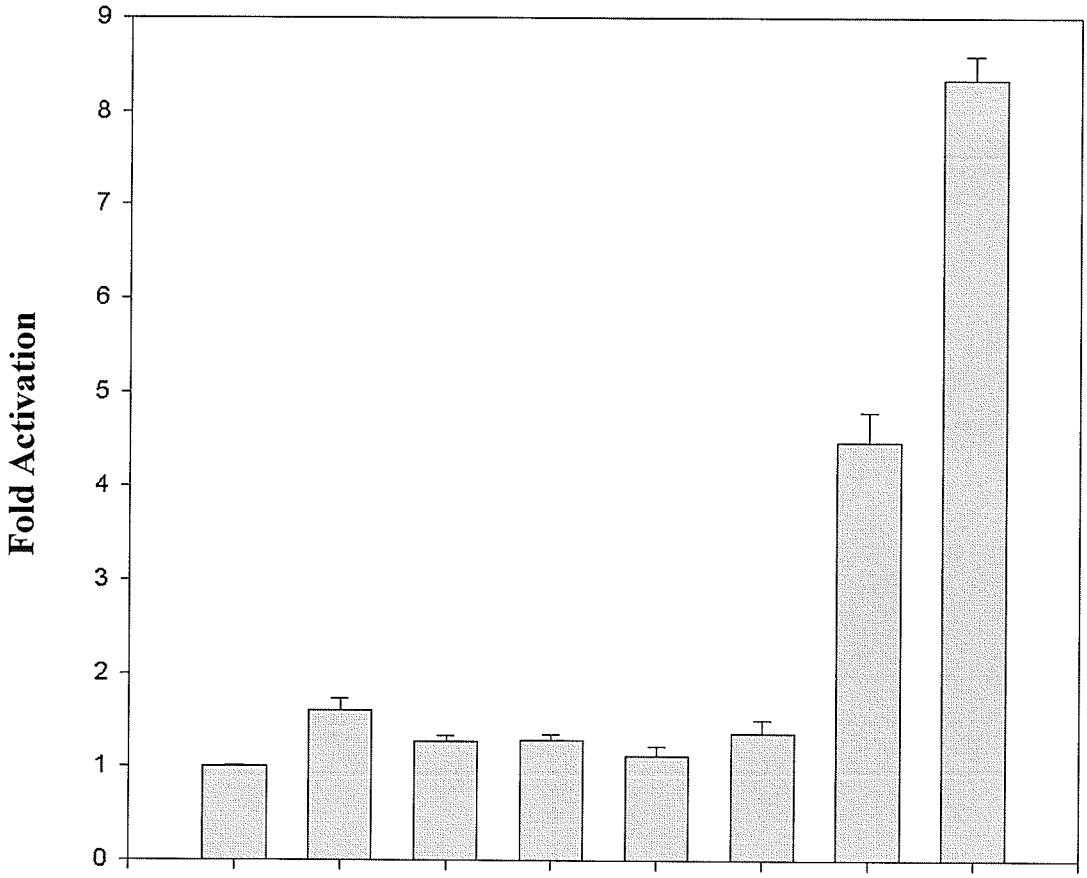

Figure 7. TLS enhances p65-directed luciferase reporter gene expression from an NF-κB-responsive element *in vitro*. Human embryonic kidney 293T cells were transiently transfected with the pGL2B-3kb reporter construct and varying amounts of the pCMV4-p65 and pCMV-tag1 constructs (μg). Fold activation values were determined from the means +/- S.E. of two independent transfections each performed in triplicate.

3.2 TNF-α-induced activation of endogenous NF-κB is impaired in TLS deficient mouse embryonic fibroblasts

Transient transfection assays are a powerful tool to assess the transcriptional activation potential of exogenously expressed proteins; however, it is often difficult to predict the physiologically relevant interactions of their respective endogenously expressed counterparts. To study TLS' role in the regulation of endogenous NF-κB-directed gene expression, we compared luciferase reporter levels between wild type and TLS deficient (TLS -/-) primary mouse embryonic fibroblasts (MEFs) in response to a physiological inducer of NF-κB. In contrast to our initial experiments (section 3.1), which involved the exogenous overexpression of both TLS and p65, the primary cells used in this experiment were transfected solely with the 3κB reporter construct, allowing us the advantage of studying a more physiologically relevant experimental system. To induce activation of NF-κB, we treated both wild type and TLS -/- reporter transfected MEF cells with 10 ng/μl of tumor necrosis factor-alpha (TNF-α) prior to the measurement of luciferase reporter levels (0, 2, 4, and 6 h).

Our results clearly demonstrate an impairment of TNF-α-induced NF-κB activation in primary TLS -/- MEF cells, as compared to wild type cells (Figure 8). After 2 h of TNF-α treatment, an approximate 7.0-fold reduction in transcriptional activation from the 3κB element, in TLS -/- versus wild type MEFs, was observed. At 4 h, the difference in activation levels was slightly lower at approximately 5.6-fold, whereas after 6 h, expression levels differed by as much as 7.6-fold. These findings demonstrate that endogenous TLS appears to be an essential cofactor for TNF-α-induced NF-κB-directed gene expression in primary MEF cells.

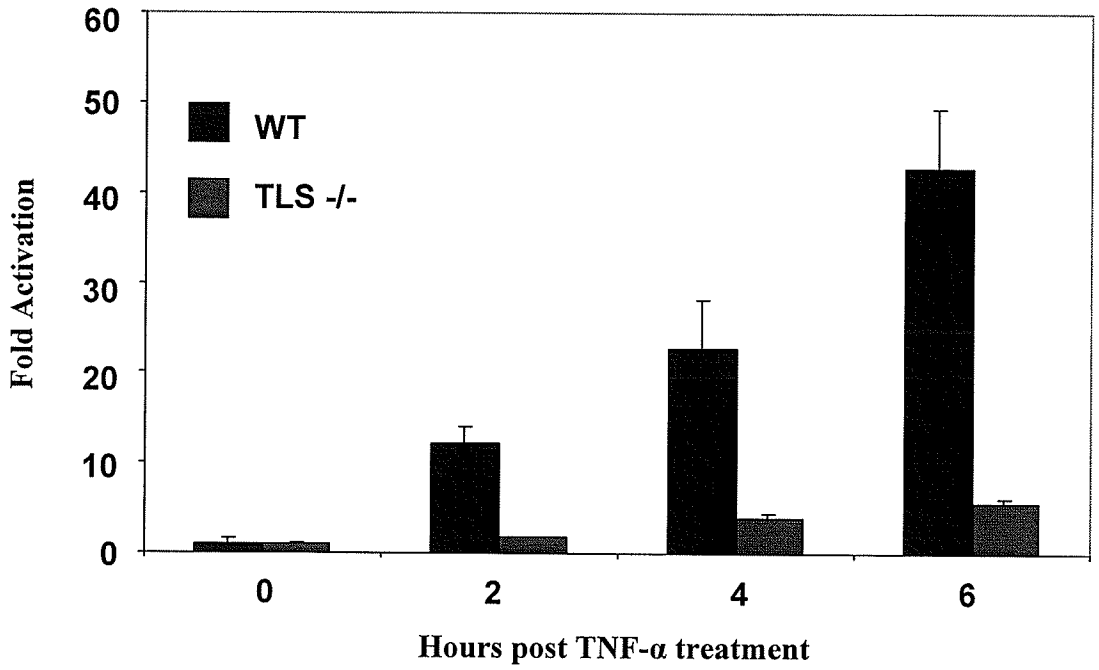

Figure 8. TNF-α-induced activation of endogenous NF-κB is impaired in TLS deficient MEF cells. Primary mouse embryonic fibroblasts (MEFs) were transiently transfected with the pGL2B-3κb reporter construct (2 μg) and treated with TNF-α (10 ng/ml) prior to analysis (0, 2, 4, 6 h). Fold activation values were determined from the means +/- S.E. of two independent transfections each performed in triplicate.

3.3 Ionizing radiation-induced activation of NF-κB is intact in TLS -/- mouse pre-B cells

Once we had established that TLS was involved in the modulation of NF-κB-directed gene expression *in vitro*, we wished to focus our efforts on the identification of TLS-dependent NF-κB target genes. Our first objective was to select an experimental model system (i.e. cell type and inducer of NF-κB) to perform microarray expression studies for the identification of the target genes. We selected an alternate model system to the TNF-α-induction of NF-κB that we used for our luciferase reporter assays in the MEF cells for two reasons. Firstly, we determined that the MEF cells, which are relatively difficult to maintain in culture, were not ideal for the large-scale nature of the

microarray analysis experiments. Secondly, we wished to determine whether TLS' modulation of NF-κB-directed gene expression was a more universal mechanism or specific only to the MEF cells.

We had previously observed a defective apoptotic response in TLS -/- mouse pre-B cells upon treatment with ionizing radiation (section 1.1.2). The NF-κB protein is known to be activated by ionizing radiation[5] and is a key regulator of apoptosis[96]. For these reasons, we chose to utilize IR-induced activation of NF-κB-directed gene expression in pre-B cells as our experimental model system. In addition, we determined that the pre-B cells, which proliferate very rapidly and are uniform in culture, were more suitable for the large-scale culturing demands of microarray analysis than the MEFs.

To ensure that potential defects in NF-κB-directed gene expression were not due to intrinsic defects in NF-κB activation in TLS -/- mouse pre-B cells, we performed immunohistochemistry to observe the nuclear translocalization of the NF-κB protein upon activation by ionizing radiation. Wild type and TLS -/- pre-B cells were irradiated with a physiologically relevant dose of ionizing radiation (2.5 Gy)[134] and visualized 1 h later with a α-p65 (sc-372) antibody. Translocation of the p65 subunit of NF-κB, from the cytoplasm to the nucleus, was observed both in wild type (panel B) and TLS -/- (Panel D) pre-B cells upon treatment with ionizing radiation (Figure 9). Our results indicate that IR-induced activation of NF-κB is intact in our TLS -/- pre-B cells. From these results, we rationalized that any observed differential gene expression discovered in our microarray experiments could be attributed to the transcriptional activity of NF-κB, rather than a defect in its upstream activation pathway. With these findings, we

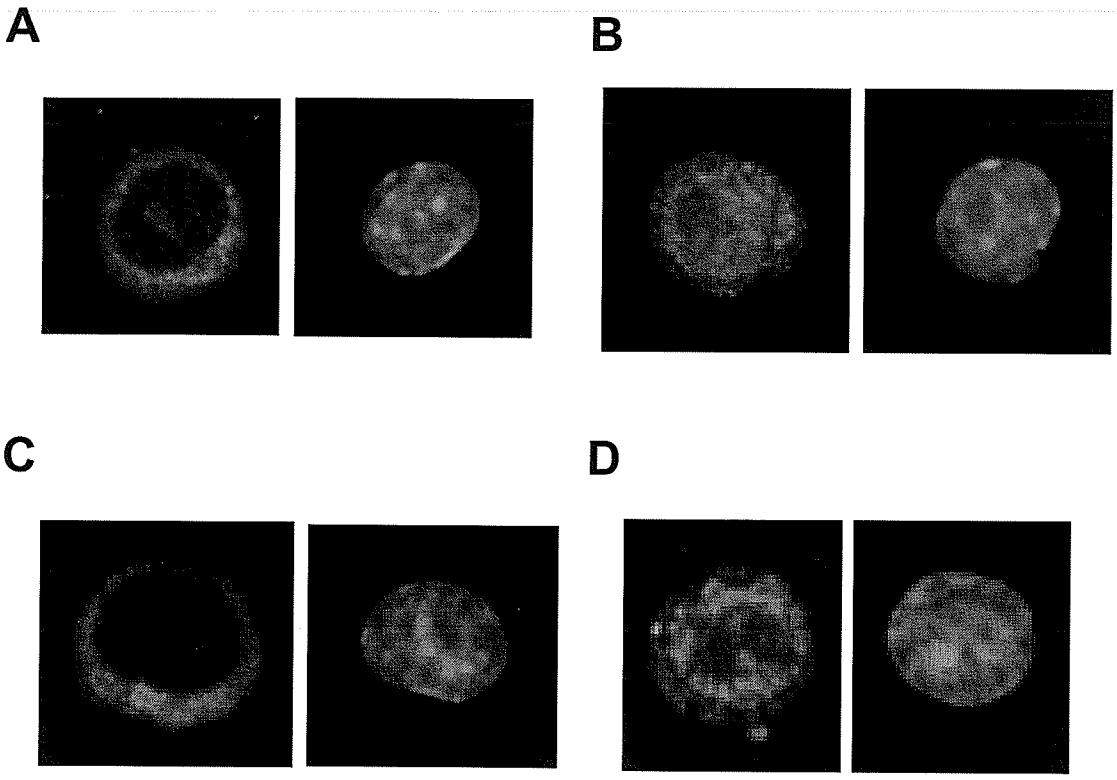

Figure 9. Ionizing radiation-induced activation of NF-κB is intact in TLS -/- mouse pre-B cells. Fixed cells were stained with goat α-p65 (sc-372) and visualized with secondary α-goat biotin followed by a strepta-vidin-fluorescein conjugate. (**A**) Untreated wild type cells. (**B**) Ionizing radiated wild type cells (1 h). (**C**) Untreated TLS -/- cells. (**D**) Ionizing radiated TLS -/- cells (1 h). Nuclear staining of all cells is displayed in the right panels with DAPI-staining.

proceeded to the microarray experiments to identify differentially expressed IR-induced NF-κB target genes between our wild type and TLS -/- pre-B cells.

3.4 Identification of ionizing radiation-induced NF-κB target genes differentially expressed between wild type and TLS deficient pre-B cells

To characterize TLS' role as a modulator of gene expression, we pursued the identification of TLS-dependent target genes. We rationalized that the best approach to determine TLS' function in NF-κB-directed gene expression was to identify NF-κB target genes that were differentially regulated upon induction in TLS deficient versus wild type cells. To accomplish this, we utilized microarray technology to simultaneously monitor thousands of genes for changes in gene expression. Before progressing to the microarray experiment, an initial pilot screen was performed to verify whether this approach could identify a subset of differentially regulated IR-induced NF-κB target genes that met our selection criteria.

3.4.1 Pilot screen

The initial pilot microarray experiment was designed to be a relatively rapid and inexpensive way to verify that we could observe IR-responsive NF-κB target genes that were differentially regulated in TLS -/- versus wild type mouse pre-B cells using Affymetrix Murine U74Av2 microarray GeneChips. These chips provided extensive coverage of approximately 12,000 mouse genes and expressed sequence tags (ESTs). Our samples consisted of single replicates of a control sample and two ionizing radiation time points (2 and 4 h post-ionizing radiation) for both wild type and TLS deficient pre-B

cells, resulting in a total of six samples (Table 3). The rationale behind the selection of the 2 and 4 h ionizing radiation time points will be discussed in section 3.4.2.

Table 3. Pilot microarray experimental samples and conditions.

Sample	Experimental Condition
1	Wild type untreated
2	Wild type 2h post-IR
3	Wild type 4h post-IR
4	TLS -/- 0h untreated
5	TLS -/- 2h post-IR
6	TLS -/- 4h post-IR

To ensure that RNA preparations were of high quality, experimental samples were resolved on a formaldehyde agarose gel and visually inspected for the integrity of the 18S and 28S ribosomal RNA (rRNA) bands (Figure 10). The integrity of our samples was also analyzed for purity by the Montreal Genome Centre using an Agilent Bioanalyzer. Our samples were determined to be of good quality by the Montreal Genome Centre's technical staff. To prepare mRNA samples for hybridization, the Montreal Genome Centre reverse transcribed the mRNA to cDNA, converted the cDNA to cRNA, labeled the cRNA, hybridized the labeled cRNA to the microarray chips and scanned the signal intensities to determine changes in gene expression, as described in detail in section 2.5.2.

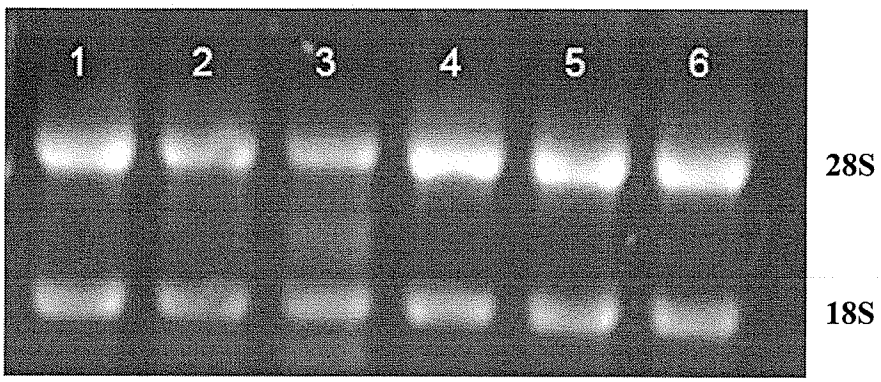

Figure 10. Quality verification of RNA preparations for pilot screen analysis. Bands represent 18S (lower) and 28S (upper) ribosomal RNA. Total cellular RNA was isolated from mouse pre-B cells using RNeasy mini kits (QIAGEN). RNA samples (1 μg) were electrophoresed on a 1.2% formaldehyde agarose gel. Lanes: (1) Wild type (WT) 0 h untreated. (2) WT 2 h post-ionizing radiation (IR). (3) WT 4 h post-IR. (4) TLS -/- 0 h untreated. (5) TLS -/- 2 h post-IR. (6) TLS -/- 4 h post-IR.

Genes that were differentially expressed between any two experimental samples were identified by comparing the average expression of each probe set to one another. The fluorescent signal intensities, which directly correlate to mRNA levels, of all genes represented on the U74Av2 microarray chip were graphically generated using Affymetrix Microarray Analysis Suite 5.0 (MAS5) scatterplots. Each dot on the scatterplot represents a direct comparison of gene expression levels of a single gene between two experimental conditions. Dots colored in green represent genes whose expression levels are deemed to be significantly different (at least 2.5 fold) between the conditions being compared (Figure 11). For further reference, the attached CD-ROM data disk (Appendix I) includes the complete set of scatterplots for the pilot microarray experiment (see Pilot screen/Scatterplots).

The expression levels of all genes could also be assigned quantitative values based on chip-to-chip analysis by the MAS5.0 software and presented in tabular form.

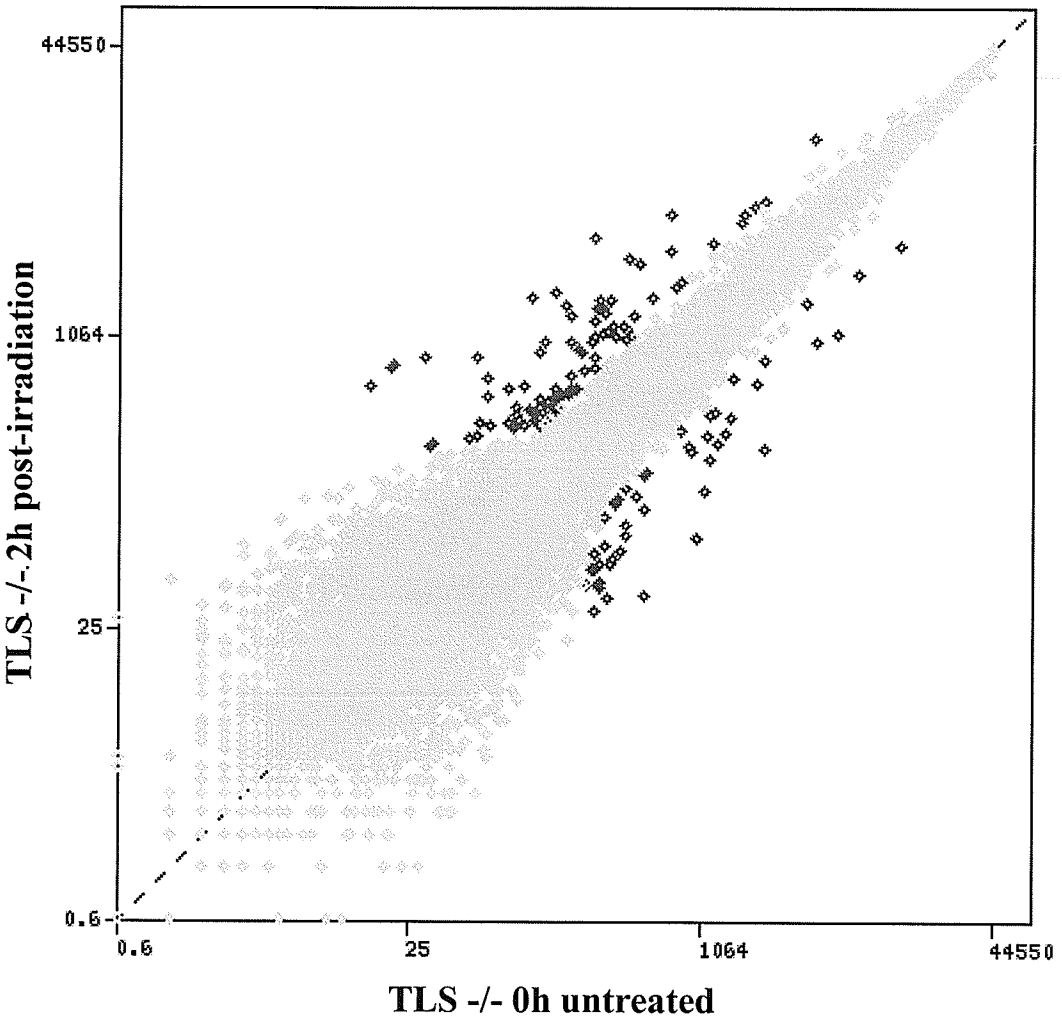

Figure 11. Determination of differentially expressed genes between untreated and ionizing radiated (2 h) TLS -/- pre-B cells from preliminary microarray data. Scatterplot indicates the average expression of each probe set from the TLS -/- 0 h untreated sample versus the TLS -/- 2 h post-ionizing radiation sample. Genes that were determined to be expressed significantly different between the two samples (at least 2.5-fold) are colored green. Numbers on axes indicate measured expression levels in the form of fluorescent signal intensities. Scatterplot was generated using Affymetrix Microarray Analysis Suite 5.0 software.

From pair-wise comparisons of chip data between experimental conditions, we were able to identify several unique IR-responsive genes. In wild type cells, we identified 62 such genes after 2 h of ionizing radiation (Table 4), while 145 genes were discovered after 4 h, as compared to control non-irradiated wild-type cells (Table 5). For TLS deficient cells, we observed 95 and 104 IR-induced genes after 2 (Table 6) and 4 h (Table 7) of ionizing radiation, respectively, as compared to control non-irradiated TLS –/– cells.

Upon identification of the IR-responsive genes, as described above, we were interested in determining whether IR-responsive NF-κB target genes were differentially expressed between wild type and TLS -/- pre-B cells. Of all IR-responsive genes that were identified (see Tables 4-7), we discovered that 15 were experimentally validated NF-κB target genes[97] (http://www.panomics.com/MA2010.cfm). Using the GeneCluster 2.0 software package, we generated an expression profile diagram, also referred to as a heat map, of the 15 IR-responsive NF-κB target genes (Figure 12).

The expression levels of the *TNFaip2* and *S100a6* genes, shown in the upper portion of the diagram, are induced in TLS -/- cells, whereas no expression was observed in wild type cells. The upper middle portion of the heat map (*Ier3, Ltb, Nfkbie, TNFrsf5, Nfkb2, Bcl2a1a* and *Tnf*) consists of genes with strong IR-induced expression levels in TLS -/- cells in comparison to weak induction levels found in the wild type cells. The lower middle section contains genes that have similar induction levels in response to ionizing radiation (*Icam1, JunB, Nfkbia, Gadd45b and RelB*). These five genes appear to be regulated in a TLS-independent manner. Finally, the *CD83* gene, found at the bottom of the diagram, is induced in wild type but not in TLS -/- cells.

Table 4. Ionizing radiation-responsive genes in wild type pre-B cells (2 h post-IR).

Downregulated genes 2 h post-IR (2.5Gy) in WT pre-B

Probename	Fold Change	Gene	Description
95728_g_at	-6.873	Apoa5	apolipoprotein A-V
99552_at	-6.650	Snai2	snail homolog 2 (Drosophila)
92512_g_at	-6.297	Aanat	arylalkylamine N-acetyltransferase
102374_at	-4.587	Dscr1l2	Down syndrome critical region gene 1-like 2
92969_at	-4.473	Ddr2	discoidin domain receptor family member 2
102300_at	-4.358	Rapsn	receptor-associated protein of the synapse
97830_at	-4.254	Pecam	platelet/endothelial cell adhesion molecule
102679_at	-4.191	Madcam1	mucosal vascular addressin cell adhesion molecule 1
99861_at	-4.143	Dhh	desert hedgehog
94429_at	-3.979	Eef1a2	eukaryotic translation elongation factor 1 alpha 2
102429_at	-3.930	Slc22al2	solute carrier family 22 (organic cation transporter)-like 2
94119_at	-3.887	Pip5k1c	phosphatidylinositol-4-phosphate 5-kinase type 1 gamma
161740_r_at	-3.817	Rag1	recombination activating gene 1
104555_at	-3.815	Myoz1	myozenin 1
160601_at	-3.804	Lfng	lunatic fringe gene homolog (Drosophila)
92639_at	-3.802	Stk6	serine/threonine kinase 6
100467_at	-3.148	Lyl1	lymphoblastomic leukemia
160821_r_at	-3.072	Ppp6c	protein phosphatase 6 catalytic subunit
104277_at	-2.970	Alg2	asparagine-linked glycosylation 2 homolog (yeast alpha-13-mannosyltransferase)
99899_at	-2.681	Ccr6	chemokine (C-C motif) receptor 6
160755_at	-2.670	Kif2c	kinesin family member 2C
101834_at	-2.553	Mapk3	mitogen activated protein kinase 3
102318_at	-2.535	Siat8d	sialyltransferase 8 (alpha-2 8-sialyltransferase) D

Upregulated genes 2 h post-IR (2.5Gy) in WT pre-B

Probename	Fold Change	Gene	Description
99392_at	28.791	Tnfaip3	tumor necrosis factor alpha-induced protein 3
97106_at	21.012	Map3k8	mitogen activated protein kinase kinase kinase 8
96752_at	12.601	Icam1	intercellular adhesion molecule
103980_at	12.322	Epha2	Eph receptor A2
94881_at	9.396	Cdkn1a	cyclin-dependent kinase inhibitor 1A (P21)
96515_at	8.479	Il4i1	interleukin 4 induced 1
100946_at	8.281	Hspa1a	heat shock protein 1A
98056_at	6.865	Phlda3	pleckstrin homology-like domain family A member 3
100631_r_at	6.520	Gstm5	glutathione S-transferase mu 5
102779_at	5.709	Gadd45b	growth arrest and DNA-damage-inducible 45 beta
161030_at	5.576	Scx	scleraxis
95356_at	5.123	Apoe	apolipoprotein E
102362_i_at	5.115	Junb	Jun-B oncogene
160895_at	4.993	Fancc	Fanconi anemia complementation group C
101727_at	4.734	Nfkbie	nuclear factor of kappa light polypeptide gene enhancer in B-cells inhibitor epsilon
93875_at	4.632	Hspa1a	heat shock protein 1A
161361_s_at	4.056	Tnnt1	troponin T1 skeletal slow
97740_at	4.044	Dusp16	dual specificity phosphatase 16
101554_at	3.850	Nfkbia	nuclear factor of kappa light chain gene enhancer in B-cells inhibitor alpha
103270_at	3.811	Gtse1	G two S phase expressed protein 1
102363_r_at	3.808	Junb	Jun-B oncogene
94891_s_at	3.801	Mea1	male enhanced antigen 1
104149_at	3.701	Nfkbia	nuclear factor of kappa light chain gene enhancer in B-cells inhibitor alpha
104155_f_at	3.628	Atf3	activating transcription factor 3
98110_at	3.620	Mdm2	transformed mouse 3T3 cell double minute 2
103091_at	3.590	Relb	avian reticuloendotheliosis viral (v-rel) oncogene related B
97681_f_at	3.543	Gstm3	glutathione S-transferase mu 3
160645_at	3.398	Birc2	baculoviral IAP repeat-containing 2
92908_at	3.393	Hivep1	human immunodeficiency virus type I enhancer binding protein 1

Table 4. continued

Upregulated genes 2 h post-IR (2.5Gy) in WT pre-B

Probename	Fold Change	Gene	Description
98067_at	3.368	Cdkn1a	cyclin-dependent kinase inhibitor 1A (P21)
97497_at	3.351	Notch1	Notch gene homolog 1 (Drosophila)
97264_r_at	3.301	Csnk1d	casein kinase 1 delta
103614_at	3.232	Nfkb2	nuclear factor of kappa light polypeptide gene enhancer in B-cells 2 p49/p100
93657_at	3.014	Spib	Spi-B transcription factor (Spi-1/PU.1 related)
96865_at	2.947	Marcks	myristoylated alanine rich protein kinase C substrate
101752_f_at	2.860	Igh-VJ558	immunoglobulin heavy chain (J558 family)
104533_at	2.848	Pim1	proviral integration site 1
96931_at	2.829	Mrp63	mitochondrial ribosomal protein 63
160127_at	2.828	Ccng1	cyclin G1
102906_at	2.807	Tgtp	T-cell specific GTPase
92666_at	2.721	Sh3bp1	SH3-domain binding protein 1
103483_at	2.696	Ercc5	excision repair cross-complementing repair deficiency complementation group 5
104046_at	2.630	Arih1	ariadne ubiquitin-conjugating enzyme E2 binding protein homolog 1

Table 5. Ionizing radiation-responsive genes in wild type pre-B cells (4 h post-IR).

Downregulated genes 4 h post-IR (2.5Gy) in WT pre-B

Probename	Fold Change	Gene	Description
94240_i_at	-24.683	Rpl29	ribosomal protein L29
92901_at	-13.402	Rara	retinoic acid receptor alpha
98559_at	-10.693	Smtn	smoothelin
92250_s_at	-7.347	Prcc	papillary renal cell carcinoma (translocation-associated)
102632_at	-5.877	Calmbp1	calmodulin binding protein 1
93985_at	-5.662	Tiparp	TCDD-inducible poly(ADP-ribose) polymerase
93320_at	-5.379	Cpt1a	carnitine palmitoyltransferase 1a liver
94748_g_at	-4.071	Csf2rb1	colony stimulating factor 2 receptor beta 1 low-affinity (granulocyte-macrophage)
92425_at	-4.060	Chd1l	chromodomain helicase DNA binding protein 1-like
99020_at	-4.059	Yy1	YY1 transcription factor
92766_at	-3.998	Hand1	heart and neural crest derivatives expressed transcript 1
100016_at	-3.987	Mmp11	matrix metalloproteinase 11
101865_at	-3.975	Pip5k2a	phosphatidylinositol-4-phosphate 5-kinase type II alpha
102759_at	-3.898	Pik3r2	phosphatidylinositol 3-kinase regulatory subunit polypeptide 2 (p85 beta)
160844_at	-3.789	Pts	6-pyruvoyl-tetrahydropterin synthase
94971_at	-3.749	Cdkn3	cyclin-dependent kinase inhibitor 3
95728_g_at	-3.724	Apoa5	apolipoprotein A-V
92755_f_at	-3.561	Sct	secretin
160463_at	-3.520	Myd116	myeloid differentiation primary response gene 116
93733_r_at	-3.323	Rgs19ip1	regulator of G-protein signaling 19 interacting protein 1
92483_g_at	-3.311	Fmnl	formin-like
97377_at	-3.222	Coil	coilin
96306_at	-3.153	Polr2i	polymerase (RNA) II (DNA directed) polypeptide I
160601_at	-3.089	Lfng	lunatic fringe gene homolog (Drosophila)
92969_at	-3.087	Ddr2	discoidin domain receptor family member 2
98489_at	-3.049	Hurp	hepatoma up-regulated protein
98580_at	-3.033	Ppm1a	protein phosphatase 1A magnesium dependent alpha isoform
103665_at	-3.009	Elovl6	ELOVL family member 6 elongation of long chain fatty acids (yeast)
98305_at	-2.914	Foxm1	forkhead box M1
100616_at	-2.890	Cenpa	centromere autoantigen A
160501_at	-2.881	Kif20a	kinesin family member 20A
103628_at	-2.856	Lef1	lymphoid enhancer binding factor 1
93670_at	-2.834	Erf	Ets2 repressor factor
96729_at	-2.819	Eif4ebp2	eukaryotic translation initiation factor 4E binding protein 2
92639_at	-2.814	Stk6	serine/threonine kinase 6
102833_at	-2.811	Cbx2	chromobox homolog 2 (Drosophila Pc class)
94332_at	-2.802	Ets1	E26 avian leukemia oncogene 1 5' domain
100424_at	-2.772	Ercc1	excision repair cross-complementing repair deficiency complementation group 1
160159_at	-2.756	Ccnb1	cyclin B1
94418_at	-2.732	Elovl6	ELOVL family member 6 elongation of long chain fatty acids (yeast)
160327_at	-2.708	Dctn6	dynactin 6
93878_at	-2.668	Mllt10	myeloid/lymphoid or mixed lineage-leukemia translocation to 10 homolog (Drosophila)
100885_at	-2.665	Nek2	NIMA (never in mitosis gene a)-related expressed kinase 2
102123_at	-2.646	Lip1	lysosomal acid lipase 1
96319_at	-2.629	Cdc20	cell division cycle 20 homolog (S. cerevisiae)
94294_at	-2.616	Ccnb2	cyclin B2
103957_at	-2.611	Trfr	transferrin receptor
160745_at	-2.597	Gcn5l2	GCN5 general control of amino acid synthesis-like 2 (yeast)
160352_at	-2.563	Pcbp4	poly(rC) binding protein 4
93403_at	-2.540	Atp2a3	ATPase Ca++ transporting ubiquitous
98969_at	-2.507	Abcd1	ATP-binding cassette sub-family D (ALD) member 1

Table 5. continued

Upregulated genes 4 h post-IR (2.5Gy) in WT pre-B

Probename	Fold Change	Gene	Description
95388_at	121.467	Hist1h1d	histone 1 H1d
92219_s_at	42.672	Mid1	midline 1
101587_at	22.661	Ephx1	epoxide hydrolase 1 microsomal
96515_at	22.513	Il4i1	interleukin 4 induced 1
96416_f_at	21.242	Hist1h3d	histone1 H3d
94202_at	16.656	Tcrb-V8.2	T-cell receptor beta variable 8.2
93834_at	13.540	Hist1h2bp	histone 1 H2bp
99392_at	12.510	Tnfaip3	tumor necrosis factor alpha-induced protein 3
103616_at	12.016	Col11a2	procollagen type XI alpha 2
93067_f_at	10.703	Hist2h2aa1	histone 2 H2aa1
96712_at	9.046	Smoc1	SPARC related modular calcium binding 1
103980_at	8.628	Epha2	Eph receptor A2
93380_at	8.365	Klrb1c	killer cell lectin-like receptor subfamily B member 1C
103022_at	7.999	Map3k1	mitogen activated protein kinase kinase kinase 1
92962_at	7.757	Tnfrsf5	tumor necrosis factor receptor superfamily member 5
160061_at	7.724	Il1rl1	interleukin 1 receptor-like 1 ligand
94141_at	7.634	Fcer2a	Fc receptor IgE low affinity II alpha polypeptide
93869_s_at	7.608	Bcl2a1a	B-cell leukemia/lymphoma 2 related protein A1a
98056_at	7.277	Phlda3	pleckstrin homology-like domain family A member 3
104268_at	7.180	Il6ra	interleukin 6 receptor alpha
93068_r_at	7.148	Hist2h2aa1	histone 2 H2aa1
94881_at	6.444	Cdkn1a	cyclin-dependent kinase inhibitor 1A (P21)
102914_s_at	6.378	Bcl2a1a	B-cell leukemia/lymphoma 2 related protein A1a
97763_at	6.273	Ncf1	neutrophil cytosolic factor 1
98873_at	6.105	Dlx4	distal-less homeobox 4
98067_at	6.085	Cdkn1a	cyclin-dependent kinase inhibitor 1A (P21)
95356_at	5.819	Apoe	apolipoprotein E
98784_at	5.766	Gpr12	G-protein coupled receptor 12
95540_r_at	5.758	Ddx27	DEAD (Asp-Glu-Ala-Asp) box polypeptide 27
93837_at	5.755	Hrg	histidine-rich glycoprotein
94988_at	5.652	Pten	phosphatase and tensin homolog
97224_at	5.575	Pnrc1	proline-rich nuclear receptor coactivator 1
103614_at	5.534	Nfkb2	nuclear factor of kappa light polypeptide gene enhancer in B-cells 2 p49/p100
160771_r_at	5.497	Ppfibp2	protein tyrosine phosphatase receptor-type F interacting protein binding protein 2
104483_at	5.419	Col9a1	procollagen type IX alpha 1
93221_at	5.313	Hoxd8	homeo box D8
160895_at	4.939	Fancc	Fanconi anemia complementation group C
101727_at	4.878	Nfkbie	nuclear factor of kappa light polypeptide gene enhancer in B-cells inhibitor
101723_r_at	4.752	Adam28	a disintegrin and metalloprotease domain 28
103483_at	4.586	Ercc5	excision repair cross-complementing rodent repair deficiencycomplementation
97965_at	4.528	Pla2g6	phospholipase A2 group VI
161361_s_at	4.336	Tnnt1	troponin T1 skeletal slow
98787_at	4.328	Kcnj11	potassium inwardly rectifying channel subfamily J member 11
161034_at	4.113	Pla2g10	phospholipase A2 group X
102578_at	4.112	Pax5	paired box gene 5
160127_at	4.098	Ccng1	cyclin G1
99931_at	4.079	Lama5	laminin alpha 5
100300_at	4.036	Cybb	cytochrome b-245 beta polypeptide
160577_at	3.999	Atp9a	ATPase class II type 9A
160645_at	3.935	Birc2	baculoviral IAP repeat-containing 2
96865_at	3.885	Marcks	myristoylated alanine rich protein kinase C substrate
93657_at	3.850	Spib	Spi-B transcription factor (Spi-1/PU.1 related)
103270_at	3.828	Gtse1	G two S phase expressed protein 1
99081_at	3.774	Serping1	serine (or cysteine) proteinase inhibitor clade G member 1
100946_at	3.767	Hspa1a	heat shock protein 1A

Table 5. continued

Upregulated genes 4 h post-IR (2.5Gy) in WT pre-B

Probename	Fold Change	Gene	Description
93875_at	3.761	Hspa1a	heat shock protein 1A
102940_at	3.712	Ltb	lymphotoxin B
92262_at	3.708	Wig1	wild-type p53-induced gene 1
103053_at	3.654	Myog	myogenin
101752_f_at	3.620	Igh-VJ558	immunoglobulin heavy chain (J558 family)
104020_at	3.588	Rap2b	RAP2B member of RAS oncogene family
92301_at	3.581	Ikbke	inhibitor of kappaB kinase epsilon
93472_at	3.577	Col5a1	procollagen type V alpha 1
103091_at	3.551	Relb	avian reticuloendotheliosis viral (v-rel) oncogene related B
92666_at	3.550	Sh3bp1	SH3-domain binding protein 1
95339_r_at	3.527	Mmp12	matrix metalloproteinase 12
160553_at	3.476	Ly6d	lymphocyte antigen 6 complex locus D
93744_at	3.439	Calm4	calmodulin 4
93078_at	3.438	Ly6a	lymphocyte antigen 6 complex locus A
96752_at	3.401	Icam1	intercellular adhesion molecule
99899_at	3.377	Ccr6	chemokine (C-C motif) receptor 6
94924_at	3.339	Prrg2	proline-rich Gla (G-carboxyglutamic acid) polypeptide 2
99629_at	3.330	Ei24	etoposide induced 2.4 mRNA
103040_at	3.321	Cd83	CD83 antigen
92356_at	3.259	Ptpn8	protein tyrosine phosphatase non-receptor type 8
93013_at	3.189	Idb2	inhibitor of DNA binding 2
97319_at	3.097	Rrad	Ras-related associated with diabetes
97497_at	3.095	Notch1	Notch gene homolog 1 (Drosophila)
100059_at	3.088	Cyba	cytochrome b-245 alpha polypeptide
97507_at	3.073	Ppicap	peptidylprolyl isomerase C-associated protein
98892_at	3.060	Lpin1	lipin 1
100439_i_at	2.921	Ank1	ankyrin 1 erythroid
96056_at	2.892	Arhc	ras homolog gene family member C
92471_i_at	2.844	Slfn2	schlafen 2
98839_at	2.822	Six2	sine oculis-related homeobox 2 homolog (Drosophila)
101046_at	2.815	Vim	vimentin
93536_at	2.800	Bax	Bcl2-associated X protein
160679_at	2.793	Kif1c	kinesin family member 1C
102014_at	2.775	Homer3	homer homolog 3 (Drosophila)
92371_at	2.713	Hrc	histidine rich calcium binding protein
104597_at	2.677	Gbp2	guanylate nucleotide binding protein 2
160133_at	2.669	Ltbp3	latent transforming growth factor beta binding protein 3
94986_at	2.658	Gng3	guanine nucleotide binding protein (G protein) gamma 3 subunit
93382_at	2.642	Pde1b	phosphodiesterase 1B Ca2+-calmodulin dependent
103215_g_at	2.631	Hspb2	heat shock protein 2
99134_at	2.577	Tcte3	t-complex-associated testis expressed 3
103796_at	2.571	Apaf1	apoptotic protease activating factor 1
100134_at	2.569	Eng	endoglin
102906_at	2.563	Tgtp	T-cell specific GTPase

Table 6. Ionizing radiation-responsive genes in TLS -/- pre-B cells (2 h post-IR).

Downregulated genes 2 h post-IR (2.5Gy) in TLS -/- pre-B

Probename	Fold Change	Gene	Description
100435_at	-12.841	Edg2	endothelial differentiation lysophosphatidic acid G-protein-coupled receptor 2
98471_f_at	-12.077	Kifc5a	kinesin family member C5A
93683_at	-9.417	Rag1	recombination activating gene 1
92504_at	-8.563	Hus1	Hus1 homolog (S. pombe)
161824_r_at	-8.457	Indo	indoleamine-pyrrole 23 dioxygenase
160601_at	-7.546	Lfng	lunatic fringe gene homolog (Drosophila)
102037_at	-6.358	Mapre2	microtubule-associated protein RP/EB family member 2
160553_at	-5.625	Ly6d	lymphocyte antigen 6 complex locus D
101855_at	-5.471	Mtap6	microtubule-associated protein 6
100467_at	-5.412	Lyl1	lymphoblastomic leukemia
104601_at	-5.354	Thbd	thrombomodulin
94521_at	-5.321	Cdkn2d	cyclin-dependent kinase inhibitor 2D (p19 inhibits CDK4)
102085_at	-4.910	Insm1	insulinoma-associated 1
100759_at	-4.852	Mrc2	mannose receptor C type 2
92639_at	-4.635	Stk6	serine/threonine kinase 6
102716_at	-4.315	Eya3	eyes absent 3 homolog (Drosophila)
161917_i_at	-4.044	Pnmt	phenylethanolamine-N-methyltransferase
100468_g_at	-3.842	Lyl1	lymphoblastomic leukemia
103201_at	-3.817	Ttk	Ttk protein kinase
102318_at	-3.797	Siat8d	sialyltransferase 8 (alpha-2 8-sialyltransferase) D
93099_f_at	-3.643	Plk	polo-like kinase (Drosophila)
103311_at	-3.474	Osbpl5	oxysterol binding protein-like 5
93285_at	-3.280	Dusp6	dual specificity phosphatase 6
160755_at	-3.043	Kif2c	kinesin family member 2C
92464_at	-2.897	Mknk1	MAP kinase-interacting serine/threonine kinase 1
92836_at	-2.801	Eln	elastin
99844_at	-2.800	Fzd9	frizzled homolog 9 (Drosophila)
92998_at	-2.671	Vav2	Vav2 oncogene
104010_at	-2.612	Zfp99	zinc finger protein 99
161740_r_at	-2.565	Rag1	recombination activating gene 1
103629_g_at	-2.527	Lef1	lymphoid enhancer binding factor 1
94821_at	-2.506	Xbp1	X-box binding protein 1

Upregulated genes 2 h post-IR (2.5Gy) in TLS -/- pre-B

Probename	Fold Change	Gene	Description
96515_at	37.614	Il4i1	interleukin 4 induced 1
99392_at	35.955	Tnfaip3	tumor necrosis factor alpha-induced protein 3
97106_at	35.862	Map3k8	mitogen activated protein kinase kinase kinase 8
100946_at	26.186	Hspa1a	heat shock protein 1A
96752_at	13.912	Icam1	intercellular adhesion molecule
102239_at	13.712	Bcl3	B-cell leukemia/lymphoma 3
103091_at	11.499	Relb	avian reticuloendotheliosis viral (v-rel) oncogene related B
102629_at	9.073	Tnf	tumor necrosis factor
101727_at	8.489	Nfkbie	nuclear factor of kappa light polypeptide gene enhancer in B-cells inhibitor epsilon
103849_at	7.947	Crkl	v-crk sarcoma virus CT10 oncogene homolog (avian)-like
102371_at	7.863	Nr4a1	nuclear receptor subfamily 4 group A member 1
101554_at	7.214	Nfkbia	nuclear factor of kappa light chain gene enhancer in B-cells inhibitor alpha
97740_at	6.931	Dusp16	dual specificity phosphatase 16
102362_i_at	6.911	Junb	Jun-B oncogene
94384_at	6.534	Ier3	immediate early response 3
93416_at	5.996	Tnfsf11	tumor necrosis factor (ligand) superfamily member 11
104149_at	5.680	Nfkbia	nuclear factor of kappa light chain gene enhancer in B-cells inhibitor alpha
101900_at	5.623	Cdkn2b	cyclin-dependent kinase inhibitor 2B (p15 inhibits CDK4)

Table 6. continued

Upregulated genes 2 h post-IR (2.5Gy) in TLS -/- pre-B

Probename	Fold Change	Gene	Description
93411_at	5.569	Sema7a	sema domain immunoglobulin domain (Ig) and GPI membrane anchor (semaphorin)
100962_at	5.310	Nab2	Ngfi-A binding protein 2
103614_at	5.136	Nfkb2	nuclear factor of kappa light polypeptide gene enhancer in B-cells 2 p49/p100
92962_at	5.046	Tnfrsf5	tumor necrosis factor receptor superfamily member 5
97745_at	4.962	Hoxa4	homeo box A4
104155_f_at	4.911	Atf3	activating transcription factor 3
99419_g_at	4.804	Bcl2l11	BCL2-like 11 (apoptosis facilitator)
102940_at	4.755	Ltb	lymphotoxin B
102363_r_at	4.581	Junb	Jun-B oncogene
101030_at	4.428	Arhb	ras homolog gene family member B
92908_at	4.066	Hivep1	human immunodeficiency virus type I enhancer binding protein 1
97319_at	3.993	Rrad	Ras-related associated with diabetes
103689_at	3.954	Abcc3	ATP-binding cassette sub-family C (CFTR/MRP) member 3
104428_s_at	3.934	Matk	megakaryocyte-associated tyrosine kinase
100022_at	3.876	Cish	cytokine inducible SH2-containing protein
160489_at	3.767	Tnfaip2	tumor necrosis factor alpha-induced protein 2
93753_at	3.730	Litaf	LPS-induced TN factor
104701_at	3.641	Bhlhb2	basic helix-loop-helix domain containing class B2
102779_at	3.617	Gadd45b	growth arrest and DNA-damage-inducible 45 beta
93657_at	3.600	Spib	Spi-B transcription factor (Spi-1/PU.1 related)
104614_at	3.549	Gpc1	glypican 1
104068_at	3.527	Strn4	striatin calmodulin binding protein 4
102860_at	3.507	Serpina3g	serine (or cysteine) proteinase inhibitor clade A member 3G
102636_at	3.417	Klc2	kinesin light chain 2
104156_r_at	3.330	Atf3	activating transcription factor 3
100298_at	3.282	Pspn	persephin
97794_at	3.192	Sema7a	sema domain immunoglobulin domain (Ig) and GPI membrane anchor (semaphorin)
94246_at	3.180	Ets2	E26 avian leukemia oncogene 2 3' domain
103248_at	3.162	Fkbp1b	FK506 binding protein 1b
93013_at	3.124	Idb2	inhibitor of DNA binding 2
94881_at	3.116	Cdkn1a	cyclin-dependent kinase inhibitor 1A (P21)
160818_at	3.082	Lrrfip2	leucine rich repeat (in FLII) interacting protein 2
92737_at	3.056	Irf4	interferon regulatory factor 4
98067_at	3.050	Cdkn1a	cyclin-dependent kinase inhibitor 1A (P21)
161067_at	2.912	Ifld2	induced in fatty liver dystrophy 2
93869_s_at	2.904	Bcl2a1a	B-cell leukemia/lymphoma 2 related protein A1a
92512_g_at	2.900	Aanat	arylalkylamine N-acetyltransferase
99384_at	2.854	Pim1	proviral integration site 1
93324_at	2.832	Zfp36l1	zinc finger protein 36 C3H type-like 1
93617_at	2.799	Ccrl2	chemokine (C-C motif) receptor-like 2
93875_at	2.784	Hspa1a	heat shock protein 1A
100024_at	2.752	Shrm	shroom
102376_r_at	2.725	Pcp2	Purkinje cell protein 2 (L7)
93958_at	2.649	Rnf14	ring finger protein 14
104531_at	2.645	Prkcd	protein kinase C delta
93425_at	2.631	Irf5	interferon regulatory factor 5
103959_at	2.610	Phf13	PHD finger protein 13
93218_at	2.595	Swap70	SWAP complex protein
93104_at	2.584	Btg1	B-cell translocation gene 1 anti-proliferative
160794_at	2.566	Smyd2	SET and MYND domain containing 2
98083_at	2.558	Copeb	core promoter element binding protein
101437_at	2.550	Stk2	serine/threonine kinase 2
160645_at	2.541	Birc2	baculoviral IAP repeat-containing 2

Table 7. Ionizing radiation-responsive genes in TLS -/- pre-B cells (4 h post-IR).

Downregulated genes 4 h post-IR (2.5Gy) in TLS -/- pre-B

Probename	Fold Change	Gene	Description
92671_f_at	-22.584	Rgl1	ral guanine nucleotide dissociation stimulator-like 1
98559_at	-9.759	Smtn	smoothelin
92300_at	-9.270	Mnt	max binding protein
92504_at	-5.858	Hus1	Hus1 homolog (S. pombe)
103629_g_at	-5.218	Lef1	lymphoid enhancer binding factor 1
93360_at	-5.014	Pmm1	phosphomannomutase 1
92449_at	-5.010	Gfra2	glial cell line derived neurotrophic factor family receptor alpha 2
92232_at	-4.815	Socs3	suppressor of cytokine signaling 3
103574_at	-4.692	Ablim1	actin-binding LIM protein 1
104276_at	-4.496	Glipr2	GLI pathogenesis-related 2
104370_s_at	-3.921	Krt2-6a	keratin complex 2 basic gene 6a
99880_at	-3.764	Rfx1	regulatory factor X 1 (influences HLA class II expression)
160601_at	-3.690	Lfng	lunatic fringe gene homolog (Drosophila)
93683_at	-3.679	Rag1	recombination activating gene 1
104712_at	-3.635	Myc	myelocytomatosis oncogene
102085_at	-3.626	Insm1	insulinoma-associated 1
160159_at	-3.495	Ccnb1	cyclin B1
95728_g_at	-3.232	Apoa5	apolipoprotein A-V
96331_at	-3.173	Snx2	sorting nexin 2
94418_at	-3.122	Elovl6	ELOVL family member 6 elongation of long chain fatty acids (yeast)
100467_at	-3.109	Lyl1	lymphoblastomic leukemia
101180_at	-3.088	Atm	ataxia telangiectasia mutated homolog (human)
103048_at	-3.060	Nmyc1	neuroblastoma myc-related oncogene 1
104735_at	-3.055	Kctd12	potassium channel tetramerisation domain containing 12
103514_at	-2.987	Tnfrsf21	tumor necrosis factor receptor superfamily member 21
93565_at	-2.981	Kns2	kinesin 2
94891_s_at	-2.964	Mea1	male enhanced antigen 1
104601_at	-2.949	Thbd	thrombomodulin
93321_at	-2.929	Ifi203	interferon activated gene 203
92666_at	-2.907	Sh3bp1	SH3-domain binding protein 1
100631_r_at	-2.856	Gstm5	glutathione S-transferase mu 5
103665_at	-2.853	Elovl6	ELOVL family member 6 elongation of long chain fatty acids (yeast)
98471_f_at	-2.803	Kifc5a	kinesin family member C5A
101868_i_at	-2.785	H2-DMb1	histocompatibility 2 class II locus Mb1
160970_at	-2.776	Odf2	outer dense fiber of sperm tails 2
160553_at	-2.731	Ly6d	lymphocyte antigen 6 complex locus D
97963_at	-2.704	Sipa1	signal-induced proliferation associated gene 1
102779_at	-2.687	Gadd45b	growth arrest and DNA-damage-inducible 45 beta
160755_at	-2.653	Kif2c	kinesin family member 2C
100468_g_at	-2.645	Lyl1	lymphoblastomic leukemia
94971_at	-2.640	Cdkn3	cyclin-dependent kinase inhibitor 3
94390_at	-2.640	Akap8	A kinase (PRKA) anchor protein 8
103585_at	-2.637	Spg4	spastic paraplegia 4 homolog (human)
93895_s_at	-2.606	Itpr1	inositol 145-triphosphate receptor 1
160501_at	-2.589	Kif20a	kinesin family member 20A
101571_g_at	-2.578	Igfbp4	insulin-like growth factor binding protein 4
95306_at	-2.549	Gpr14	G protein-coupled receptor 14
92668_at	-2.527	Btk	Bruton agammaglobulinemia tyrosine kinase
160748_at	-2.526	Asb6	ankyrin repeat and SOCS box-containing protein 6

Upregulated genes 4 h post-IR (2.5Gy) in TLS -/- pre-B

Probename	Fold Change	Gene	Description
96515_at	48.445	Il4i	interleukin 4 induced 1
161030_at	25.484	Scx	scleraxis
103091_at	11.957	Relb	avian reticuloendotheliosis viral (v-rel) oncogene related B

Table 7. continued

Probename	Fold Change	Gene	Description
97106_at	11.066	Map3k8	mitogen activated protein kinase kinase kinase 8
102314_at	10.980	Slc2a4	solute carrier family 2 (facilitated glucose transporter) member 4
103849_at	7.833	Crkl	v-crk sarcoma virus CT10 oncogene homolog (avian)-like
101927_at	7.520	Prkar1b	protein kinase cAMP dependent regulatory type I beta
99664_at	6.974	Pcnt2	pericentrin 2
102239_at	6.966	Bcl3	B-cell leukemia/lymphoma 3
93869_s_at	6.927	Bcl2a1a	B-cell leukemia/lymphoma 2 related protein A1a
101705_at	6.605	Dclre1c	DNA cross-link repair 1C PSO2 homolog (S. cerevisiae)
93386_at	6.486	Amacl	acyl-malonyl condensing enzyme
103614_at	6.368	Nfkb2	nuclear factor of kappa light polypeptide gene enhancer in B-cells 2 p49/p100
94564_at	6.149	Sult4a1	sulfotransferase family 4A member 1
102940_at	5.692	Ltb	lymphotoxin B
104428_s_at	5.559	Matk	megakaryocyte-associated tyrosine kinase
92223_at	5.440	C1qg	complement component 1 q subcomponent gamma polypeptide
104462_at	5.345	Hic1	hypermethylated in cancer 1
103248_at	4.926	Fkbp1b	FK506 binding protein 1b
160489_at	4.849	Tnfaip2	tumor necrosis factor alpha-induced protein 2
102918_at	4.575	Muc1	mucin 1 transmembrane
160786_f_at	4.486	Actr1b	ARP1 actin-related protein 1 homolog B (yeast)
92962_at	4.345	Tnfrsf5	tumor necrosis factor receptor superfamily member 5
99000_at	4.266	Mapk7	mitogen-activated protein kinase 7
102629_at	4.078	Tnf	tumor necrosis factor
93682_at	4.039	Ldb2	LIM domain binding 2
104068_at	3.994	Strn4	striatin calmodulin binding protein 4
101054_at	3.959	Ii	Ia-associated invariant chain
92422_at	3.918	Chga	chromogranin A
94735_s_at	3.908	Cma2	chymase 2 mast cell
103433_at	3.806	Pscd3	pleckstrin homology Sec7 and coiled-coil domains 3
160818_at	3.678	Lrrfip2	leucine rich repeat (in FLII) interacting protein 2
93608_at	3.659	Ebi3	Epstein-Barr virus induced gene 3
160133_at	3.540	Ltbp3	latent transforming growth factor beta binding protein 3
100298_at	3.534	Pspn	persephin
101727_at	3.521	Nfkbie	nuclear factor of kappa light polypeptide gene enhancer in B-cells inhibitor epsilon
94285_at	3.512	H2-Eb1	histocompatibility 2 class II antigen E beta
160655_at	3.451	Cpd	carboxypeptidase D
93617_at	3.427	Ccrl2	chemokine (C-C motif) receptor-like 2
98011_at	3.419	Gabbr1	gamma-aminobutyric acid (GABA-B) receptor 1
101554_at	3.288	Nfkbia	nuclear factor of kappa light chain gene enhancer in B-cells inhibitor alpha
97319_at	3.257	Rrad	Ras-related associated with diabetes
103046_at	3.144	Car4	carbonic anhydrase 4
94246_at	3.141	Ets2	E26 avian leukemia oncogene 2 3' domain
104467_at	3.125	Cpd	carboxypeptidase D
102914_s_at	3.086	Bcl2a1a	B-cell leukemia/lymphoma 2 related protein A1a
104170_at	3.085	Mapk8ip	mitogen activated protein kinase 8 interacting protein
160645_at	3.079	Birc2	baculoviral IAP repeat-containing 2
94384_at	2.982	Ier3	immediate early response 3
97740_at	2.894	Dusp16	dual specificity phosphatase 16
104531_at	2.871	Prkcd	protein kinase C delta
93218_at	2.858	Swap70	SWAP complex protein
95012_at	2.848	Slc22a17	solute carrier family 22 (organic cation transporter) member 17
92770_at	2.845	S100a6	S100 calcium binding protein A6 (calcyclin)
96752_at	2.805	Icam1	intercellular adhesion molecule
104597_at	2.627	Gbp2	guanylate nucleotide binding protein 2
93013_at	2.561	Idb2	inhibitor of DNA binding 2
92667_at	2.552	Ar	androgen receptor
104149_at	2.549	Nfkbia	nuclear factor of kappa light chain gene enhancer in B-cells inhibitor alpha
103549_at	2.542	Nes	nestin

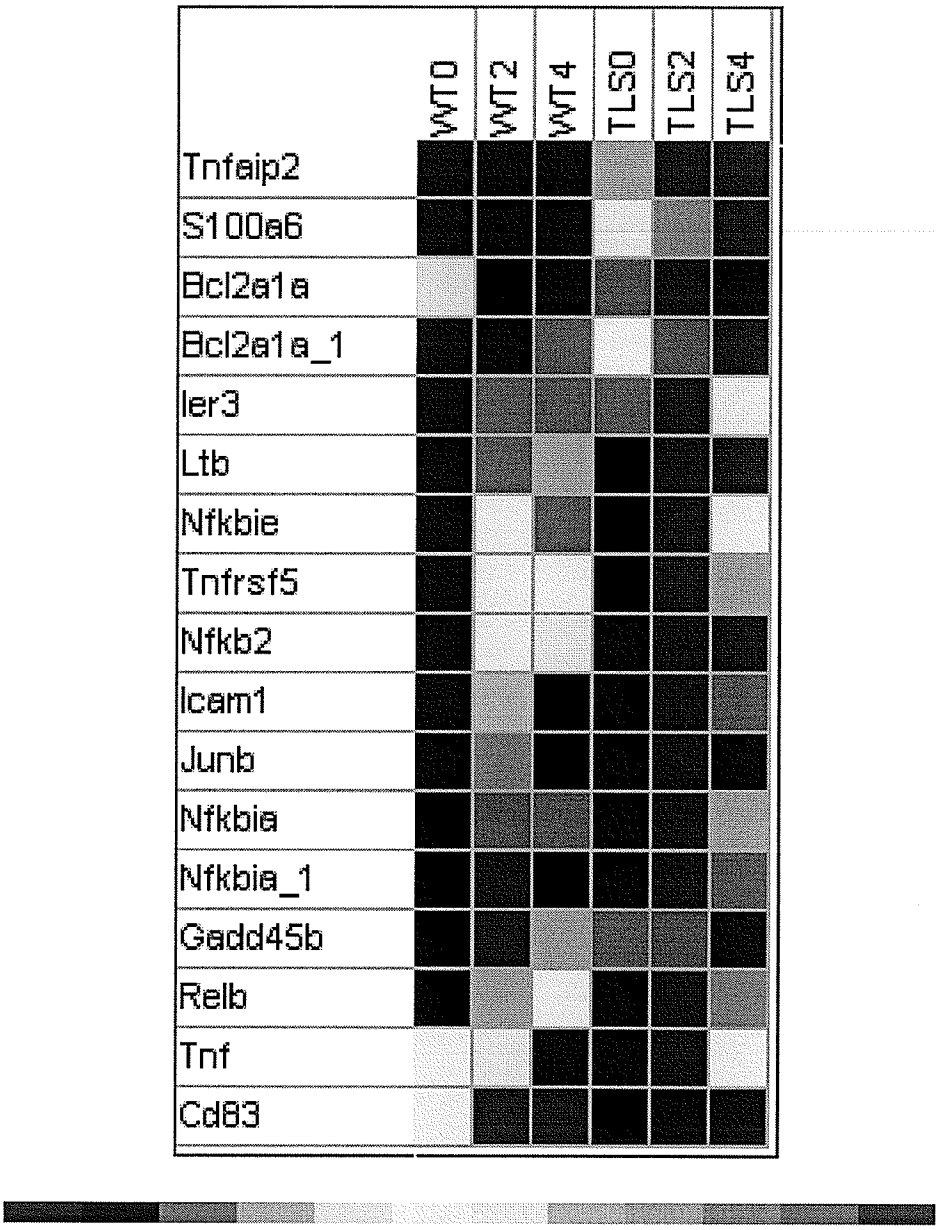

Figure 12. Ionizing radiation-induced NF-κB target genes identified in the preliminary microarray experiment. Each column represents an experimental condition: wild type (WT) 0 h untreated (WT0), WT 2 h post-ionizing radiation (IR) (WT2), WT 4 h post-IR (WT4), TLS -/- 0 h untreated (TLS0), TLS -/- 2 h post-IR (TLS2), and TLS -/- 4 h post-IR (TLS4). Legend indicates color scheme used to represent low (blue) and high (red) expression levels. The heat map was generated by GeneCluster 2.0 software.

Taken together, we have identified 10 IR-induced NF-κB target genes that are differentially expressed between wild type and TLS deficient pre-B cells. Although these conclusions were based solely on our qualitative assessment of the heat map data, our putative identification of 10 differentially expressed IR-responsive NF-κB target genes allowed us to proceed with the full microarray experiment.

3.4.2 Microarray analysis

The microarray experiment was designed to perform a genomewide analysis of IR-induced changes in gene expression between wild type and TLS -/- mouse pre-B cells for the purpose of identifying TLS-dependent NF-κB target genes. To observe both the optimal NF-κB and pre-apoptotic gene expression responses to ionizing radiation of our pre-B cells, we isolated total RNA from irradiated cells after 2 and 4 h, respectively. Optimal NF-κB-induced gene expression changes have been shown to occur between 2 and 4 h[135]. The 4h time point was also selected to identify genes involved in the defective IR-induced apoptotic signaling that was observed in our TLS -/- pre-B cells (Figure 2 – section 1.1.4). Based on our experience with these cells, execution of the apoptotic program occurs between 4-8 h post ionizing radiation, and as such, the 4 h timepoint should be free of apoptotic-related events that would interfere with gene expression analysis. To minimize our chances of identifying false positive candidate genes, we performed three independent experiments. In addition to the ionizing radiation time points mentioned above, we included an unirradiated control sample for both wild type and TLS -/- pre-B cells for a total of 18 biological samples (Table 8).

Table 8. Microarray experimental samples and their respective assigned chip designations.

Sample	Experimental Condition
1-3	Wild type untreated
4-6	Wild type 2h post-IR
7-9	Wild type 4h post-IR
10-12	TLS -/- 0h untreated
13-15	TLS -/- 2h post-IR
16-18	TLS -/- 4h post-IR

As in the pilot screen, the quality of the RNA samples was examined by visual inspection of the integrity of the 18S and 28S rRNA bands (Figure 13), and determined to be fit for experimentation. The samples were sent to the Montreal Genome Centre and also determined to be of high quality, as determined by inspection using an RNA Bioanalyzer (Agilent). RNA samples were reverse transcribed into cDNA, converted to cRNA, labeled and hybridized to Affymetrix Murine 430A 2.0 microarray GeneChips. These chips, which were available through the Montreal Genome Centre, employed newly developed technology to provide the most updated and comprehensive coverage of approximately 39,000 mouse genes and expressed sequence tags (ESTs) on a single amalgamated array chip.

Interestingly, it was determined that the hybridization of two of the three WT 4 h post-ionizing radiation samples (7 and 8) to their microarray chips was deemed to have been marginally unsuccessful by the Montreal Genome Centre. This may have been

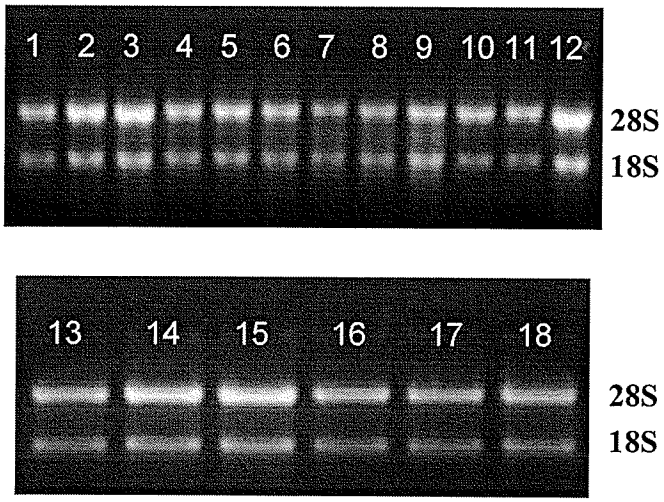

Figure 13. Quality verification of RNA preparations for microarray analysis experiment. Lanes (1-18) correspond to the full microarray RNA samples outlined in Table 7 (see section 3.4.2). Bands represent 18S (lower) and 28S (upper) ribosomal RNA. Approximately 2 μg of each sample was resolved on a 1.2% formaldehyde agarose gel.

attributed to the fact that these particular samples were isolated from cells that were beginning to undergo apoptosis. However, this was unexpected, given that the samples were deemed to be of high quality by both us and the Montreal Genome Centre (MGC) prior to the hybridization step. We were informed by the MGC technical staff that the data obtained from these chips could still be utilized, given that the hybridization had only been marginally unsuccessful. However, we decided to exclude the 4 h time point for the analysis of the microarray data to ensure that our data were as free of false positive and false negative results as possible.

Robust Multiple-array Averaging (RMA) software was used to process the data from the microarray experiment. In comparison to the MAS5.0 software that was used in the pilot screen, RMA has the added advantage of being able to simultaneously compare all microarray chip data together, thereby resulting in more reliable chip-to-chip comparisons than the pair-wise approach used in the pilot study. RMA-processed data are provided in a $\log_2$ scale, but can easily be converted algebraically to determine the fold change differences of gene expression of individual genes between experimental conditions. Another unique feature of RMA is that it underestimates the changes in gene expression, thereby lowering the likelihood of obtaining false positive genes.
Based on publicly available experimental literature[97]
(http://www.panomics.com/MA2010.cfm), I determined that 108 unique and established NF-κB target genes were represented on the murine 430A 2.0 microarray chip. Upon analysis of the RMA-processed microarray data, microarray experimental data were initially visualized utilizing Cluster/TreeView software to examine the expression profile of all 108 NF-κB target genes (Figure 14 - Panel A). Upon closer inspection of the

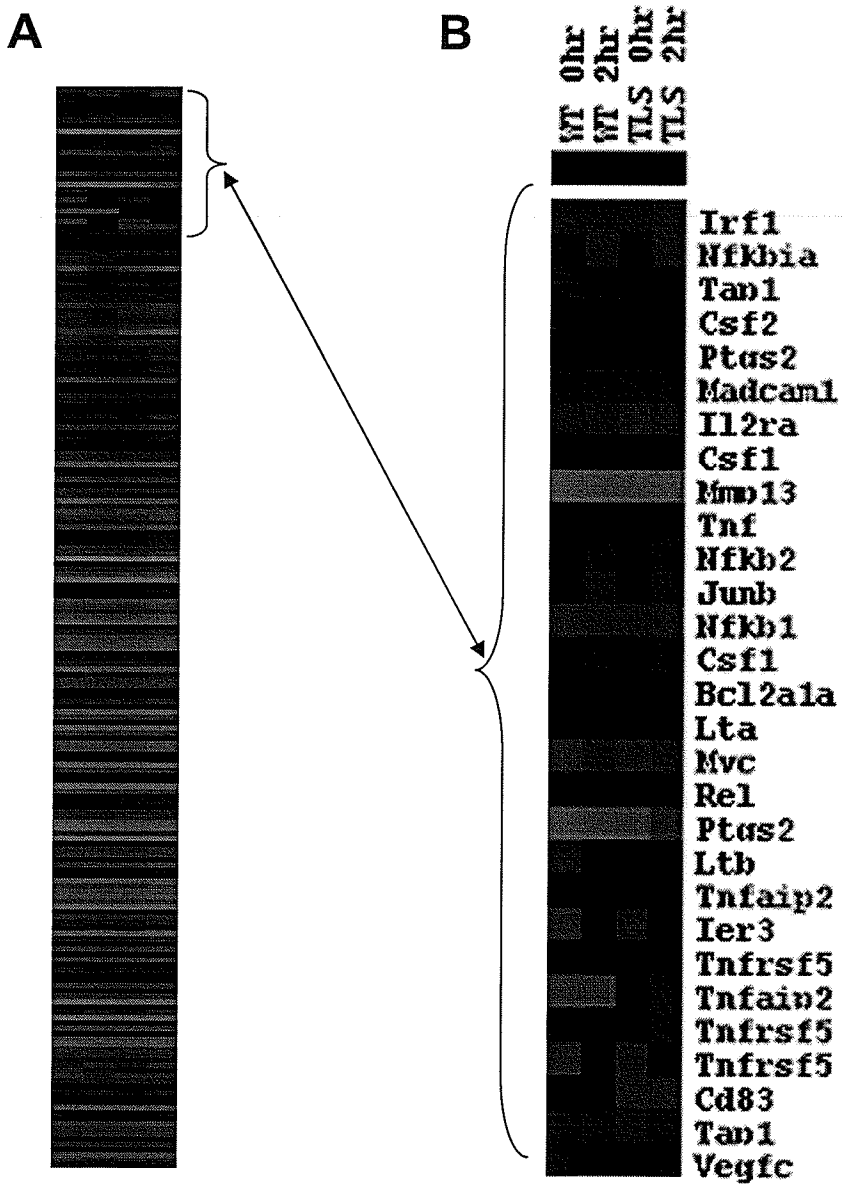

Figure 14. Analysis of expression levels of NF-κB target genes represented on the 430A 2.0 microarray chip. **(A)** Expression profile of all NF-κB genes represented on the murine 430A 2.0 chips. **(B)** An expanded view of a subset of NF-κB genes, several of which were differentially expressed between wild type and TLS -/- pre-B cells. Each column represents an experimental condition (i.e. cell type and time post-ionizing radiation (IR)) and each row represents a gene or oligo set. Green represents low expression while red indicates high expression. Expression profile diagrams were generated by Cluster and TreeView software packages. Wild type untreated (WT0), wild type 2 h post-IR (WT2), TLS -/- untreated (TLS0), and TLS -/- 2 h post-IR (TLS2).

expression profile diagram (Panel B), a subset of the NF-κB target genes were visually identified as being differentially expressed in response to ionizing radiation between wild type and TLS -/- cells (*Ltb, TNFaip2, Ier3, TNFrsf5* and *CD83*).

We also determined that of the 108 NF-κB target genes represented on the 430A 2.0 chip only 59 were deemed to be "expressed". Typically, our experiments yielded RMA values in the range of 3.5 to 14.0 ($\log_2$). Genes were considered to be "expressed" if RMA expression values were measured above 7.0. This expression level value was empirically determined to be too low to detect by RT-PCR and therefore was selected as the threshold between "expressed" and "not expressed" genes. Of the 59 expressed NF-κB genes, only 10 were determined to be IR-induced (at least 2-fold) in either WT or TLS -/- cells (Figure 15). Of the 10 IR-induced NF-κB target genes, 3 were identified as being differentially regulated at least 2.5-fold between wild type and TLS deficient cells (*TNFaip2, TNFrsf5* and *Ier3*). These three genes were of particular interest to our lab and will be discussed in detail throughout the remainder of the thesis. A sample calculation and detailed explanation of how fold change differences in gene expression were determined from RMA values are provided in Appendix II.

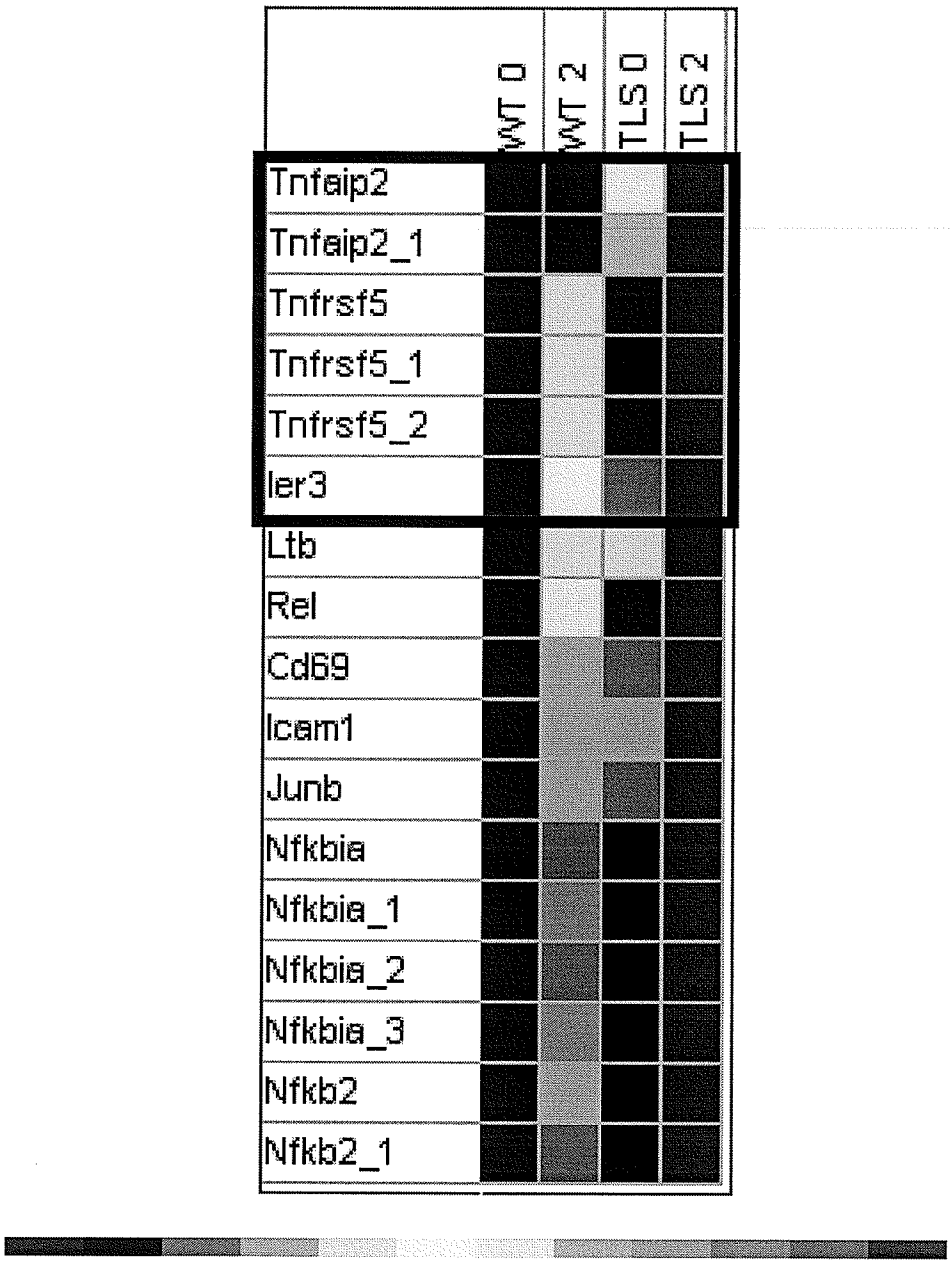

Figure 15. Ionizing radiation-induced NF-kB target genes identified in the full microarray experiment. Each column represents an experimental condition (i.e. cell type and time post-irradiation). Legend indicates color scheme used to represent low (blue) and high (red) expression levels. The black box encircles the ionizing radiation-responsive target genes that are differentially expressed between wild type and TLS -/- cells. The heat map was generated by GeneCluster 2.0 software.

In addition to the three IR-induced NF-κB target genes that we have discussed above, we were also able to identify 33 unique IR-responsive genes that were differentially expressed between wild type and TLS deficient pre-B cells (Tables 9 and 10). Several genes were represented more than once on the microarray chips, comprised of different oligonucleotide sets spanning different regions of the transcript, and therefore can be found multiple times in tables. Table 9 displays the 24 unique genes that were induced after 2 h of ionizing radiation in wild type cells with at least 2.5-fold higher expression than in TLS -/- cells. Table 10 displays the 9 unique genes, including the 3 previously mentioned NF-κB targets, which had expression levels that were induced at least 2.5-fold higher in TLS -/- cells than in wild type cells. Although these differentially expressed genes may contribute to the cellular defects that we have observed in TLS -/- mice and cells, our focus in this study was the identification of TLS-dependent NF-κB target genes.

In addition to the 33 differentially expressed IR-responsive genes that we identified, we also discovered 201 genes that appear to have intrinsic, non-IR-related differences in expression levels between wild type and TLS deficient pre-B cells. These genes were at least 2.5-fold differentially expressed in non-irradiated wild type versus TLS -/- pre-B cells. Appendix I should be referred to for the complete data set of genes with intrinsic gene expression differences between wild type and TLS -/- pre-B cells. Of these 201 genes, 6 were identified as NF-κB target genes (Table 11). It should be noted that the *TNFaip2* gene was the only gene that was scored as both a differentially expressed intrinsic and IR-responsive gene. This unique feature of the *TNFaip2* gene

Table 9. Genes with significantly higher ionizing radiation-induced gene expression levels in wild type versus TLS -/- mouse pre-B cells.

Affymetrix Gene ID	Gene Symbol	Gene Description	WT0	WT2	TLS0	TLS2	Fold Change
1441315_s_at	Slc19a2	Solute carrier family 19	6.549	9.716	6.018	6.185	7.996
1420965_a_at	Enc1	Ectodermal neural cortex 1	7.355	9.464	7.447	6.763	6.932
1418483_a_at	Ggta1	Galactosyltransferase 13	8.573	9.099	8.930	7.042	5.330
1417902_at	Slc19a2	Solute carrier family 19	9.110	11.657	8.710	8.867	5.241
1416926_at	Trp53inp1	P53-inducible protein 1	10.602	11.778	11.008	9.949	4.710
1416969_at	Gtse1	G2/S phase expressed 1	8.651	9.823	8.784	7.773	4.539
1450680_at	Rag1	Recombination activating gene 1	4.936	4.651	9.557	7.151	4.347
1426117_a_at	Slc19a2	Solute carrier family 19	7.720	10.159	7.253	7.573	4.344
1449002_at	Phlda3	Pleckstrin homology-like	8.531	10.782	7.667	7.863	4.151
1416927_at	Trp53inp1	P53-inducible protein 1	8.430	9.518	8.778	7.966	3.733
1449877_s_at	Kifc1	Kinesin family c1	9.060	9.490	8.852	7.409	3.663
1449483_at	Polk	Polymerase kappa	8.035	9.813	7.700	7.677	3.483
1423315_at	Bbc3	Bcl-2 binding component 3	8.747	11.330	7.751	8.546	3.451
1417323_at	Dda3-pending	Differential display and activated by p53	10.212	11.224	7.688	6.927	3.420
1424638_at	Cdkn1a	Cyclin-dependent kinase inhibitor 1A (p21)	8.838	12.018	9.297	10.783	3.235
1450017_at	Ccng1	Cyclin G1	10.213	11.691	8.914	8.714	3.199
1450541_at	Pvt1	Plasmacytoma variant translocation 1	7.623	9.344	6.948	6.993	3.196
1417143_at	Edg2	Endothelial differentiation G-protein-coupled 2	6.450	6.224	8.832	6.938	3.176
1420827_a_at	Ccng1	Cyclin G1	10.463	11.768	9.192	8.914	2.996
1449414_at	Zfp118	Zinc finger protein 118	7.332	8.170	8.905	8.169	2.977
1425416_s_at	Dda3-pending	Differential display and activated by p53	8.940	10.057	7.195	6.743	2.967
1450016_at	Ccng1	Cyclin G1	10.411	11.810	9.222	9.060	2.951
1440481_at	Stat1	Signal transducer/activator of transcription 1	6.382	7.322	6.239	5.632	2.923
1424332_at	Rab40c	RAS oncogene family	6.839	7.664	7.059	6.366	2.863
1448606_at	Edg2	Endothelial differentiation G-protein-coupled 2	8.265	7.704	10.853	8.825	2.764
1421397_a_at	Lrdd	Leucine-rich and death domain containing	8.556	10.069	8.599	8.672	2.712
1424331_at	Rab40c	RAS oncogene family	8.393	9.258	8.697	8.123	2.711
1450935_at	Ercc5	Excision repair cross-complement 5	7.689	8.893	7.807	7.629	2.605
1422513_at	Ccnf	Cyclin F	9.970	10.182	9.724	8.567	2.583
1427416_x_at	Dusp7	Dual specificity phosphatase 7	8.656	8.258	9.393	7.637	2.563
1448529_at	Thbd	Thrombomodulin	8.098	6.410	9.770	6.739	2.539
1450061_at	Enc1	Ectodermal neural cortex 1	8.134	9.239	7.978	7.739	2.538
1437279_x_at	Sdc1	Syndecan 1	5.236	6.357	6.998	6.786	2.519

RMA-processed expression data (in $\log_2$ scale) from the full microarray experiment. Each column corresponds to an experimental condition (wild type unirradiated (WT0), wild type irradiated 2h (WT2), TLS -/- unirradiated (TLS0) and TLS -/- irradiated 2h (TLS2)). Fold change column indicates fold difference in ionizing radiation-induced gene expression levels between wild type and TLS -/- cells.

Table 10. Genes with significantly higher ionizing radiation-induced gene expression levels in TLS -/- versus wild type pre-B cells.

Affymetrix Gene ID	Gene Symbol	Gene Description	WT0	WT2	TLS0	TLS2	Fold Change
1419083_at	Tnfsf11	TNF superfamily member 11	6.048	5.596	6.588	10.029	14.852
1451944_a_at	Tnfsf11	TNF superfamily member 11	5.626	5.441	6.262	8.825	6.716
1439221_s_at	Tnfrsf5	TNF receptor superfamily member 5	6.011	6.997	6.186	9.759	6.010
1459903_at	Sema7a	Semaphorin 7a	7.824	7.902	8.160	10.786	5.847
1452417_x_at	Igk-V8	Immunoglobulin κ chain variable	11.565	12.060	6.500	9.525	5.775
1460415_a_at	Tnfrsf5	TNF receptor superfamily member 5	6.873	7.531	7.170	9.763	3.824
1449473_s_at	Tnfrsf5	TNF receptor superfamily member 5	6.477	7.049	6.550	9.044	3.789
1418280_at	Copeb	Core promoter element binding	7.095	6.363	7.729	8.830	3.563
1438855_x_at	Tnfaip2	TNF alpha induced protein 2	5.250	5.345	8.023	9.888	3.408
1453228_at	Stx11	Syntaxin 11	7.082	8.311	7.351	10.334	3.373
1427660_x_at	Igk-V8	Immunoglobulin κ chain variable	11.943	12.483	7.687	9.912	3.216
1433508_at	Copeb	Core promoter element binding	7.286	6.669	7.993	9.013	3.109
1419647_a_at	Ier3	Immediate early response 3	5.808	6.693	6.192	8.668	3.012
1427742_a_at	Copeb	Core promoter element binding	8.137	7.680	8.442	9.364	2.600
1449363_at	Atf3	Activating transcription factor	7.448	7.964	7.585	9.433	2.517

RMA-processed expression data (in $\log_2$ scale) from the full microarray experiment. Each column corresponds to an experimental condition (wild type unirradiated (WT0), wild type irradiated 2h (WT2), TLS -/- unirradiated (TLS0) and TLS -/- irradiated 2h (TLS2)). Fold change column indicates fold difference in ionizing radiation-induced gene expression levels between wild type and TLS -/- cells.

Table 11. NF-κB target genes that have intrinsic differences in gene expression levels between wild type and TLS -/- mouse pre-B cells.

Affymetrix Gene ID	Gene Symbol	Gene Description	WT0	TLS0	Fold change
1421375_a_at	S100a6	S100 calcium binding protein A6 (calcyclin)	5.457	9.553	17.108
1450140_a_at	Cdkn2a	Cyclin-dependent kinase inhibitor 2A (ARF)	5.868	9.035	8.984
1438855_x_at	Tnfaip2	TNF alpha induced protein	5.25	8.023	6.835
1422003_at	Blr1	Burkett lymphoma receptor 1	5.47	8.228	6.767
1455897_x_at	Hmgn1	High mobility group nucleosomal binding	9.86	12.305	5.447
1422495_a_at	Hmgn1	High mobility group nucleosomal binding	10.27	12.488	4.651
1438940_x_at	Hmgn1	High mobility group nucleosomal binding	10.128	12.257	4.373
1416111_at	Cd83	CD83 antigen	7.384	5.729	3.148

RMA-processed expression data (in $\log_2$ scale) from the full microarray experiment. Each column corresponds to an experimental condition (wild type unirradiated (WT0) and TLS -/- unirradiated (TLS0)). Fold change column indicates fold difference in ionizing radiation-induced gene expression levels between wild type and TLS -/- cells.

make it an attractive candidate to test our hypothesized model of TLS as a modulator of NF-κB-directed gene expression.

To avoid potential visualization bias inherent to an individual algorithm, we performed independent analysis of our microarray data, using the R and Bioconductor software packages[129](http://www.bioconductor.org/). Using all three approaches we were able to identify the same set of differentially expressed intrinsic and IR-responsive NF-κB target genes described above (Figure 16). These findings clearly indicate that these NF-κB target genes are differentially expressed in the absence of funtional TLS. To characterize the role of TLS in the modulation of NF-κB-directed gene expression, we selected *TNFaip2, TNFrsf5* and *Ier3* as our candidate genes to validate our microarray analysis.

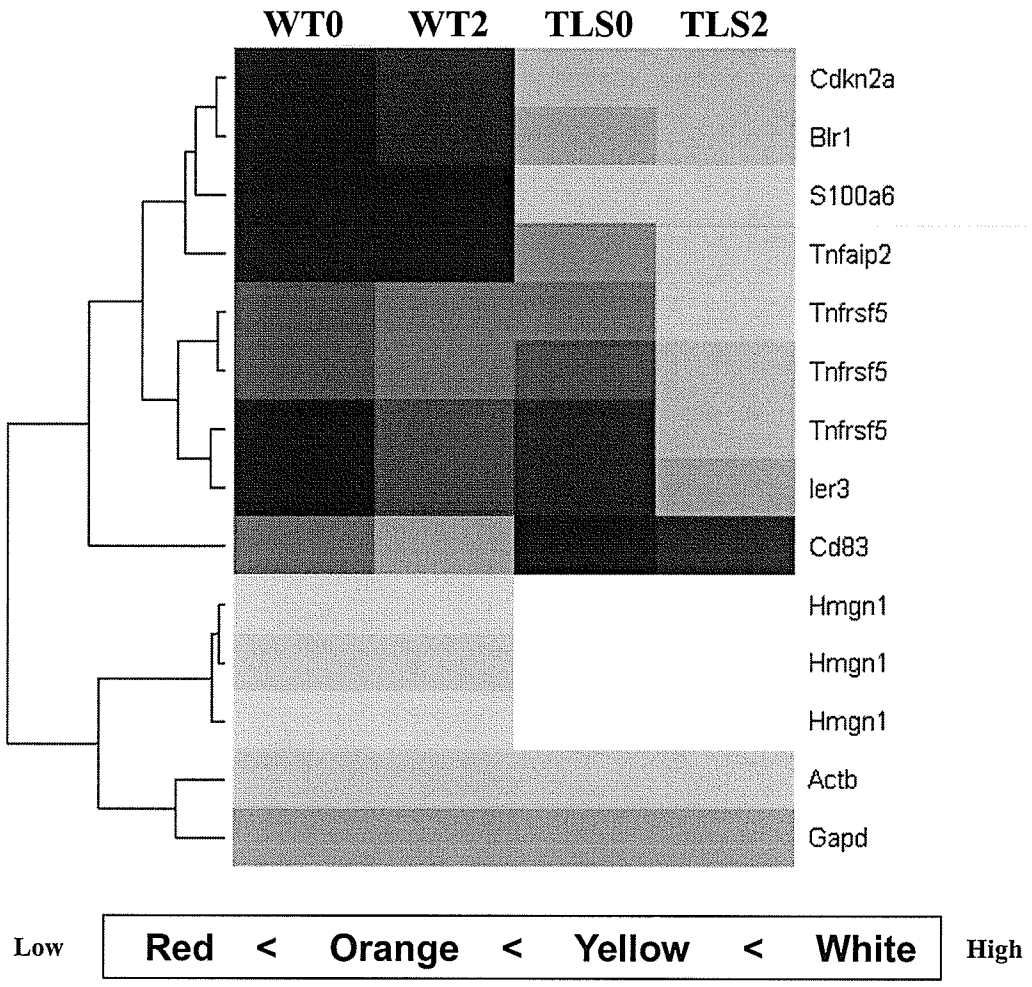

Figure 16. Classification of differentially regulated NF-κB target genes identified in the microarray experiment. Cluster analysis was performed to classify genes according to their gene expression patterns. Genes that are similarily expressed were grouped together. Each column represents an experimental condition (i.e. cell type and time post-ionizing radiation (IR)). Legend indicates color scheme used to represent low (red) and high (white) expression levels. The heat map was generated using the R and Bioconductor software packages. Wild type untreated (WT0), wild type 2 h post-IR (WT2), TLS -/- untreated (TLS0), and TLS -/- 2 h post-IR (TLS2).

3.5 Validation of expression levels of candidate genes

To validate the expression levels of the *TNFaip2, TNFrsf5* and *Ier3* candidate target genes that we observed in our microarray experiment, we used reverse transcriptase-polymerase chain reaction (RT-PCR) to measure mRNA levels from whole RNA extracts from both irradiated and unirradiated wild type and TLS deficient mouse pre-B cells. RT-PCR involves the initial synthesis of cDNA from an mRNA template followed by the amplification of the specific cDNA. We designed gene specific primers to the 3' untranslated region of our candidate gene transcripts for first strand synthesis. Gene specific amplification cycles were performed using a pair of coding region specific primers. The number of PCR amplification cycles to be used was determined empirically for each individual candidate gene to ensure the amplification process was still in the linear range. Amplified DNA fragments, which correspond to the relative levels of mRNA for a particular gene, were resolved on agarose gels for quantification (section 2.6).

Transcript levels for the *TNFaip2* gene were measured, and determined to be consistent with our microarray experimental data (Figure 17). No PCR bands were observed in the wild type samples, while an approximate 3.4-fold induction was observed in TLS -/- pre-B upon ionizing radiation. The expression patterns of the IR-induced *TNFrsf5* gene were also consistent with those measured in the microarray experiments (Figure 18). We observed an approximate 2.0-fold higher post-ionizing radiation induction of the *TNFrsf5* gene in TLS -/- versus wild type pre-B cells. However, due to low expression levels in mouse pre-B cells, we were unable to validate the transcript levels of the *Ier3* gene by RT-PCR. Taken together, we were successful in validating our

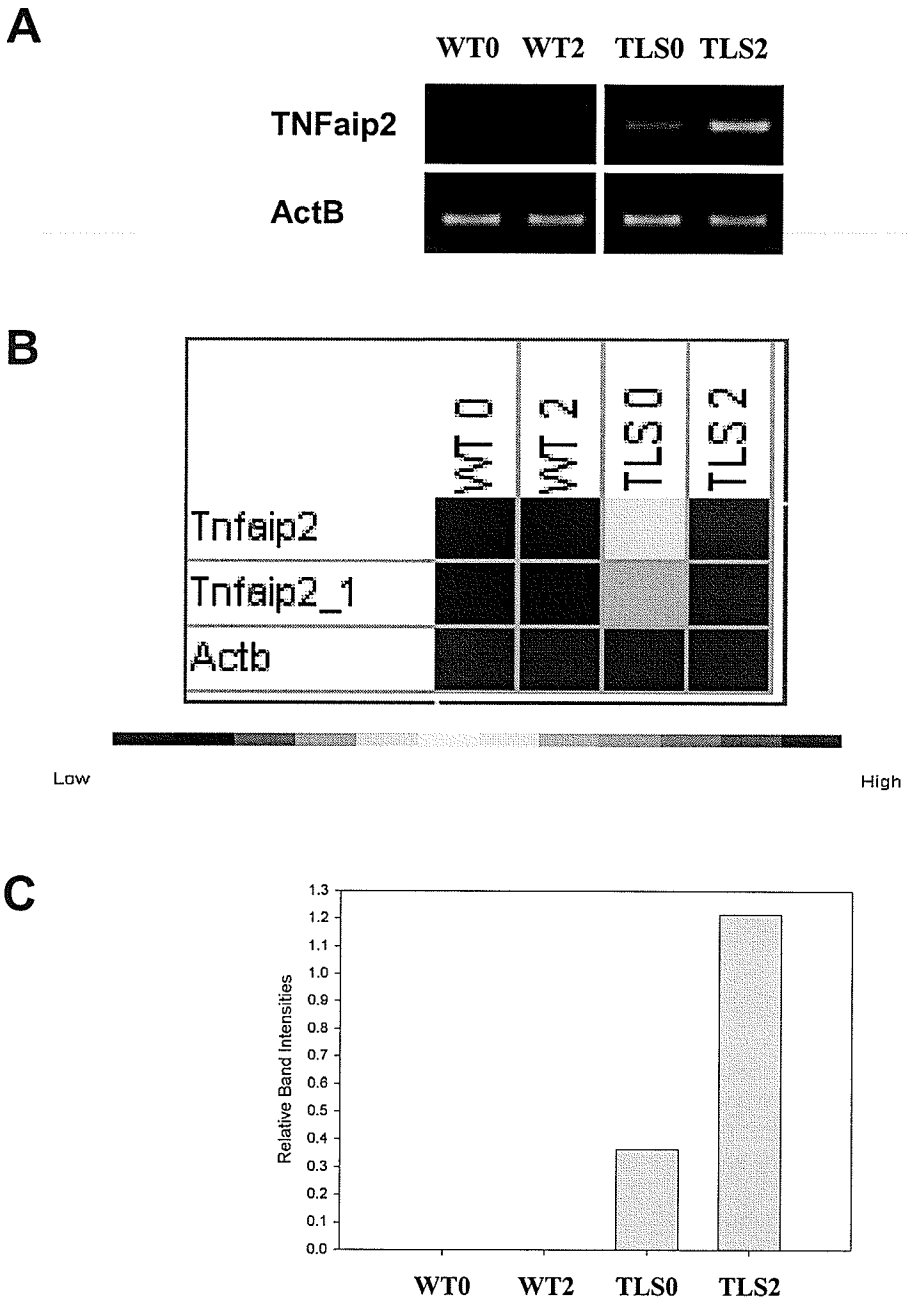

Figure 17. Validation of TNFaip2 transcript levels in mouse pre-B cells. (A) Messenger RNA levels of TNFaip2 were validated by RT-PCR on RNA preparations from mouse pre-B cells. Gene specific primers were used for first strand cDNA synthesis, while 22 (ActB control) and 40 (TNFaip2) cycles were used for the amplification step. **(B)** Expression profile of the mRNA levels of the TNFaip2 and ActB genes (GeneCluster 2.0). **(C)** Graphical representation of the semi-quantified band intensities of TNFaip2 compared to ActB.

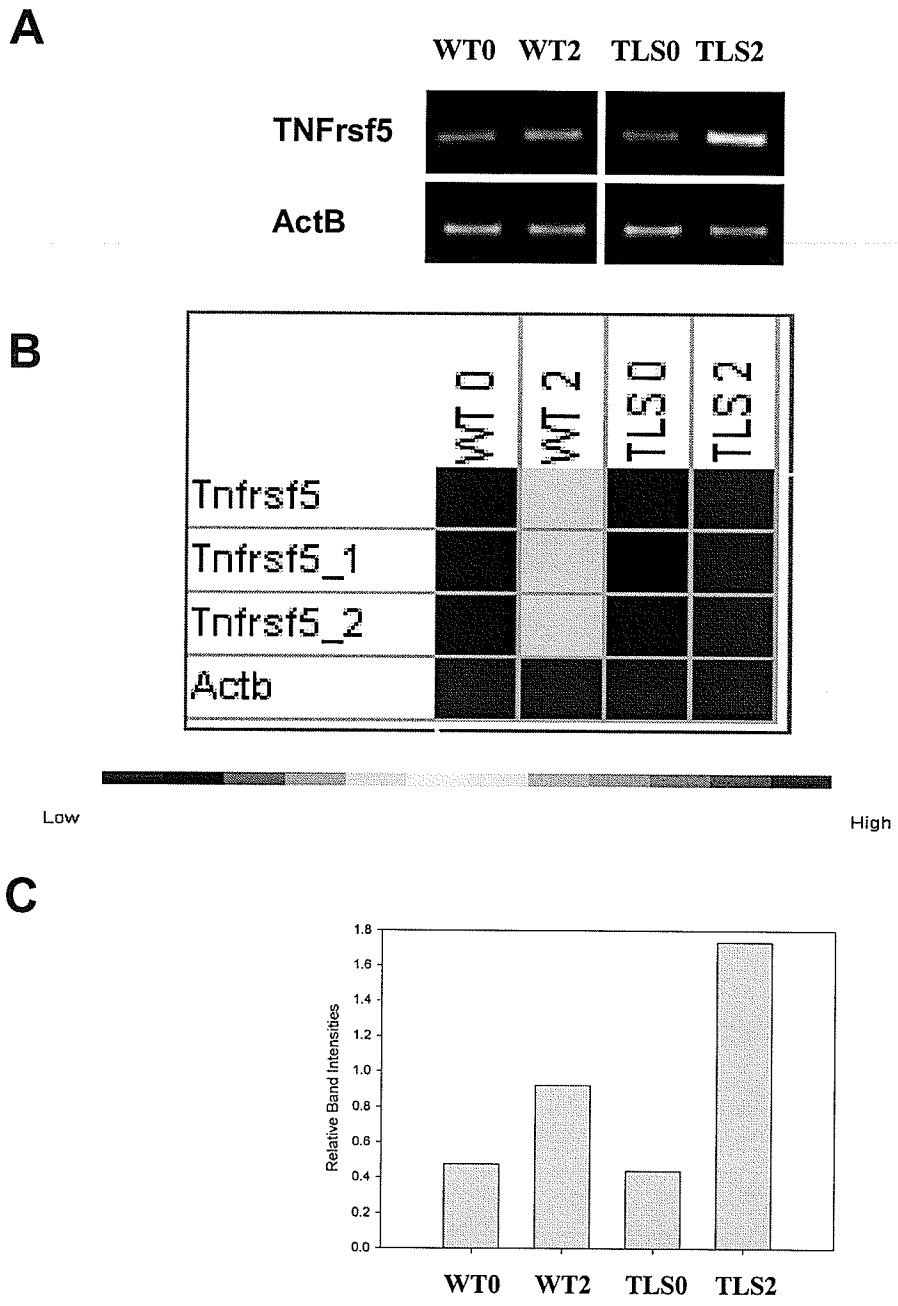

Figure 18. Validation of TNFrsf5 transcript levels in mouse pre-B cells. (A) Messenger RNA levels of TNFrsf5 were validated by RT-PCR on RNA preparations from mouse pre-B cells. Gene specific primers were used for first strand cDNA synthesis, while 22 (ActB control) and 40 (TNFrsf5) cycles were used for the amplification step. **(B)** Expression profile of the mRNA levels of the TNFrsf5 and ActB genes (GeneCluster 2.0). **(C)** Graphical representation of the semi-quantified band intensities of TNFrsf5 compared to ActB.

microarray data by observing the same differential gene expression patterns for *TNFaip2* and *TNFrsf5* mRNA in TLS -/- cells.

3.6 Characterization of the candidate gene promoters of *TNFaip2* and *TNFrsf5*

To begin to understand the possible mechanisms involved in TLS modulation of IR-induced NF-κB target genes, we analyzed the promoter sequences of the *TNFaip2* and *TNFrsf5* genes for both NF-κB- and TLS-binding sites. To search for NF-κB-binding sites, we used the TFSEARCH transcription factor binding-site search database (http://www.cbrc.jp/research/db/TFSEARCH.html)[130] to search for sequences with high nucleotide sequence identity to the known consensus NF-κB-binding sequence GGGACTTTCC[131]. To identify putative TLS-binding sites, we manually searched the promoter sequences of the *TNFaip2* and *TNFrsf5* genes for regions with high sequence similarity to a previously reported 21 base pair TLS-binding element (5' TTTTCTCCC CACTTTTAGATC 3')[14]. Promoter sequences deemed to be potential TLS-binding sites required at least 6 continuous base pairs of sequence identity to the known TLS-binding element. Transcription factors are known to bind short degenerate sequences in the range of 6-20 base pairs[132]. Mismatched base pairs were allowed, however, sequences needed to maintain an overall sequence similarity of at least 80% (i.e. 6 out of 7 base pairs matched (85.7%) or 8 of 10 matched (80%)).

The *TNFaip2* and *TNFrsf5* gene promoters were also examined for potential regions of overlap between the predicted NF-κB- and TLS-binding sites (Figure 19). The results of the analysis indicated that all potential NF-κB-binding sites were in close proximity, at least within 91 base pairs, to putative TLS-binding sites in both candidate

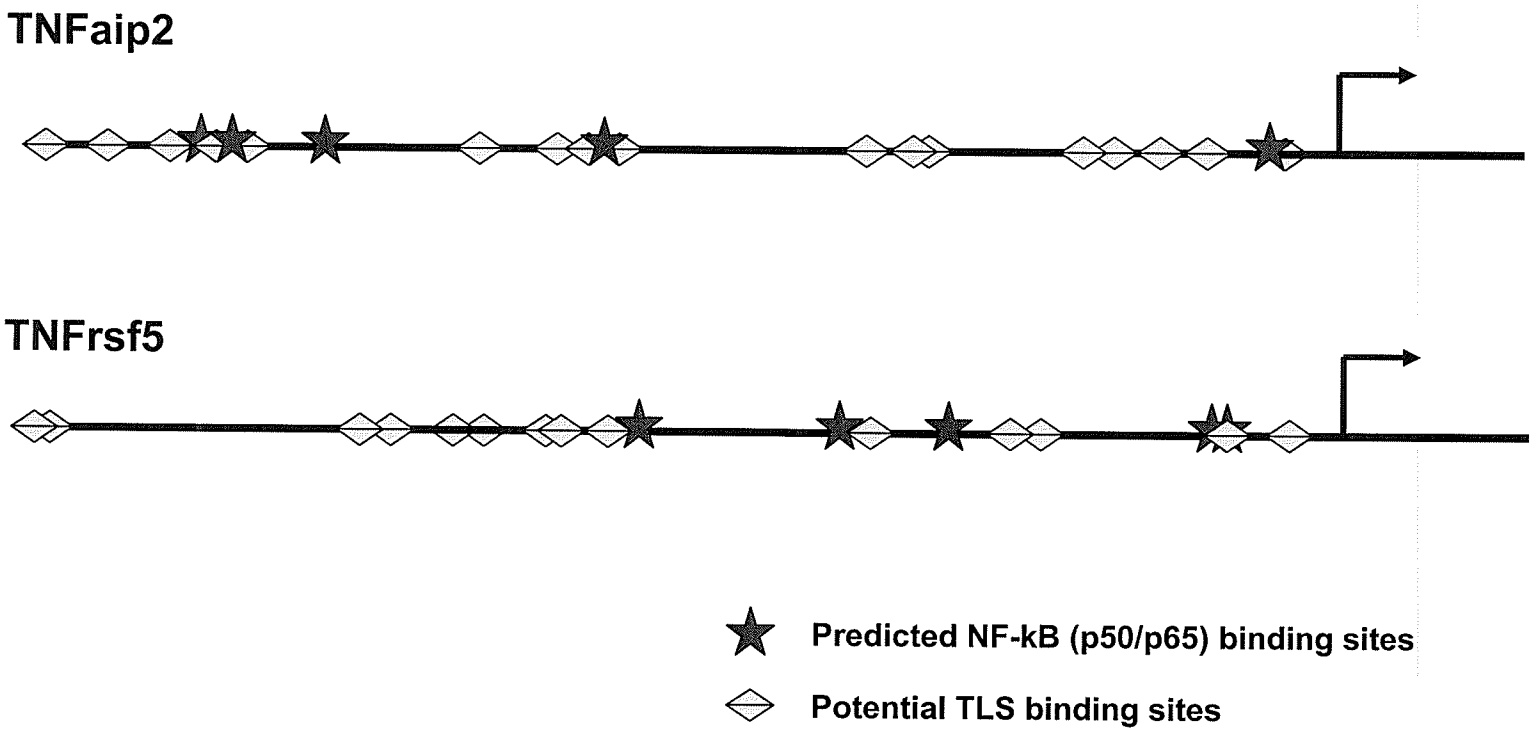

Figure 19. Promoter analysis of the candidate genes: *TNFaip2* and *TNFrsf5*. Promoter sequences for the TNFaip2 (-1637 to +1) and TNFrsf5 (-1621 to +1) genes were searched for NF-kB-binding sites using TFSEARCH (www.cbrc.jp/research/db/TFSEARCH.html). Predicted TLS-binding sites were manually determined by identifying sequences with high homology to known TLS-binding elements.

promoters. Whether TLS is able to bind the promoter regions of the *TNFaip2* and *TNFrsf5* genes directly, or if there is competition between NF-κB and TLS for the same promoter binding sites of these same genes, remains to be elucidated. The possible mechanisms for TLS' modulation of NF-κB-directed gene expression of the *TNFaip2* and *TNFrsf5* genes will be discussed in detail later.

In summary, we have confirmed that TLS modulates NF-κB-directed gene expression and have identified two NF-κB target genes that are differentially expressed in TLS -/- versus wild type pre-B cells by microarray analysis. We have also validated the differential expression of mRNA of these genes by RT-PCR. Initial analysis of the promoter sequences of the *TNFaip2* and *TNFrsf5* genes have revealed several potential TLS-binding sites that are in close proximity to NF-κB sites. Through the identification of these candidate genes, we now possess a powerful genetic tool that will allow us to deduce the molecular mechanisms involved in TLS' modulation of NF-κB-directed gene expression.

Chapter 4: Discussion

The *TLS* gene is translocated in several human cancers, including myxoid liposarcoma and acute myeloid leukemia[1,3,27]. Our lab has rationalized that the best approach to determine the role of TLS in the initiation and progression of these cancers is to first characterize the normal cellular function of the TLS protein. We have previously identified high levels of genomic instability and defects in lymphocyte maturation in cells deficient for TLS[4]. We have also observed a defective DNA damage-induced apoptotic response in TLS -/- pre-B cells (Cann, *et al.*, manuscript in preparation).

Based on our work and others, TLS is thought to be involved in the regulation of gene expression at multiple levels, including as a transcription cofactor, as a splicing factor, and as factor involved in targeted subcellular translation (section 1.1.3). Our hypothesis is that TLS is initially loaded onto the promoters of the target genes and modulates expression through interactions with gene-specific factors at multiple levels. Furthermore, we expect that at least some of these target genes are involved in cellular processes that were determined to be defective in our TLS -/- mice. To test our hypothesis, we chose to focus on TLS' ability to regulate NF-κB-directed gene expression. TLS has been described as an *in vitro* transcriptional coactivator to the p65 subunit of the well characterized NF-κB transcription factor[6].

In this study, we report that endogenous NF-κB-directed gene expression is impaired in TLS -/- MEF cells. In addition, we have identified the IR-induced NF-κB target genes: *TNFaip2*, *TNFrsf5*, and *Ier3,* as putative TLS-dependent target genes by microarray analysis. Finally, we have validated the differential expression of endogenous

transcripts for the *TNFaip2* and *TNFrsf5* candidate genes by RT-PCR. The identification of these putative TLS-dependent target genes will allow us to further investigate the mechanisms involved in TLS' modulation of NF-κB-directed gene expression.

4.1 TLS modulates NF-κB-directed gene expression *in vivo*

TLS has been identified as an interaction partner to the p65 subunit of NF-κB and acts as a transcriptional co-activator to NF-κB-directed gene expression *in vitro*[6]. While we were able to confirm TLS' transcriptional activation potential in the same classical transient transfection-reporter assay, it is often difficult to interpret the relevance of this potential *in vivo*. To directly address this issue, we used physiological levels of TNF-α to activate endogenous NF-κB. Our results clearly establish endogenous NF-κB-directed gene expression induced by TNF-α was impaired in TLS deficient cells, as compared to wild-type MEF cells. Immunohistochemical analysis of TLS -/- cells confirmed normal NF-κB expression in these cells and that IR-induced NF-κB nuclear translocation was intact, indicating that the transcriptional defects observed were not a consequence of NF-κB misexpression or the inability of NF-κB to be activated. Taken together, this is the first functional evidence that TLS is a transcriptional cofactor *in vivo*. With this information in hand, we carried on with the microarray experiments to identify TLS-dependent NF-κB target genes.

4.2 Identification of candidate TLS-dependent NF-κB target genes

Here we report the identification of *TNFaip2*, *TNFrsf5*, and *Ier3* as IR-induced NF-κB target genes that are differentially expressed in wild type cells as compared to

TLS -/- cells. Moreover, these putative TLS-dependent candidate genes have also been implicated in cellular processes that we have previously found to be defective in our TLS deficient mice.

4.2.1 TNFaip2

We have identified Tumor Necrosis Factor alpha-induced protein 2 (*TNFaip2*) as a putative TLS-dependent candidate gene by microarray analysis. TNFaip2, or B94, was originally identified as a TNF-α-inducible peptide that was shown to be expressed during mouse development in embryonic liver cells[136]. The function of TNFaip2 is largely unknown.

From our microarray data, we did not observe expression of TNFaip2 in either pre- or post-ionizing radiated wild type mouse pre-B cells. This is consistent with a previous study in which postnatal expression of mouse TNFaip2 was not observed in any hematopoietic precursor cells[137]. In TLS -/- pre-B cells, however, we did observe a basal level of expression in unirradiated cells and an approximate 3-fold induction of TNFaip2 mRNA levels was detected 2 h post-ionizing radiation. These results demonstrate that the *TNFaip2* gene is an ionizing radiation-inducible target gene in the absence of functional TLS protein.

It can be speculated that the increased levels of TNFaip2 expression may interfere with the maturation process of lymphocytes, given that expression levels are not normally observed in hematopoietic cells[137]. If true, this would help explain the differentiation block in pre-B to mature B cells that we observed in our TLS -/- mice[4]. At the molecular level, TLS may normally function to inhibit both basal and IR-induced expression levels

of the *TNFaip2* gene in lymphocytes. The former may be a result of direct binding of the TLS protein to the promoter resulting in the inhibition of transcriptional initiation. The latter inhibition of IR-induced expression of *TNFaip2,* may be due to TLS' interference in NF-κB promoter binding to its consensus sequences. Proposed models of TLS modulation of the NF-κB target genes will be discussed in detail in section 4.3.

4.2.2 TNFrsf5

We have discovered that Tumor Necrosis Factor receptor superfamily member 5 (*TNFrsf5*) as a putative TLS-dependent target gene. The B cell surface-expressed TNFrsf5 (CD40) is a major B cell receptor (BCR) cofactor and associates with its T cell expressed ligand CD40L resulting in B cell receptor activation. B cell receptor activation is important in the induction of cell differentiation, proliferation, and Ig isotype class switching[138]. Moreover, each of these processes is defective in TLS-deficient cells[4].

From our microarray data, we measured minimal expression levels of TNFrsf5 both in unirradiated wild type and TLS -/- pre-B cells. This is consistent with a previous study that found that TNFrsf5 is normally found expressed on all mature B cells, but at low to undetectable levels on the surfaces of pre- and pro-B cells, respectively[139]. In cells subjected to ionizing radiation, we observed TNFrsf5 expression levels that were induced 4.7-fold higher in TLS -/- cells compared to wild type cells. These results demonstrate that the *TNFsf5* gene, like *TNFaip2*, is an ionizing radiation-inducible target gene in the absence of functional TLS protein.

We have hypothesized that TLS may be involved in the transport of TNFrsf5 mRNA to the B cell receptor activation "synaptic" cap, which occurs at the junction

between B and T cells, for local protein synthesis. In support of this hypothesis, in a recent collaboration, it was demonstrated that TLS could transport mRNA to post-synaptic sites in hippocampal neurons[10]. We are in the process of designing an experiment to investigate whether exogenously expressed GFP-tagged TLS can relocalize from the nucleus to the synaptic cap structures on the surface of activated B cells. This experiment will be performed in collaboration with Dr. Aaron Marshall of the Department of Immunology at the University of Manitoba. This model would be consistent with our previous observation that α-CD40-induced B cell receptor activation and subsequent cell proliferation is impaired in TLS -/- lymphocytes[4]. The lack of TLS to correctly transport TNFrsf5 (CD40) mRNA to the cell surface, or the existence of a new isoform of the transcript that is preferentially expressed in TLS -/- cells could provide the molecular mechanism for this phenotypic defect. This hypothesis is directly testable and further experimentation can now focus on the potential molecular mechanisms involved.

TNFrsf5 has been described as both a target gene and a known inducer of the NF-κB transcription factor. Examples of such signaling pathway crosstalk include synergistic interferon-gamma-induced expression of the *TNFrsf5* gene in the presence of activated NF-κB[140], and NF-κB-dependent expression of the anti-apoptotic *Bfl-1* gene upon TNFrsf5-mediated B cell receptor activation[141]. It is interesting to speculate that TLS modulation of NF-κB-directed gene expression may provide a mechanism by which crosstalk between signaling pathways or seemingly divergent activation responses can be coordinated. If true, one could predict the outcome of these signaling pathways would also be disrupted in TLS –/– cells. Indeed, we do observe a 1.4-fold increase in Bfl-1

(Bcl2-related gene 1)) expression levels in TLS -/- cells. This would suggest that the IR-induced increase in TNFrsf5 expression in TLS -/- pre-B cells may result in elevated levels of Bfl-1 expression and contribute to the protective anti-apoptotic response that we had observed (section 1.1.4).

Finally, as was speculated with the *TNFaip2* gene, IR-induced NF-κB-directed expression of *TNFrsf5* may normally be inhibited by TLS in wild type cells. The proposed molecular mechanisms involved in TLS' modulation of NF-κB-directed TNFrsf5 expression will be discussed in detail in section 4.3.

4.2.3 Ier3

We have identified the ionizing radiation inducible immediate early response-3 (*Ier3*), or *Iex-1*, gene[142] as a putative TLS-dependent target gene. Through our microarray experiment and subsequent attempts at validation using RT-PCR, we have determined that expression of Ier3 is undetectable both in unirradiated wild type and TLS -/- mouse pre-B cells. Upon induction by ionizing radiation, we observed an approximate 3–fold higher level of expression of the *Ier3* gene in TLS -/- versus wild type pre-B cells. To our knowledge, we are the first to report the expression of Ier3 in lymphocytes. These results demonstrate that in the absence of functional TLS, the *Ier3* gene is induced in response to DNA damage.

Ier3 has been determined to be a target gene of both NF-κB and p53 *in vitro*[143,144]. It was also shown that NF-κB and p53 were able to activate Ier3 expression levels in a synergistic manner[145]. The p53 tumor suppressor protein is an IR-induced transcription factor that is integral in the regulation of cell cycle progression, apoptosis, and DNA

repair (see review[146]). The Ier3 protein itself has been implicated in the regulation of apoptosis; however, it has also been described as both an anti-[147,148] and pro-apoptotic factor[149,150]. It can be speculated that in TLS-deficient lymphocytes, the Ier3 protein may function as an anti-apoptotic factor to lower IR-induced apoptosis levels. If true, this would be consistent with the reduced apoptotic response that we have observed in our TLS -/- pre-B cells upon ionizing radiation.

Here we have shown that IR-induced expression of the *Ier3* gene is higher in TLS -/- cells as compared to wild type pre-B cells. This is consistent with the IR-induced expression levels of the *TNFaip2* and *TNFrsf5* genes that we have discussed above. The proposed molecular mechanisms involved in TLS' modulation of all three candidate genes will be discussed in detail in the next section.

4.3 Proposed model for TLS modulation of ionizing radiation-induced NF-κB target genes

My hypothesis is that the oncoprotein TLS modulates NF-κB-directed gene expression. Based on our work and others, TLS has the potential to influence gene expression at multiple levels, ranging from being a transcriptional cofactor to RNA processing to protein translation. Irrespective of whether any or all of these functions are correct, my model predicts that TLS is first loaded onto the promoter of its target genes. Once TLS is associated with the promoter it is able to modulate gene expression levels through interactions with gene-specific factors. My model predicts three potential molecular mechanisms, based on known functions of the TLS, EWS and TAF15 proteins, which explain TLS' co-regulation of these candidate genes at the promoter level.

Through sequence analysis of the TNFaip2 and TNFrsf5 promoters, one can predict putative TLS-binding sites based on sequence identity with a known TLS-binding element[14]. Putative TLS binding sites are in close proximity to the predicted NF-κB-binding elements. In the first proposed mechanism (Figure 20 - Panel A), TLS binds directly to these putative binding sites within the candidate promoter and inhibits the binding affinity of NF-κB to its consensus κB-binding elements, thereby repressing NF-κB's transactivational potential for specific target genes. Competition between TLS and NF-κB for the occupancy of overlapping binding sites within the promoter may result in lower expression levels of the target gene, as we observed in the target genes identified in response to DNA damage in wild type versus TLS -/- cells.

In the second proposed mechanism (Panel B), TLS interacts directly with NF-κB as it is bound to its consensus κB element and modulates its ability to activate transcription of the candidate gene by preventing its association with its known coactivator proteins, such as CBP/p300[109,110] or $TAF_{II}105$[113]. In support of this model, TLS was shown to retain its association with the thyroid receptor transcription factor upon its binding to the hormone receptor-specific target DNA[75].

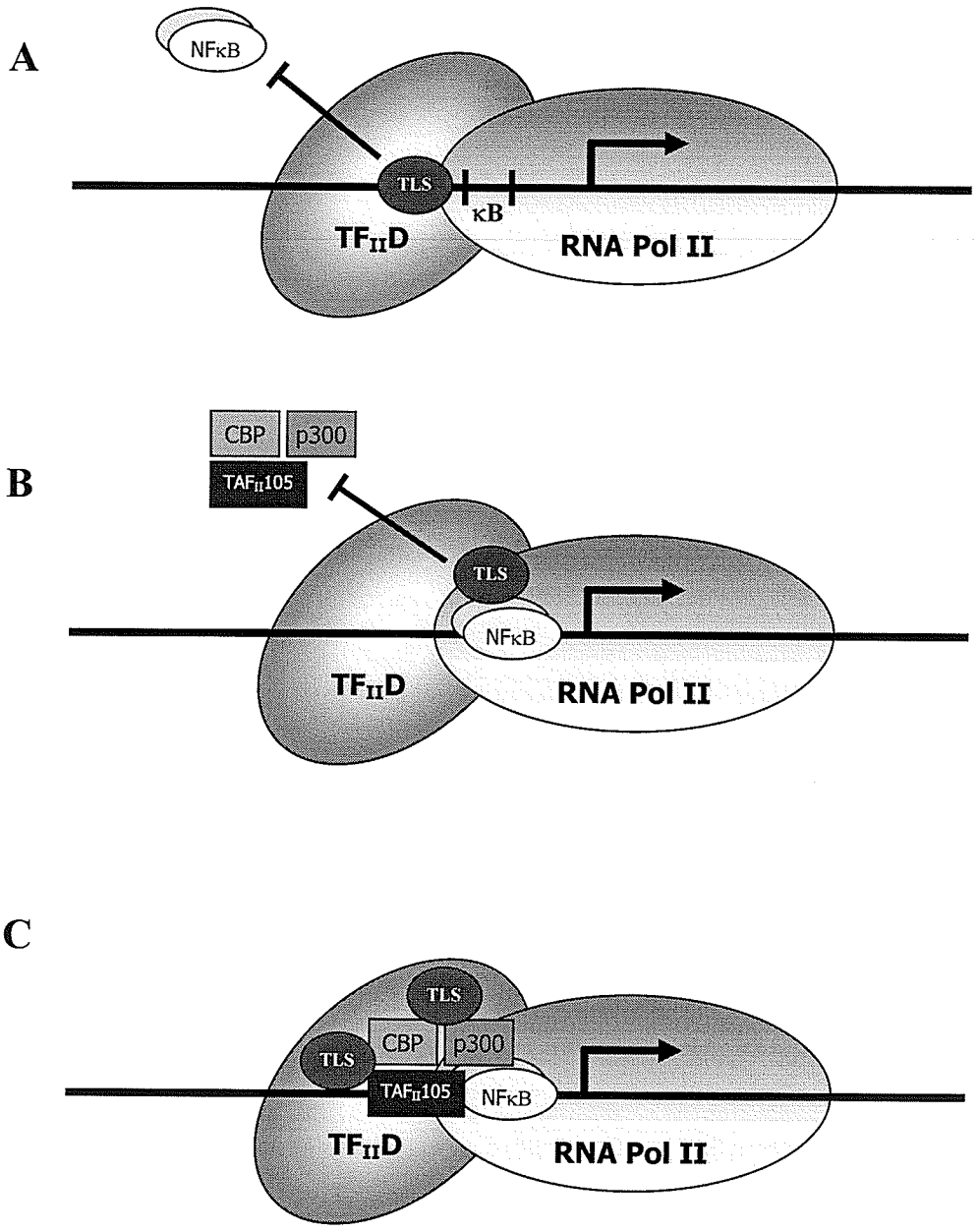

Figure 20. Schematic representation of the proposed mechanisms of repression involved in TLS' modulation of NF-κB-directed gene expression. **(A)** TLS binds directly to target promoter and represses the ability of NF-κB to bind its consensus κB site **(B)** TLS interacts with NF-κB and represses its ability to associate with the CBP/p300 coactivator proteins. **(C)** TLS interacts with the NF-κB-bound CBP/ p300 coactivator proteins and represses their histone acetyl-transferase (HAT) activity.

In the third proposed mechanism (Panel C), TLS interacts directly with the NF-κB-bound coactivator proteins and interferes with their histone acetyl-transferase activity, or other relevant transcriptional functions. The EWS protein has been shown to interact with both the CBP and p300 coactivator proteins[86], and thus it can be inferred that TLS may also associate with these same factors. Additionally, the TET proteins have been shown to interact with various TAF_{II} proteins[16,67], which are part of the $TF_{II}D$ complex. Therefore, it is possible that TLS may also interact with the NF-κB coactivator protein $TAF_{II}105$ to modulate the gene expression of specific target genes.

The role of TLS in the modulation of the three IR-induced NF-κB candidate genes may also be explained by an alternative molecular mechanism to those that were described above. TLS is known to associate with RNA and known components of gene splicing (section 1.1.3). It is possible that TLS may inhibit gene expression of the three candidate genes at the splicing level. This may involve the prevention of proper spliceosome assembly onto the RNA polymerase II enzyme, or the elongation of the transcription complex. Regardless of which mechanism is determined to be valid, we hypothesize that TLS is initially loaded onto the promoter regions of the candidate genes. Moreover, with candidate target genes now in hand, each of these models can be directly tested experimentally, as will be discussed in section 4.5.

4.4 TLS modulates p53-directed gene expression

We have not discounted the possibility that TLS may also function as a transcriptional activator. The same mechanisms that were described above may also enhance and activate transcriptional activation of target genes rather than only function in

a repressive capacity. The dynamic interaction of the components involved in these mechanisms may have different effects on gene expression levels from one gene to another. Indeed, we have preliminary microarray data that suggest TLS may act as an activator to modulate IR-induced p53-directed gene expression (Figure 21). Of the 17 IR-induced p53 target genes that were represented on the murine 430A 2.0 microarray chip, 11 were determined to be differentially expressed between wild type and TLS -/- pre-B cells.

In contrast to the expression pattern of the differentially expressed NF-κB target genes that we identified, the p53 genes are induced in wild type cells upon ionizing radiation, but not in TLS -/- cells. While p53 target genes are beyond the direct focus of this thesis project, validation of transcript levels and subsequent analysis of the promoter sequences of p53-associate genes will determine whether TLS is involved in the modulation of p53-directed gene expression.

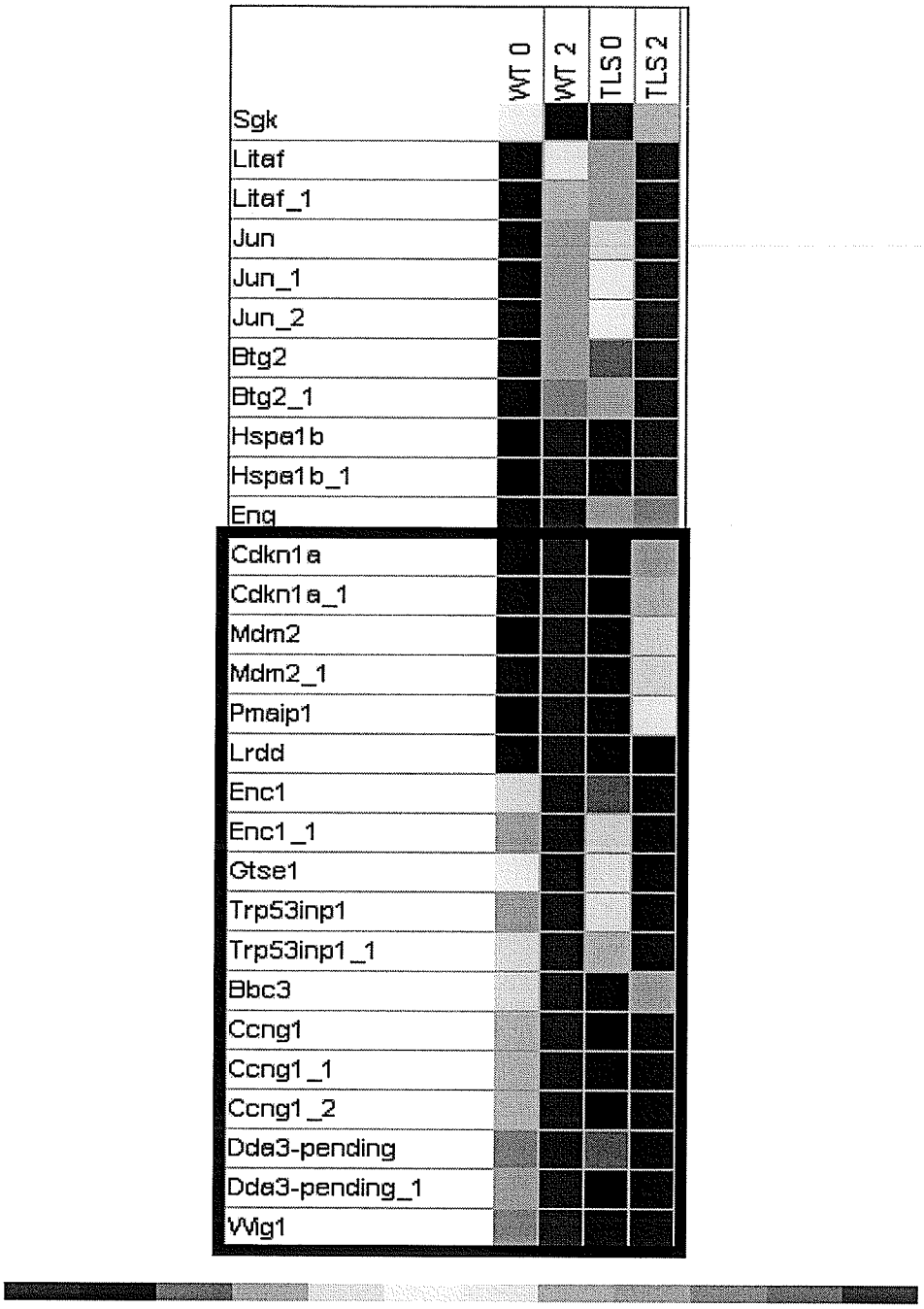

Figure 21. Ionizing radiation-induced p53 target genes identified in the full microarray experiment. Each column represents an experimental condition (i.e. cell type and time post-ionizing radiation (IR)). Legend indicates color scheme used to represent low (blue) and high (red) expression levels. The black box encircles the IR-responsive target genes that are differentially expressed between wild type and TLS -/- cells. The heat map was generated by GeneCluster 2.0 software.

4.5 Future Directions

In summary, we have established that TLS modulates NF-κB-directed gene expression *in vivo* and have identified and validated the candidate TLS-dependent NF-κB target genes *TNFaip2* and *TNFrsf5*. The identification of these genes will allow us the opportunity to directly investigate the molecular mechanisms involved in TLS' ability to modulate NF-κB-directed gene expression. Our hypothesis is that TLS associates with the promoter regions of the candidate genes, either directly or through an association with NF-κB, or its coactivator proteins (CBP/p300 and $TAF_{II}105$), and acts to modulate NF-κB-directed gene expression.

Future experiments will initially be performed by myself as part of a newly funded CIHR grant based in large part on this thesis work. We will perform chromatin immunoprecipitation (ChIP) experiments, in collaboration with Dr. Jim Davie of the Manitoba Institute of Cell Biology at the University of Manitoba, to assess whether TLS can bind the promoter regions of the *TNFaip2* and *TNFrsf5* genes directly, or as an NF-κB cofactor. We have identified NF-κB binding sites in these two gene promoters using the TFSEARCH database (http://www.cbrc.jp/research/db/TFSEARCH.html)[130] and potential TLS binding sites were predicted by sequence identity to a reported double-stranded TLS-binding site[14](section 3.6). These binding sites will allow us to select which region of each promoter will be analyzed in our ChIP experiments. Oligonucleotide primers specific to regions flanking the potential TLS and NF-κB binding sites within the *Tnfaip2* and *Tnfrsf5* promoters will be used to PCR amplify candidate target promoters. Positive ChIP results will be verified by mutation of DNA binding sites in promoter binding assays. We expect to establish that TLS binds to

specific promoter regions through its interaction with NF-κB, or possibly directly. Further characterization of the molecular interactions between TLS, NF-κB, and its coactivator proteins, through coimmunoprecipitation experiments, will also allow us to confirm our proposed models.

Upon further validation and characterization of the p53 candidate promoters, we will also use the same criteria to perform ChIP experiments on these particular genes. Although the p53 target genes are beyond the scope of my thesis work, they remain a powerful tool that may be used to determine a molecular mechanism for TLS in the modulation of gene expression. Furthermore, the p53 candidate genes may directly contribute to the TLS -/- phenotypic defects that we have observed. Modulation of NF-κB- or p53-directed gene expression in response to DNA damage will have widespread significance in our understanding of tumor promotion. Furthermore, it may provide a molecular mechanism for the integration of multiple signaling pathways as they converge on major transcription factors that control the biological consequences to such signals.

The results presented in this thesis advance our current understanding of TLS' normal cellular function in the mammalian cell. Ultimately, these findings will assist in the elucidation of the molecular mechanisms underlying the role of the TLS-fusion proteins in the oncogenic progression of myxoid liposarcoma and acute myeloid leukemia.

Chapter 5: References

(1) Ichikawa H, Shimizu K, Hayashi Y, Ohki M. An RNA-binding protein gene, TLS/FUS, is fused to ERG in human myeloid leukemia with t(16;21) chromosomal translocation. Cancer Res. 1994;54:2865-2868.

(2) Prasad DD, Ouchida M, Lee L, Rao VN, Reddy ES. TLS/FUS fusion domain of TLS/FUS-erg chimeric protein resulting from the t(16;21) chromosomal translocation in human myeloid leukemia functions as a transcriptional activation domain. Oncogene. 1994;9:3717-3729.

(3) Crozat A, Aman P, Mandahl N, Ron D. Fusion of CHOP to a novel RNA-binding protein in human myxoid liposarcoma. Nature. 1993;363:640-644.

(4) Hicks GG, Singh N, Nashabi A et al. Fus deficiency in mice results in defective B-lymphocyte development and activation, high levels of chromosomal instability and perinatal death. Nat Genet. 2000;24:175-179.

(5) Brach MA, Hass R, Sherman ML et al. Ionizing radiation induces expression and binding activity of the nuclear factor kappa B. J Clin Invest. 1991;88:691-695.

(6) Uranishi H, Tetsuka T, Yamashita M et al. Involvement of the pro-oncoprotein TLS (translocated in liposarcoma) in nuclear factor-kappa B p65-mediated transcription as a coactivator. J Biol Chem. 2001;276:13395-13401.

(7) Aman P, Panagopoulos I, Lassen C et al. Expression patterns of the human sarcoma-associated genes FUS and EWS and the genomic structure of FUS. Genomics. 1996;37:1-8.

(8) Zinszner H, Albalat R, Ron D. A novel effector domain from the RNA-binding protein TLS or EWS is required for oncogenic transformation by CHOP. Genes Dev. 1994;8:2513-2526.

(9) Yang L, Embree LJ, Tsai S, Hickstein DD. Oncoprotein TLS interacts with serine-arginine proteins involved in RNA splicing. J Biol Chem. 1998;273:27761-27764.

(10) Fujii R, Okabe S, Urushido T et al. The RNA binding protein TLS is translocated to dendritic spines by mGluR5 activation and regulates spine morphology. Curr Biol. 2005;15:587-593.

(11) Lerga A, Hallier M, Delva L et al. Identification of an RNA binding specificity for the potential splicing factor TLS. J Biol Chem. 2001;276:6807-6816.

(12) Baechtold H, Kuroda M, Sok J et al. Human 75-kDa DNA-pairing protein is identical to the pro-oncoprotein TLS/FUS and is able to promote D-loop formation. J Biol Chem. 1999;274:34337-34342.

(13) Cassiday LA, Maher LJ, III. Having it both ways: transcription factors that bind DNA and RNA. Nucleic Acids Res. 2002;30:4118-4126.

(14) Perrotti D, Bonatti S, Trotta R et al. TLS/FUS, a pro-oncogene involved in multiple chromosomal translocations, is a novel regulator of BCR/ABL-mediated leukemogenesis. EMBO J. 1998;17:4442-4455.

(15) Zinszner H, Sok J, Immanuel D, Yin Y, Ron D. TLS (FUS) binds RNA in vivo and engages in nucleo-cytoplasmic shuttling. J Cell Sci. 1997;110 (Pt 15):1741-1750.

(16) Bertolotti A, Lutz Y, Heard DJ, Chambon P, Tora L. hTAF(II)68, a novel RNA/ssDNA-binding protein with homology to the pro-oncoproteins TLS/FUS and EWS is associated with both TFIID and RNA polymerase II. EMBO J. 1996;15:5022-5031.

(17) Ohno T, Ouchida M, Lee L et al. The EWS gene, involved in Ewing family of tumors, malignant melanoma of soft parts and desmoplastic small round cell tumors, codes for an RNA binding protein with novel regulatory domains. Oncogene. 1994;9:3087-3097.

(18) Lee HJ, Kim S, Pelletier J, Kim J. Stimulation of hTAFII68 (NTD)-mediated transactivation by v-Src. FEBS Lett. 2004;564:188-198.

(19) Query CC, Bentley RC, Keene JD. A common RNA recognition motif identified within a defined U1 RNA binding domain of the 70K U1 snRNP protein. Cell. 1989;57:89-101.

(20) Rappsilber J, Friesen WJ, Paushkin S, Dreyfuss G, Mann M. Detection of arginine dimethylated peptides by parallel precursor ion scanning mass spectrometry in positive ion mode. Anal Chem. 2003;75:3107-3114.

(21) Belyanskaya LL, Delattre O, Gehring H. Expression and subcellular localization of Ewing sarcoma (EWS) protein is affected by the methylation process. Exp Cell Res. 2003;288:374-381.

(22) Iko Y, Kodama TS, Kasai N et al. Domain architectures and characterization of an RNA-binding protein, TLS. J Biol Chem. 2004;279:44834-44840.

(23) Ladomery M, Dellaire G. Multifunctional zinc finger proteins in development and disease. Ann Hum Genet. 2002;66:331-342.

(24) Enzinger FM, Weiss SW. Soft tissue tumors. 3rd ed ed. St. Louis: Mosby; 1995.

(25) Kilpatrick SE, Doyon J, Choong PF, Sim FH, Nascimento AG. The clinicopathologic spectrum of myxoid and round cell liposarcoma. A study of 95 cases. Cancer. 1996;77:1450-1458.

(26) Heim S, Mitelman F. Cancer cytogenetics. 2nd ed ed. New York: Wiley-Liss; 1995.

(27) Rabbitts TH, Forster A, Larson R, Nathan P. Fusion of the dominant negative transcription regulator CHOP with a novel gene FUS by translocation t(12;16) in malignant liposarcoma. Nat Genet. 1993;4:175-180.

(28) Butterwith SC. Molecular events in adipocyte development. Pharmacol Ther. 1994;61:399-411.

(29) Barone MV, Crozat A, Tabaee A, Philipson L, Ron D. CHOP (GADD153) and its oncogenic variant, TLS-CHOP, have opposing effects on the induction of G1/S arrest. Genes Dev. 1994;8:453-464.

(30) Sanchez-Garcia I, Rabbitts TH. Transcriptional activation by TAL1 and FUS-CHOP proteins expressed in acute malignancies as a result of chromosomal abnormalities. Proc Natl Acad Sci U S A. 1994;91:7869-7873.

(31) Perez-Losada J, Pintado B, Gutierrez-Adan A et al. The chimeric FUS/TLS-CHOP fusion protein specifically induces liposarcomas in transgenic mice. Oncogene. 2000;19:2413-2422.

(32) Perez-Mancera PA, Perez-Losada J, Sanchez-Martin M et al. Expression of the FUS domain restores liposarcoma development in CHOP transgenic mice. Oncogene. 2002;21:1679-1684.

(33) Pereira DS, Dorrell C, Ito CY et al. Retroviral transduction of TLS-ERG initiates a leukemogenic program in normal human hematopoietic cells. Proc Natl Acad Sci U S A. 1998;95:8239-8244.

(34) Kong XT, Ida K, Ichikawa H et al. Consistent detection of TLS/FUS-ERG chimeric transcripts in acute myeloid leukemia with t(16;21)(p11;q22) and identification of a novel transcript. Blood. 1997;90:1192-1199.

(35) Hiyoshi M, Yamane T, Hirai M et al. Establishment and characterization of IRTA17 and IRTA21, two novel acute non-lymphocytic leukaemia cell lines with t(16;21) translocation. Br J Haematol. 1995;90:417-424.

(36) Panagopoulos I, Mandahl N, Ron D et al. Characterization of the CHOP breakpoints and fusion transcripts in myxoid liposarcomas with the 12;16 translocation. Cancer Res. 1994;54:6500-6503.

(37) Panagopoulos I, Mandahl N, Mitelman F, Aman P. Two distinct FUS breakpoint clusters in myxoid liposarcoma and acute myeloid leukemia with the translocations t(12;16) and t(16;21). Oncogene. 1995;11:1133-1137.

(38) Waters BL, Panagopoulos I, Allen EF. Genetic characterization of angiomatoid fibrous histiocytoma identifies fusion of the FUS and ATF-1 genes induced by a chromosomal translocation involving bands 12q13 and 16p11. Cancer Genet Cytogenet. 2000;121:109-116.

(39) Storlazzi CT, Mertens F, Nascimento A et al. Fusion of the FUS and BBF2H7 genes in low grade fibromyxoid sarcoma. Hum Mol Genet. 2003;12:2349-2358.

(40) Bonin G, Scamps C, Turc-Carel C, Lipinski M. Chimeric EWS-FLI1 transcript in a Ewing cell line with a complex t(11;22;14) translocation. Cancer Res. 1993;53:3655-3657.

(41) Sorensen PH, Liu XF, Delattre O et al. Reverse transcriptase PCR amplification of EWS/FLI-1 fusion transcripts as a diagnostic test for peripheral primitive neuroectodermal tumors of childhood. Diagn Mol Pathol. 1993;2:147-157.

(42) Peter M, Mugneret F, Aurias A et al. An EWS/ERG fusion with a truncated N-terminal domain of EWS in a Ewing's tumor. Int J Cancer. 1996;67:339-342.

(43) Sorensen PH, Lessnick SL, Lopez-Terrada D et al. A second Ewing's sarcoma translocation, t(21;22), fuses the EWS gene to another ETS-family transcription factor, ERG. Nat Genet. 1994;6:146-151.

(44) Urano F, Umezawa A, Hong W, Kikuchi H, Hata J. A novel chimera gene between EWS and E1A-F, encoding the adenovirus E1A enhancer-binding protein, in extraosseous Ewing's sarcoma. Biochem Biophys Res Commun. 1996;219:608-612.

(45) Benjamin LE, Fredericks WJ, Barr FG, Rauscher FJ, III. Fusion of the EWS1 and WT1 genes as a result of the t(11;22)(p13;q12) translocation in desmoplastic small round cell tumors. Med Pediatr Oncol. 1996;27:434-439.

(46) Kim J, Lee K, Pelletier J. The desmoplastic small round cell tumor t(11;22) translocation produces EWS/WT1 isoforms with differing oncogenic properties. Oncogene. 1998;16:1973-1979.

(47) Rauscher FJ, III, Benjamin LE, Fredericks WJ, Morris JF. Novel oncogenic mutations in the WT1 Wilms' tumor suppressor gene: a t(11;22) fuses the Ewing's sarcoma gene, EWS1, to WT1 in desmoplastic small round cell tumor. Cold Spring Harb Symp Quant Biol. 1994;59:137-146.

(48) Shimizu Y, Mitsui T, Kawakami T et al. Novel breakpoints of the EWS gene and the WT1 gene in a desmoplastic small round cell tumor. Cancer Genet Cytogenet. 1998;106:156-158.

(49) Dal Cin P, Sciot R, Panagopoulos I et al. Additional evidence of a variant translocation t(12;22) with EWS/CHOP fusion in myxoid liposarcoma: clinicopathological features. J Pathol. 1997;182:437-441.

(50) Panagopoulos I, Hoglund M, Mertens F et al. Fusion of the EWS and CHOP genes in myxoid liposarcoma. Oncogene. 1996;12:489-494.

(51) Clark J, Benjamin H, Gill S et al. Fusion of the EWS gene to CHN, a member of the steroid/thyroid receptor gene superfamily, in a human myxoid chondrosarcoma. Oncogene. 1996;12:229-235.

(52) Labelle Y, Bussieres J, Courjal F, Goldring MB. The EWS/TEC fusion protein encoded by the t(9;22) chromosomal translocation in human chondrosarcomas is a highly potent transcriptional activator. Oncogene. 1999;18:3303-3308.

(53) Fujimura Y, Ohno T, Siddique H et al. The EWS-ATF-1 gene involved in malignant melanoma of soft parts with t(12;22) chromosome translocation, encodes a constitutive transcriptional activator. Oncogene. 1996;12:159-167.

(54) Speleman F, Delattre O, Peter M et al. Malignant melanoma of the soft parts (clear-cell sarcoma): confirmation of EWS and ATF-1 gene fusion caused by a t(12;22) translocation. Mod Pathol. 1997;10:496-499.

(55) Zucman J, Delattre O, Desmaze C et al. EWS and ATF-1 gene fusion induced by t(12;22) translocation in malignant melanoma of soft parts. Nat Genet. 1993;4:341-345.

(56) Jeon IS, Davis JN, Braun BS et al. A variant Ewing's sarcoma translocation (7;22) fuses the EWS gene to the ETS gene ETV1. Oncogene. 1995;10:1229-1234.

(57) Martini A, La Starza R, Janssen H et al. Recurrent rearrangement of the Ewing's sarcoma gene, EWSR1, or its homologue, TAF15, with the transcription factor CIZ/NMP4 in acute leukemia. Cancer Res. 2002;62:5408-5412.

(58) Attwooll C, Tariq M, Harris M et al. Identification of a novel fusion gene involving hTAFII68 and CHN from a t(9;17)(q22;q11.2) translocation in an extraskeletal myxoid chondrosarcoma. Oncogene. 1999;18:7599-7601.

(59) Panagopoulos I, Mencinger M, Dietrich CU et al. Fusion of the RBP56 and CHN genes in extraskeletal myxoid chondrosarcomas with translocation t(9;17)(q22;q11). Oncogene. 1999;18:7594-7598.

(60) Sjogren H, Meis-Kindblom J, Kindblom LG, Aman P, Stenman G. Fusion of the EWS-related gene TAF2N to TEC in extraskeletal myxoid chondrosarcoma. Cancer Res. 1999;59:5064-5067.

(61) Kornblihtt AR, de la MM, Fededa JP, Munoz MJ, Nogues G. Multiple links between transcription and splicing. RNA. 2004;10:1489-1498.

(62) Yang L, Embree LJ, Hickstein DD. TLS-ERG leukemia fusion protein inhibits RNA splicing mediated by serine-arginine proteins. Mol Cell Biol. 2000;20:3345-3354.

(63) Immanuel D, Zinszner H, Ron D. Association of SARFH (sarcoma-associated RNA-binding fly homolog) with regions of chromatin transcribed by RNA polymerase II. Mol Cell Biol. 1995;15:4562-4571.

(64) Blazek E, Mittler G, Meisterernst M. The mediator of RNA polymerase II. Chromosoma. 2005;113:399-408.

(65) Sims RJ, III, Belotserkovskaya R, Reinberg D. Elongation by RNA polymerase II: the short and long of it. Genes Dev. 2004;18:2437-2468.

(66) Chen BS, Hampsey M. Transcription activation: unveiling the essential nature of TFIID. Curr Biol. 2002;12:R620-R622.

(67) Bertolotti A, Melot T, Acker J et al. EWS, but not EWS-FLI-1, is associated with both TFIID and RNA polymerase II: interactions between two members of

the TET family, EWS and hTAFII68, and subunits of TFIID and RNA polymerase II complexes. Mol Cell Biol. 1998;18:1489-1497.

(68) Hartmuth K, Urlaub H, Vornlocher HP et al. Protein composition of human prespliceosomes isolated by a tobramycin affinity-selection method. Proc Natl Acad Sci U S A. 2002;99:16719-16724.

(69) Kameoka S, Duque P, Konarska MM. p54(nrb) associates with the 5' splice site within large transcription/splicing complexes. EMBO J. 2004;23:1782-1791.

(70) Meissner M, Lopato S, Gotzmann J, Sauermann G, Barta A. Proto-oncoprotein TLS/FUS is associated to the nuclear matrix and complexed with splicing factors PTB, SRm160, and SR proteins. Exp Cell Res. 2003;283:184-195.

(71) Kohno K, Izumi H, Uchiumi T, Ashizuka M, Kuwano M. The pleiotropic functions of the Y-box-binding protein, YB-1. Bioessays. 2003;25:691-698.

(72) Chansky HA, Hu M, Hickstein DD, Yang L. Oncogenic TLS/ERG and EWS/Fli-1 fusion proteins inhibit RNA splicing mediated by YB-1 protein. Cancer Res. 2001;61:3586-3590.

(73) Rapp TB, Yang L, Conrad EU, III, Mandahl N, Chansky HA. RNA splicing mediated by YB-1 is inhibited by TLS/CHOP in human myxoid liposarcoma cells. J Orthop Res. 2002;20:723-729.

(74) Yang L, Chansky HA, Hickstein DD. EWS.Fli-1 fusion protein interacts with hyperphosphorylated RNA polymerase II and interferes with serine-arginine protein-mediated RNA splicing. J Biol Chem. 2000;275:37612-37618.

(75) Powers CA, Mathur M, Raaka BM, Ron D, Samuels HH. TLS (translocated-in-liposarcoma) is a high-affinity interactor for steroid, thyroid hormone, and retinoid receptors. Mol Endocrinol. 1998;12:4-18.

(76) McKercher SR, Torbett BE, Anderson KL et al. Targeted disruption of the PU.1 gene results in multiple hematopoietic abnormalities. EMBO J. 1996;15:5647-5658.

(77) Moreau-Gachelin F, Tavitian A, Tambourin P. Spi-1 is a putative oncogene in virally induced murine erythroleukaemias. Nature. 1988;331:277-280.

(78) Scott EW, Simon MC, Anastasi J, Singh H. Requirement of transcription factor PU.1 in the development of multiple hematopoietic lineages. Science. 1994;265:1573-1577.

(79) Barkett M, Gilmore TD. Control of apoptosis by Rel/NF-kappaB transcription factors. Oncogene. 1999;18:6910-6924.

(80) Kucharczak J, Simmons MJ, Fan Y, Gelinas C. To be, or not to be: NF-kappaB is the answer--role of Rel/NF-kappaB in the regulation of apoptosis. Oncogene. 2003;22:8961-8982.

(81) Hallier M, Lerga A, Barnache S, Tavitian A, Moreau-Gachelin F. The transcription factor Spi-1/PU.1 interacts with the potential splicing factor TLS. J Biol Chem. 1998;273:4838-4842.

(82) Delva L, Gallais I, Guillouf C et al. Multiple functional domains of the oncoproteins Spi-1/PU.1 and TLS are involved in their opposite splicing effects in erythroleukemic cells. Oncogene. 2004;23:4389-4399.

(83) Gascoyne DM, Thomas GR, Latchman DS. The effects of Brn-3a on neuronal differentiation and apoptosis are differentially modulated by EWS and its oncogenic derivative EWS/Fli-1. Oncogene. 2004;23:3830-3840.

(84) Thomas GR, Latchman DS. The pro-oncoprotein EWS (Ewing's Sarcoma protein) interacts with the Brn-3a POU transcription factor and inhibits its ability to activate transcription. Cancer Biol Ther. 2002;1:428-432.

(85) Thomas GR, Faulkes DJ, Gascoyne D, Latchman DS. EWS differentially activates transcription of the Brn-3a long and short isoform mRNAs from distinct promoters. Biochem Biophys Res Commun. 2004;318:1045-1051.

(86) Rossow KL, Janknecht R. The Ewing's sarcoma gene product functions as a transcriptional activator. Cancer Res. 2001;61:2690-2695.

(87) Zhang D, Paley AJ, Childs G. The transcriptional repressor ZFM1 interacts with and modulates the ability of EWS to activate transcription. J Biol Chem. 1998;273:18086-18091.

(88) Wu S, Green MR. Identification of a human protein that recognizes the 3' splice site during the second step of pre-mRNA splicing. EMBO J. 1997;16:4421-4432.

(89) Bargou RC, Jurchott K, Wagener C et al. Nuclear localization and increased levels of transcription factor YB-1 in primary human breast cancers are associated with intrinsic MDR1 gene expression. Nat Med. 1997;3:447-450.

(90) Mertens PR, Harendza S, Pollock AS, Lovett DH. Glomerular mesangial cell-specific transactivation of matrix metalloproteinase 2 transcription is mediated by YB-1. J Biol Chem. 1997;272:22905-22912.

(91) Ohga T, Uchiumi T, Makino Y et al. Direct involvement of the Y-box binding protein YB-1 in genotoxic stress-induced activation of the human multidrug resistance 1 gene. J Biol Chem. 1998;273:5997-6000.

(92) Mertens PR, Alfonso-Jaume MA, Steinmann K, Lovett DH. YB-1 regulation of the human and rat gelatinase A genes via similar enhancer elements. J Am Soc Nephrol. 1999;10:2480-2487.

(93) Baldwin AS, Jr. The NF-kappa B and I kappa B proteins: new discoveries and insights. Annu Rev Immunol. 1996;14:649-683.

(94) Ghosh S, May MJ, Kopp EB. NF-kappa B and Rel proteins: evolutionarily conserved mediators of immune responses. Annu Rev Immunol. 1998;16:225-260.

(95) Mercurio F, Manning AM. NF-kappaB as a primary regulator of the stress response. Oncogene. 1999;18:6163-6171.

(96) Ghosh S, Karin M. Missing pieces in the NF-kappaB puzzle. Cell. 2002;109 Suppl:S81-S96.

(97) Pahl HL. Activators and target genes of Rel/NF-kappaB transcription factors. Oncogene. 1999;18:6853-6866.

(98) Sen R, Baltimore D. Inducibility of kappa immunoglobulin enhancer-binding protein Nf-kappa B by a posttranslational mechanism. Cell. 1986;47:921-928.

(99) Sen R, Baltimore D. Multiple nuclear factors interact with the immunoglobulin enhancer sequences. Cell. 1986;46:705-716.

(100) Alt FW, Blackwell TK, DePinho RA, Reth MG, Yancopoulos GD. Regulation of genome rearrangement events during lymphocyte differentiation. Immunol Rev. 1986;89:5-30.

(101) Chen FE, Ghosh G. Regulation of DNA binding by Rel/NF-kappaB transcription factors: structural views. Oncogene. 1999;18:6845-6852.

(102) Baeuerle PA, Henkel T. Function and activation of NF-kappa B in the immune system. Annu Rev Immunol. 1994;12:141-179.

(103) Zhong H, May MJ, Jimi E, Ghosh S. The phosphorylation status of nuclear NF-kappa B determines its association with CBP/p300 or HDAC-1. Mol Cell. 2002;9:625-636.

(104) Karin M, Ben Neriah Y. Phosphorylation meets ubiquitination: the control of NF-[kappa]B activity. Annu Rev Immunol. 2000;18:621-663.

(105) Bonizzi G, Karin M. The two NF-kappaB activation pathways and their role in innate and adaptive immunity. Trends Immunol. 2004;25:280-288.

(106) Vermeulen L, De Wilde G, Notebaert S, Vanden Berghe W, Haegeman G. Regulation of the transcriptional activity of the nuclear factor-kappaB p65 subunit. Biochem Pharmacol. 2002;64:963-970.

(107) Zhong H, SuYang H, Erdjument-Bromage H, Tempst P, Ghosh S. The transcriptional activity of NF-kappaB is regulated by the IkappaB-associated PKAc subunit through a cyclic AMP-independent mechanism. Cell. 1997;89:413-424.

(108) Zhong H, Voll RE, Ghosh S. Phosphorylation of NF-kappa B p65 by PKA stimulates transcriptional activity by promoting a novel bivalent interaction with the coactivator CBP/p300. Mol Cell. 1998;1:661-671.

(109) Gerritsen ME, Williams AJ, Neish AS et al. CREB-binding protein/p300 are transcriptional coactivators of p65. Proc Natl Acad Sci U S A. 1997;94:2927-2932.

(110) Perkins ND, Felzien LK, Betts JC et al. Regulation of NF-kappaB by cyclin-dependent kinases associated with the p300 coactivator. Science. 1997;275:523-527.

(111) Cheung WL, Briggs SD, Allis CD. Acetylation and chromosomal functions. Curr Opin Cell Biol. 2000;12:326-333.

(112) Kingston RE, Narlikar GJ. ATP-dependent remodeling and acetylation as regulators of chromatin fluidity. Genes Dev. 1999;13:2339-2352.

(113) Yamit-Hezi A, Dikstein R. TAFII105 mediates activation of anti-apoptotic genes by NF-kappaB. EMBO J. 1998;17:5161-5169.

(114) Raj GV, Safak M, MacDonald GH, Khalili K. Transcriptional regulation of human polyomavirus JC: evidence for a functional interaction between RelA (p65) and the Y-box-binding protein, YB-1. J Virol. 1996;70:5944-5953.

(115) Diamond P, Shannon MF, Vadas MA, Coles LS. Cold shock domain factors activate the granulocyte-macrophage colony-stimulating factor promoter in stimulated Jurkat T cells. J Biol Chem. 2001;276:7943-7951.

(116) Klemsz MJ, McKercher SR, Celada A, Van Beveren C, Maki RA. The macrophage and B cell-specific transcription factor PU.1 is related to the ets oncogene. Cell. 1990;61:113-124.

(117) Linderson Y, French NS, Neurath MF, Pettersson S. Context-dependent Pax-5 repression of a PU.1/NF-kappaB regulated reporter gene in B lineage cells. Gene. 2001;262:107-114.

(118) Chee M, Yang R, Hubbell E et al. Accessing genetic information with high-density DNA arrays. Science. 1996;274:610-614.

(119) Schena M, Shalon D, Davis RW, Brown PO. Quantitative monitoring of gene expression patterns with a complementary DNA microarray. Science. 1995;270:467-470.

(120) Schulze A, Downward J. Navigating gene expression using microarrays--a technology review. Nat Cell Biol. 2001;3:E190-E195.

(121) Chen C, Okayama H. High-efficiency transformation of mammalian cells by plasmid DNA. Mol Cell Biol. 1987;7:2745-2752.

(122) Jordan M, Schallhorn A, Wurm FM. Transfecting mammalian cells: optimization of critical parameters affecting calcium-phosphate precipitate formation. Nucleic Acids Res. 1996;24:596-601.

(123) Hubbell E, Liu WM, Mei R. Robust estimators for expression analysis. Bioinformatics. 2002;18:1585-1592.

(124) Liu WM, Mei R, Di X et al. Analysis of high density expression microarrays with signed-rank call algorithms. Bioinformatics. 2002;18:1593-1599.

(125) Irizarry RA, Bolstad BM, Collin F et al. Summaries of Affymetrix GeneChip probe level data. Nucleic Acids Res. 2003;31:e15.

(126) Eisen MB, Spellman PT, Brown PO, Botstein D. Cluster analysis and display of genome-wide expression patterns. Proc Natl Acad Sci U S A. 1998;95:14863-14868.

(127) Golub TR, Slonim DK, Tamayo P et al. Molecular classification of cancer: class discovery and class prediction by gene expression monitoring. Science. 1999;286:531-537.

(128) Tamayo P, Slonim D, Mesirov J et al. Interpreting patterns of gene expression with self-organizing maps: methods and application to hematopoietic differentiation. Proc Natl Acad Sci U S A. 1999;96:2907-2912.

(129) Gentleman RC, Carey VJ, Bates DM et al. Bioconductor: open software development for computational biology and bioinformatics. Genome Biol. 2004;5:R80.

(130) Heinemeyer T, Wingender E, Reuter I et al. Databases on transcriptional regulation: TRANSFAC, TRRD and COMPEL. Nucleic Acids Res. 1998;26:362-367.

(131) Zabel U, Schreck R, Baeuerle PA. DNA binding of purified transcription factor NF-kappa B. Affinity, specificity, Zn2+ dependence, and differential half-site recognition. J Biol Chem. 1991;266:252-260.

(132) Moses AM, Chiang DY, Pollard DA, Iyer VN, Eisen MB. MONKEY: identifying conserved transcription-factor binding sites in multiple alignments using a binding site-specific evolutionary model. Genome Biol. 2004;5:R98.

(133) Ledebur HC, Parks TP. Transcriptional regulation of the intercellular adhesion molecule-1 gene by inflammatory cytokines in human endothelial cells. Essential roles of a variant NF-kappa B site and p65 homodimers. J Biol Chem. 1995;270:933-943.

(134) Criswell T, Leskov K, Miyamoto S, Luo G, Boothman DA. Transcription factors activated in mammalian cells after clinically relevant doses of ionizing radiation. Oncogene. 2003;22:5813-5827.

(135) Brach MA, Gruss HJ, Kaisho T et al. Ionizing radiation induces expression of interleukin 6 by human fibroblasts involving activation of nuclear factor-kappa B. J Biol Chem. 1993;268:8466-8472.

(136) Sarma V, Wolf FW, Marks RM, Shows TB, Dixit VM. Cloning of a novel tumor necrosis factor-alpha-inducible primary response gene that is differentially expressed in development and capillary tube-like formation in vitro. J Immunol. 1992;148:3302-3312.

(137) Wolf FW, Sarma V, Seldin M et al. B94, a primary response gene inducible by tumor necrosis factor-alpha, is expressed in developing hematopoietic tissues and the sperm acrosome. J Biol Chem. 1994;269:3633-3640.

(138) Foy TM, Aruffo A, Bajorath J, Buhlmann JE, Noelle RJ. Immune regulation by CD40 and its ligand GP39. Annu Rev Immunol. 1996;14:591-617.

(139) Castigli E, Young F, Carossino AM, Alt FW, Geha RS. CD40 expression and function in murine B cell ontogeny. Int Immunol. 1996;8:405-411.

(140) Nguyen VT, Benveniste EN. Critical role of tumor necrosis factor-alpha and NF-kappa B in interferon-gamma -induced CD40 expression in microglia/macrophages. J Biol Chem. 2002;277:13796-13803.

(141) D'Souza BN, Edelstein LC, Pegman PM et al. Nuclear factor kappa B-dependent activation of the antiapoptotic bfl-1 gene by the Epstein-Barr virus latent membrane protein 1 and activated CD40 receptor. J Virol. 2004;78:1800-1816.

(142) Kondratyev AD, Chung KN, Jung MO. Identification and characterization of a radiation-inducible glycosylated human early-response gene. Cancer Res. 1996;56:1498-1502.

(143) Schafer H, Diebel J, Arlt A, Trauzold A, Schmidt WE. The promoter of human p22/PACAP response gene 1 (PRG1) contains functional binding sites for the p53 tumor suppressor and for NFkappaB. FEBS Lett. 1998;436:139-143.

(144) Schafer H, Trauzold A, Sebens T et al. The proliferation-associated early response gene p22/PRG1 is a novel p53 target gene. Oncogene. 1998;16:2479-2487.

(145) Huang YH, Wu JY, Zhang Y, Wu MX. Synergistic and opposing regulation of the stress-responsive gene IEX-1 by p53, c-Myc, and multiple NF-kappaB/rel complexes. Oncogene. 2002;21:6819-6828.

(146) Fei P, El Deiry WS. P53 and radiation responses. Oncogene. 2003;22:5774-5783.

(147) Gonzalez S, Perez-Perez MM, Hernando E, Serrano M, Cordon-Cardo C. p73beta-Mediated apoptosis requires p57kip2 induction and IEX-1 inhibition. Cancer Res. 2005;65:2186-2192.

(148) Kumar R, Lutz W, Frank E, Im HJ. Immediate early gene X-1 interacts with proteins that modulate apoptosis. Biochem Biophys Res Commun. 2004;323:1293-1298.

(149) Arlt A, Grobe O, Sieke A et al. Expression of the NF-kappa B target gene IEX-1 (p22/PRG1) does not prevent cell death but instead triggers apoptosis in Hela cells. Oncogene. 2001;20:69-76.

(150) Arlt A, Kruse ML, Breitenbroich M et al. The early response gene IEX-1 attenuates NF-kappaB activation in 293 cells, a possible counter-regulatory process leading to enhanced cell death. Oncogene. 2003;22:3343-3351.

Appendix I – Supplementary microarray data

See attached CD-ROM disk. The software required to open files within a given folder is indicated in brackets ( ).

Pilot Screen

Fold change comparisons (Microsoft Excel)
Pilot raw data (Microsoft Excel)
Scatterplots (Windows Picture and Fax Viewer or any other basic graphics viewing software)

Microarray Analysis

Microarray data (Microsoft Excel)
Microarray raw data (Microsoft Excel)
MVA plots (Windows Picture and Fax Viewer or any other basic graphics viewing software)

Appendix II – Microarray data calculations

The fold change differences in the irradiation-responses between wild type and TLS -/- cells for individual genes were calculated from RMA-processed data using the following equation:

$$2^{(\text{treated control cells-untreated control cells}) - (\text{treated experimental cells-untreated experimental cells})}$$

For our experiments, we used the following RMA-processed chip data in the equation to determine the fold change difference in irradiation-induced gene expression responses between wild type and TLS -/- pre-B cells:

$$2^{(WT2 - WT0) - (TLS2 - TLS\ 0)}$$

For example, the *Slc19a2* gene in Table 9 is calculated as follows:

$2^{(9.716 - 6.549) - (6.185 - 6.018)} = 8.0$ (actual value before rounding off is 7.996).

Therefore, the level of induction of the *Slc19a2* gene upon irradiation is approximately 8-fold higher in wild type cells than in TLS -/- pre-B cells.